AD-783 185

DEVELOPMENT AND TEST OF LOW IMPACT RESISTANCE STRUCTURES. VOLUME I. STRUCTURAL AND DYNAMIC ASPECTS

Robert W. Harralson, et al

ASE, Incorporated

Prepared for:

Federal Aviation Administration

February 1974

The contents of this report reflect the views of ASE, Inc. which is responsible for the facts and the accuracy of the data presented herein. The contents do not necessarily reflect the official views or policy of the Department of Transportation. This report does not constitute a standard, specification or regulation.

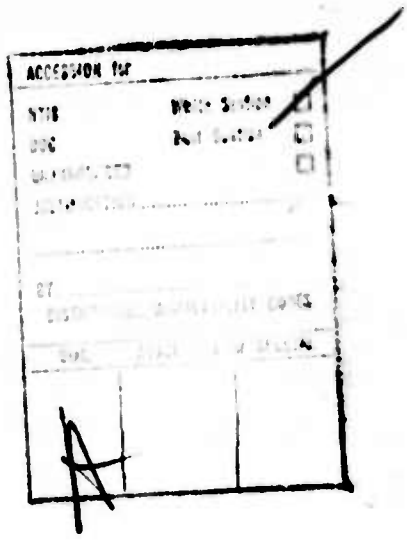

Technical Report Documentation Page

1. Report No.	2. Government Accession No.	3. Recipient's Catalog No.
FAA-RD-73-187 -I		AD 783 185

4. Title and Subtitle	5. Report Date
DEVELOPMENT AND TEST OF LOW IMPACT RESISTANCE STRUCTURES VOLUME I - STRUCTURAL AND DYNAMIC ASPECTS	February, 1974
	6. Performing Organization Code
7. Author(s) Robert W. Harralson, Charles W. Laible and John Lazarin	8. Performing Organization Report No.
9. Performing Organization Name and Address ASE, Inc. 5090 Central Highway Pennsauken, N.J. 08109	10. Work Unit No. (TRAIS)
	11. Contract or Grant No. DOT-FA72WA-3043
12. Sponsoring Agency Name and Address Department of Transportation Federal Aviation Administration Systems Research & Development Service Washington, D. C. 20590	13. Type of Report and Period Covered Final Report-Phase I
	14. Sponsoring Agency Code

15. Supplementary Notes

16. Abstract

A "Breakaway Pole" has been designed and developed and tested to satisfy the requirements for a frangible light support structure. This pole consists of four tapered sections and one straight section assembled to form a unitary structure approximately 20 feet high. The basic structure is shown by analysis to satisfy the requirements for survival in a 75 mph wind with ½" of radial ice, and a 100 mph wind with no radial ice, with factors of safety of 4.3 and 3.2 respectively. Deflection under a 45 mph wind is 0.6 of the allowable value. Tests of the joints in the pole were performed to optimize the pole performance.

An impact test using an instrumented impactor was designed and developed under this contract. Utilizing the impactor mounted on a catapult carriage at the NASA Langley Research Center, the newly developed pole is shown to exhibit frangibility superior to other structures currently in use by factors ranging from 2.5 to 10.0. Volume II of this report describes the effect of the light support structures upon the electromagnetic signals of the Instrument Landing System (ILS).

Note: References to Canadian and Belgian poles or structures throughout this report do not apply to any official Canadian or Belgian Government Agency.

17. Key Words	18. Distribution Statement
Structures, Frangible Impact Tests Light Supports, Frangible Approach Light Structures	Document is available to the public through the National Technical Information Service, Springfield, Virginia 22151.

19. Security Classif. (of this report)	20. Security Classif. (of this page)	21. No. of Pages	22. Price
Unclassified	Unclassified	164	$5.00

Form DOT F 1700.7 (8-72) Reproduction of completed page authorized

PREFACE

In order to provide greater safety for aircraft and passengers on landing or takeoff, the Systems Research and Development Service of the Federal Aviation Administration contracted with ASE, Inc. for the development, design and test of a lightweight frangible (breakable) light support structure. This final report describes the successful conclusion of Phase I of the contract.

ASE, Inc. wishes to express its appreciation to the Visual Aids Section of the Federal Aviation Administration for the guidance and assistance which helped so much to bring this effort to a successful and timely conclusion. Special mention must be made of the efforts of Mr. Bertram L. Smith, now retired, Mr. Stephen A. Cannistra, Mr. Philip A. Darmody, Program Manager; and Mr. Walter C. Fisher, Section Chief. Mr. Leon Reamer provided valuable guidance in general, and in particular the construction and installation efforts at the National Air Facility Engineering Center (NAFEC) at Atlantic City, N.J. The assistance of Mr. John McCarty, of the NASA Langley Research Center, is acknowledged with gratitude for help in conducting the impact tests at the Center.

February 1974

TABLE OF CONTENTS

TABLE OF CONTENTS (continued)

TABLE OF CONTENTS (continued)

LIST OF ILLUSTRATIONS

LIST OF TABLES

Section 1

Introduction

1.1 Background

Currently, rigid structures are being used to support the lights for airport Approach Lighting Systems (ALS), where the mounting heights of the lamps are over 6 feet above terrain. These structures are constructed of self supporting wooden poles, or self supporting towers of steel angles. Occasionally, aircraft have impacted the structures during landings or takeoffs causing major damage to the aircraft, and injury or death to passengers.

The Federal Aviation Administration has therefore issued Contract DOT-FA72WA-3043 to ASE, Inc., to provide for the development of lightweight, frangible, light support structures to support the lights of the ALS. As these structures will be installed directly in the electronic localizer beam of the Instrument Landing System (ILS), the final structural designs must permit acceptable operation of the ILS localizer.

1.2 Contract Requirements

Phase I of the contract provides for the design and development of a frangible light support structure to satisfy the structural and electronic requirements of the Approach Lighting and the Instrument Landing Systems. Structural and electromagnetic tests of the support are included to verify the performance of the final design. After final Government approval of the design, a number of the supports will be fabricated. In addition, the inner 1100 feet of the existing ALS on Runway 13 at the National Air Facility Engineering Center (NAFEC) at Atlantic

City, N.J., was to be converted to a Category II ALS. Phase II of the contract provides for the installation of a complete Category II ALS at the threshold of Runway 31 at NAFEC, using the newly designed light supports and other newly developed equipment.

1.3 Contract Objective

The basic objective of this phase of the contract is to design the lightest weight, most frangible structure consistent with the design parameters enumerated in Section 3. In order to reduce the mass and rigidity requirements of the present designs, no provisions shall be made for personnel climbing the towers. In lieu thereof, structures shall be designed so that all maintenance, including lamp replacements can be accomplished by lowering the entire structure. To achieve both a structurally and electronically acceptable system, extremely close cooperation between the structural and electronic aspects of the design is provided.

1.4 Report Organization

In accordance with the terms of the contract, this Final Report describes the accomplishments under Phase I of the contract. Section 2 summarizes the results, including the electromagnetic investigations which are reported in detail in Volume II of this report. Section 3 provides the constraints governing the design of the support structures, and construction to be provided. Section 4 describes the ASE frangible pole design which was developed, and discusses the frangibility considerations in design. Section 5 describes the rationale and the impact tests which were performed to prove the performance of the ASE pole, and the Belgian and the Canadian structures which have been used in some ALS installations. Section 6 reports on the conversion of a portion of the NAFEC Runway 13 ALS from a Category I System to a Category II System. Section 7 provides the conclusions resulting from the effort.

SECTION 2

SUMMARY

2.1 General

The accomplishments described in more detail further in this report include the development of the ASE pole as the basic light support structure; analyses and tests to prove compliance with the structural design parameters; a description of the impact test and test equipment used to determine the frangibility characteristics; results of the electromagnetic scale modelling tests and analyses; and completion and acceptance of the NAFEC Runway 13 ALS conversion construction effort.

2.2 Light Support Structure

The tapered aluminum segmented pole developed by ASE as the Light Support Structure is shown in Figure 2-1. The lower 16 feet is tapered from a diameter of 4.50 inches to a diameter of 2.87 inches with a uniform 1/8 inch wall thickness. The upper four feet consists of 2" aluminum Electrical Metallic Tubing (EMT) and the lamp fixture. The EMT may be field cut to provide for a planar light plane in the presence of minor variations in terrain. The tapered portion of the pole is sectionalized, consisting of four sections which are wedged together. This sectionalization provides the desired frangibility.

2.2.1 Stress Analysis and Static Tests

Analyses and joint bend tests have been performed (see Appendix D) which prove the compliance of the ASE pole with the structural and deflection criteria of the contract.

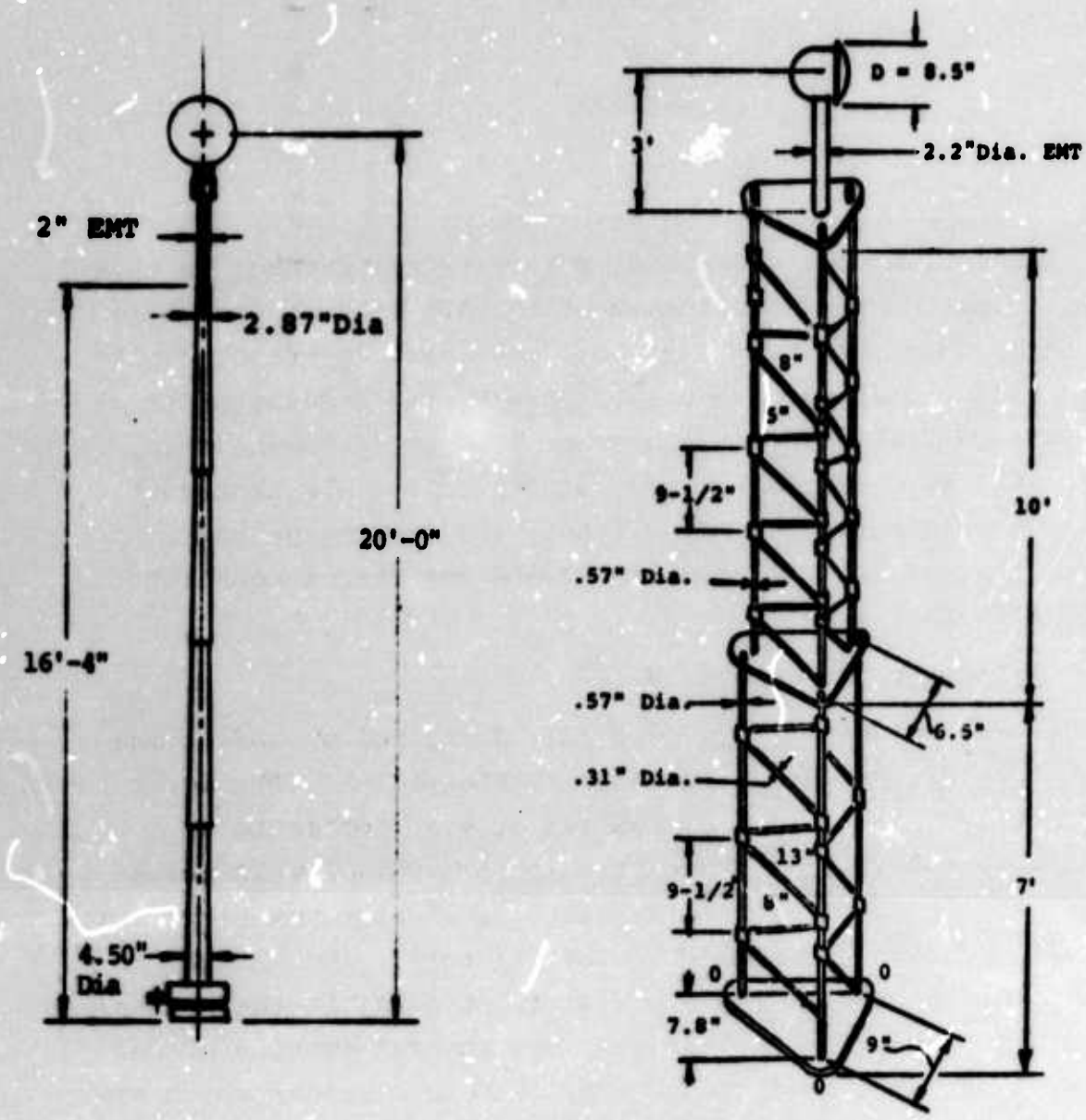

ASE Breakaway Pole

Canadian Light
Support Structure

Figure 2-1 ASE Pole and Canadian Light Support Structure

Similar analyses and tests which verify the compliance with criteria have been conducted of the Canadian structure, see Appendix E. Both structures satisfy the contractual survival criteria (75 mph with 1/2" of radial ice) as well as an additional criterion recommended by ASE (100 mph with no ice).

Table 2-1 Summary of Pole Analyses and Tests

	Basic ASE Pole	Canadian
Survival Wind		
100 mph - no ice		
Pole Stress, psi	10,180	8,973
Factor of Safety	3.2[a]	2.4 min[b]
75 mph - 1/2" ice		
Pole Stress, psi	7,636	13,220
Factor of Safety	4.3[a]	1.7 min[b]
Operational Wind - 45 mph		
Lamp Deflection, inches	1.84	0.80
Slope of Lamp, degrees	0.71	Undet.

[a]Factor of Safety is defined as yield stress/maximum stress.

[b]Factor of Safety is defined as buckling strength/maximum load.

2.3 Impact Tests

Impact tests of the ASE pole were conducted in accordance with contractual requirements. A few additional tests were conducted of the Belgian and Canadian structures for spot comparison purposes. The ASE pole exhibits frangibility in tests superior to the Belgian structure by factors of 2.4 to 5.8 on the basis of fracture energy. The superiority increases to factors of 5.3 to 10.0 on the basis of time to fracture. See Section ..

The tests were conducted with an impactor mounted on the large catapult at the NASA Langley Research Center at Hampton, Virginia. The impactor is designed so that aerodynamic forces would not be introduced into the test results. Although typical aircraft wing construction is used to simulate the interaction between the structures under test and an aircraft, the impactor is sturdy enough to provide for repeated testing under normal conditions. Electronic instrumentation was selected and conditioning equipment was designed, fabricated and installed in the impactor. The impactor was installed on the Langley catapult carriage using a truss structure designed and fabricated by ASE. All equipment, except for accelerometers, were designed, fabricated, and installed by ASE.

2.4 Electromagnetic Investigations

Volume II of this report describes the electomagnetic scattering effects of the ASE pole and the Belgian and Canadian structures upon the Instrument Landing System (ILS) Course Antenna radiation field. It is concluded that scattering of radiation by the Approach Lighting System (ALS) light supports in front of the Course Angenna will not result in course errors, particularly if the ASE design is used.

There are three reasons for this conclusion:

1. The forward scattering from the poles is weak.
2. Each pole is so close to the center line that no detectable phase change could be noted by an incoming aircraft.
3. The symmetric arrangement of poles cancels out any asymmetrical effect of one pole.

Independent analyses by ASE and by Prof. H. N. Kritikos under subcontract to ASE, indicate 6 ASE poles scatter much less than a single monitor dipole at the same point.

This is borne out by the University of Michigan full scale measurements under subcontract to ASE. These measurements

showed that the Canadian supports scattered about 10 dB more than the ASE poles, while the Belgian supports scattered about 18 dB more than the ASE poles. The six Canadian supports scattered about 1 dB more at the middle than a dipole at a height of half a wavelength, 4.5 feet.

For a complete description of the accomplishments and results of the electromagnetic investigations, refer to Volume II.

2.5 Conversion of Runway 13 ALS at NAFEC

The conversion of Runway 13 ALS at NAFEC, Atlantic City, New Jersey, was completed on 11 April 1973 and completed by grading and seeding on 14 May 1973 in accordance with contract requirements. The drawings which describe the demolition, construction, and installations are identified in Section 6.

Section 3

Contract Requirements

3.1 Structural Parameters

3.1.1 Wind Loading

All structures shall be designed to withstand without permanent set, a wind loading of 75 miles per hour with an ice loading of 1/2 inch on all structural members.

3.1.2 Deflection

All structures shall be sufficiently rigid so that the lamps mounted thereon shall not deviate more than 3 inches from the vertical when subjected to winds up to 45 miles per hour. This limit may be exceeded for wind velocities between 45 miles per hour and up to 75 miles per hour; however, in this case, the structure shall return to its normal position immediately after the wind ceases. Structures may be guyed if necessary, to provide the required rigidity.

3.1.3 Frangibility

Structures with mounting heights up to 20 feet, and the upper 20 feet of structures with mounting heights between 20 feet and 70 feet shall be as light as possible and shall be designed to break off or collapse with a minimum transfer of energy, compatible with the above requirements, when impacted by a fast moving body. This impact will be applied at the top and each 5-foot section down to 5 feet above the attachment to the rigid portion of the structure.

3.2 Design Requirements

3.2.1 Structures From 6 Feet to 20 Feet

All structures from 6 feet to 20 feet shall be composed of single vertical members; each member shall support one each

PAR-56 lamp and its holder (estimated weight 7 lbs.). Electrical cable supplying power to the lamp shall be run inside the vertical support. Provision shall be made for lowering the structure so that routine lamp replacement can be accomplished by a man standing on the ground. The design shall be such that one man can raise or lower the structure without additional help. The up to 20-foot structures shall be hinged for lowering and shall be designed to mount on the Type LB cans and the Type "A" adaptor plates. The Type "A" adaptor plates have a 2-inch tapped hole in the center. If necessary, these plates may be modified to accept the light pole base adaptor. If a special lowering device is required, it must be furnished and be such that one man can conveniently transport it from structure to structure.

3.2.2 Structures From 20 Feet to 70 Feet

For mounting heights between 20 feet and 70 feet, the upper 20 feet shall meet the requirements enumerated for the 6-foot to 20-foot mounting heights. The base section consisting of the structure between ground level and 20 feet below the lamp mounting height may be a rigid, self supporting structure, it may be rigid and guyed, or the entire height of the structure may be frangible with provision so that one man can retract either the structure or the lamp mounting bar for maintenance. If the lower portion must be climbed to a level where the top 20 feet can be lowered for maintenance and lamp changing accomplished at that level, the following additional requirements must be met: If necessary for personnel to climb this portion of the tower, a metal ladder shall be furnished. In addition to this, the work space platform shall be of sufficient size to adequately perform routine maintenance and lamp replacement functions. The work area shall be protected by a guard rail or rails and the floor shall be made of expanded steel mesh: The upper 20 feet may be a single vertical member having a non-

metallic horizontal bar mounted on top of which will be mounted 6 each PAR-56 lamp holders spaced as shown on Drawing D-5870-12 or it may be composed of 6 each single pole structures. Again, all cables supplying power to the five lamps shall be installed within the vertical support structure: The upper 20-foot section may telescope inside the lower tower section, or be hinged so that lamp replacement can be accomplished at a lower level.

3.2.3 Materials

The structures may be fabricated of metallic or non-metallic materials. They shall not warp, bend, deform, or change physical characteristics under outdoor environmental conditions. If guying is necessary, guying material shall be non-metallic, such as nylon or fiber glass and shall be self tensioning. Provision shall be made for a quick disconnecting means which shall also be protected against unauthorized operation.

3.2.4 General Requirements

(1) All hinged or telescoping sections shall have provision for latching in the vertical or extended position so that unauthorized personnel cannot operate the mechanism for lowering the assembly.

(2) All structures shall be designed so that exact structure heights can be obtained by field cutting. The objective of this requirement is to provide for lamp mounting heights throughout the mounting height range from 6 feet to 70 feet.

(3) Where the cross bar is required for structures over 20 feet in height, it shall be furnished and shall perform the functions shown on Drawing D-5870-12 which is furnished for guidance purposes and is included in FAA Handbook 6850.3.

(4) Complete detail construction drawings shall be furnished for all piers or other methods used to mount the structures. Special base sections, plates, bolts, washers, and other required parts shall be provided with each structure.

3.3 Electronic Parameters

The ALS structures shall be designed so that their installation in either a Category I or II ALS configuration will not result in the unacceptable degradation of the electronic signals emitted by the VHF ILS localizer when the localizer is installed in an area where an ALS is installed. Investigation of the degradation effects shall be accomplished by both scale modelling techniques and by mathematical analysis.

3.3.1 Electronic Scale Modelling

A typical flat terrain will be investigated by appropriate electronic, mathematical, empirical and scale modelling techniques to prove that the existence of the various types and heights of the structures will have an insignificant effect on the ILS guidance signal. The modelling technique used shall provide a beam which closely approximates the beam radiated from the Texas Instrument Parabolic Reflector.

There are two other frangible type structures in widespread use throughout the world - structures used by the Canadian Government and structures used worldwide produced in Brussels, Belgium. Both of these designs shall be tested along with the ones developed under this contract.

3.3.2 Mathematical Analyses

Mathematical analysis shall be performed on the system terrain selected and compared with the actual electronic modelling results.

Mathematical techniques shall also be used to show the relative performance to all of the requirements using the following types of arrays (6 arrays).

(1) 8-loop array
(2) V-ring array
(3) Texas Instrument/Thompson CSF (French), 80- and 170-foot aperture Parabolic Reflector array
(4) British STAN/37 array

(5) FAA Traveling Wave Antenna Arrays with 40-160 foot apertures

(6) Air Force MRN/7 array

For guidance, the total allowable deviation of the ILS beam for all siting effects is determined by the following documents:

(1) Category I, II, and III localizer requirements set forth in Paragraph 3.1.3 of International Civil Aviation Organization (ICAO), Annex 10, Volume I.

(2) Category I and II localizer requirements of Section 217 of the United States Standard Flight Inspection Manual, FAA Handbook OA-P-8200.1.

(3) Category I and II localizer requirements of FAA Handbook 6750.16 (Siting Criteria for Instrument Landing Systems).

3.4 ALS Conversion for NAFEC Runway 13

A standard Category I ALS and supplemental experimental lighting systems are installed on Runway 13 at NAFEC. The mounting structures in the inner 1100 feet of this installation shall be replaced with the newly-designed supports to form a complete Category II ALS. The elevation of these lights shall be on a slope not over 50:1 starting 200 feet from the threshold, so that the lighting fixtures will clear a new ILS localizer antenna which will be installed between 1100' and 1200' from the runway threshold. All existing structures now installed from the threshold out to and including station 11 + 00 shall be removed at one time and the foundations shall be removed and the ground shall be graded to a smooth surface without bumps or holes. The threshold bar will not be removed. The removal of this equipment will be started when directed by the Government representative. Such salvageable equipment as IL transformers, PAR-36 lamps, lamp holders, cable assemblies, etc., as can be used either on the Runway 13 or 31 installations shall be carefully removed and stored for future use. Underground cables shall not be removed but shall be cut

off below ground. No work will be required on the system between station 12 + 00 and 30 + 00 and no equipment shall be removed from that portion of the Runway 13 ALS. Configuration of the completed system shall be as shown in Figure 2-2 of Agency Handbook Number 6850.2.

3.5 ALS Installation for NAFEC Runway 31

A complete Category II ALS with additional experimental lighting equipment shall be installed on Runway 31 at NAFEC as Phase II of the contract. A description of the contract requirements and accomplishments will be contained in the Phase II Final Report.

Section 4

Frangible Pole

4.1 Description

The basic Light Support Structure developed by ASE is an aluminum pole 20 feet in height from the base to the center of the lamp. The lower 16 feet in height is tapered from a diameter of 4.50 inches to a diameter of 2.87 inches with a uniform 1/8 inch wall thickness. The upper 4 feet consists of 2 inch aluminum Electrical Metallic Tubing (EMT) and the lamp fixture. The EMT may be field cut to provide for the desired planar light field in the presence of minor variations in terrain. Substantially shorter heights may be accommodated by omitting lower pole sections. The tapered portion of the pole is sectionalized, consisting of four sections which are wedged together to form the composite. See Figure 2-1. It is this sectionalization of the pole that provides the desired frangibility characteristics.

4.2 Concepts Considered

4.2.1 Type of Member

The contract specifies that a single vertical member shall be used for the light support structures. The advantages of a single vertical member over a member assembled from trusses are:

a) minimum secondary radiation and consequent distortion of the horizontally polarized ILS beam - there are no horizontal or slanted members to reradiate.

b) simpler and less expensive field erection.

A tapered pole similar to those used extensively in the United States for light standards was selected in lieu of

a uniform diameter pole. This selection was made because

(a) the resultant structure is lighter in weight - material is present only where needed.
(b) flexibility is provided in the methods available to introduce frangibility.
(c) vibration induced by vortex shedding is negated.
(d) electromagnetic scattering is minimized.

4.2.2 Frangibility Considerations

Two concepts were considered to provide the desired frangibility in the pole; the use of stress risers and the use of breakaway joints.

4.2.2.1 Stress Riser

This construction would use sharp cornered holes in the pole wall to introduce stress concentrations combined with an aluminum alloy with brittle failure characteristics. Appropriately designed, this concept would provide adequate strength to withstand the specified wind forces and would break when subjected to impact. Deflection would not be a factor in material selection as long as the material remains an aluminum alloy and the cross section remains the same.

The major objection to this concept is the high cost of sawing, drilling, punching or broaching the many sharp cornered holes in the pole wall that would be required. Discussions with the Aluminum Company of America (ALCOA) indicate that Alloy 6005 would provide the required characteristics. However, substantial amounts of energy are still required when the material is bent, stretched, or fractured.

4.2.2.2 Breakaway Joints

The tapered pole selected by ASE lends itself admirably to the use of breakaway joints. The poles are comprised of four sections of equal length and of equal taper, and

are assembled by wedging the sections onto one another. This concept is not sensitive to the type of material used. However, although compliance with windloading and deflection requirements of the basic design may be established by analytical techniques, the pole joints are not amenable to such analysis. Joints with varying socket ratios (length of joint/joint diameter) were therefore subjected to bend tests to determine the characteristics of the joints.

The analyses and tests which prove the compliance of the ASE Breakaway Pole design with the structural and deflection criteria are contained in Appendix D. A stress analyses of the Canadian Light Support Structure, together with a description of a Load/Deflection Test conducted on this structure is contained in Appendix E. Impact tests of all these structures as well as the Belgian unit, are described in Section 5. Table 4-1 summarizes the results of the analyses and static tests described in Appendices D and E.

Table 4-1 - Summary of Pole Analyses and Tests

	Basic ASE Pole	Canadian
Survival Wind		
100 mph - no ice		
Pole Stress, psi	10,180	8,973
Factor of Safety	3.2	2.4 min
75 mph - 1/2" ice		
Pole Stress, psi	7,636	13,220
Factor of Safety	4.3	1.7 min
Operational Wind - 45 mph		
Lamp Deflection, inches	1.84	0.80
Slope of Lamp, degrees	0.71	Undet.

4.2.3 Production Design

The dimensional parameters of the breakaway poles which were tested in this program were established by considerations of available suitable materials, test schedules, and production expediting. The design of the pole assembly is currently being reviewed for production, with a view toward decreasing weight, a major parameter in impact considerations. As currently envisaged, the pole assembly consists of a lamp-holder assembly supported by a four foot length of 2.4" OD aluminum alloy thin wall tubing, four sections of tapered aluminum alloy tubing approximately 4 feet long and a cast aluminum base, see Figure 2-1.

4.2.3.1 Weight Considerations

Analysis shows that the wall of the 2.4" OD tubing may be reduced to about .06 inches, and still provide an adequate margin of safety against the specified environment. The walls of the tapered sections are substantially influenced by manufacturing consideration. Reductions of 20% are expected in the wall thickness of the tapered sections as a result of investigations currently underway with manufacturers of these poles. Table 4-2 compares the weights of the tested poles with the anticipated weight of the production poles.

4.2.3.2 Section Length Considerations

The potential quantity requirements for light support structures dictates that careful attention be paid to costs as well as frangibility and producibility considerations. The pole was accordingly sectionalized into equal lengths of four feet each. This simplifies manufacture, shipping, and field assembly, with a concomitant minimization of associated costs.

This subdivision has proven by test to provide excellent frangibility characteristics. Although shorter and lighter

Table 4-2 Comparison of Weights of ASE Tested Pole with Anticipated Production Pole

Item	Weight of	
	ASE Tested Pole, lbs.	Anticipated Production Pole, lbs.
Lampholder Assembly		
Par 56 with color filter	6.5	6.5
Flasher assembly	-	11.0
2.4" OD Thin Wall Tubing	4.0	2.0
Upper Tapered Tubing Section	7.0	5.6
Second Tapered Tubing Section	7.5	6.0
Third Tapered Tubing Section	8.0	6.4
Lowest Tapered Tubing Section	7.8	6.2

sections together with an increased number of joints can be provided, it is conceivable that the added joints could increase the energy transfer. If a substantial change in the design were to be made, it would appear advisable to verify the frangibility and the desirability of the revised design by tests.

SECTION 5

Impact Tests

5.1 Introduction

Frangibility is not amenable to linear analysis and therefore dynamic impact testing is utilized to obtain valid data. The contract document therefore requires the light support structure designed under this contract to be subjected to impact tests. The impacts are to be applied at the top and each 5-foot section down to 5 feet above the attachment to the rigid portion of the structure. The impact test method selected for this program is described in Section 5.2. The alternates to this method are considered and evaluated in Appendix B. The test equipment is discussed in detail in Section 5.3. The test results are given in Section 5.4, and are evaluated in Section 5.5.

5.2 Description of Impact Test

5.2.1 Test Parameters

The light support structures may be impacted by a wide variety of airplanes with impact velocities from 60 mph to 140 mph. The effective mass of the aircraft parts colliding with the light support structure may range from 300 pounds, (Beechcraft nose landing gear coupled to main fuselage) to several tons, (Boeing 747 jet pod or landing gear).

5.2.2 Impact Test Method

The impact test method selected for this program consisted of striking the light support test structures with an impactor, see Section 5.3.1, mounted on the catapult carriage at the NASA Langley Research Center, Hampton, Va., see Section 5.3.2. The impactor was mounted on, and outboard of, the carriage in such a way that it could move relative to the carriage and in

a direction parallel to its direction of travel. Compression springs positioned the impactor in a neutral position. Each test structure, mounted on a foundation alongside the carriage tracks, was struck by the impactor as the carriage travelled past. Ideally, on impact, the impactor moved backward relative to the carriage, compressing the positioning springs. This compression and the change in impactor velocity provide a measure of the kinetic energy required to break, bend or twist the test structure.

Test instrumentation, see Section 5.3.3, installed within the impactor measured and recorded the acceleration. High speed cameras, mounted on the catapult carriage and on the ground behind the impact point normal to the carriage direction of travel, provided visual records of the actual impacts.

Three different designs of light support structures were tested, the ASE pole, the Belgian structure, and the Canadian structure. A quantity of the ASE pole was tested, varying the height of impact relative to the structure base, the velocity of impact, and the type of electric power cable within the structure. Three tests of the Belgian structure and one of the Canadian were conducted. Because of repairs to the impactor and instrumentation required after the first impact with a Canadian structure, two series of runs were required.

Each test structure consisted of one of the three light support structures including the lampholder mounted on top of the 2-inch tubing. A cable was run from the lamp into the foundation support structure at the base of the structure to simulate an actual airport installation.

5.3 Test Equipment Description

The equipment used to conduct the impact tests may be divided into three groups; the impactor, the test facility (catapult/ modified carriage), and the instrumentation.

5.3.1 Impactor

The impactor is an all aluminum aerodynamically stable

structure designed so that aerodynamic forces will not be introduced into the test results. Although typical aircraft wing construction is used to simulate the interaction between the structures under test and an aircraft, the impactor is sturdy enough to provide for repeated testing under normal conditions. The heavy impactor head is made from a 1/2" wall, 10" diameter pipe. The head is faired with 1/8" aluminum sheet, assembled with high strength aircraft rivets and reinforced with typical aircraft construction to simulate an aircraft wign section, see Figure 5-1. Covers in the top of the "wing" provide access to the batteries and the electronic instrumentation. The original weight of the impactor was 305 lbs., and after repairs, the weight was 325 lbs.

5.3.2 Test Facility

Impact tests were conducted at the NASA Langley Research Center in Hampton, Virginia. An overview of the catapult site where the tests were run is given in Figure 5-2, which is not to scale.

The test vehicle was the large test carriage which weighs approximately 120,000 lbs. The test track is approximately 2200 feet long. The test carriage is accelerated in the first 300 or 400 feet, coasts for approximately 1000 feet and then is arrested in approximately 600 or 700 feet at the end of the track.

5.3.2.1 Carriage Modifications

After careful study and analysis, ASE modified the test carriage by adding an impactor support structure. This addition was planned so as to minimize the effects upon the carriage performance, both from a structural integrity viewpoint and from a velocity viewpoint. See Appendix C. The support structure was mounted in such a way that at completion of all the tests, the entire support structure assembly may be removed and the carriage returned to its original condition. The support structure extends outboard of the carriage and supports the impactor. See Figure 5-3.

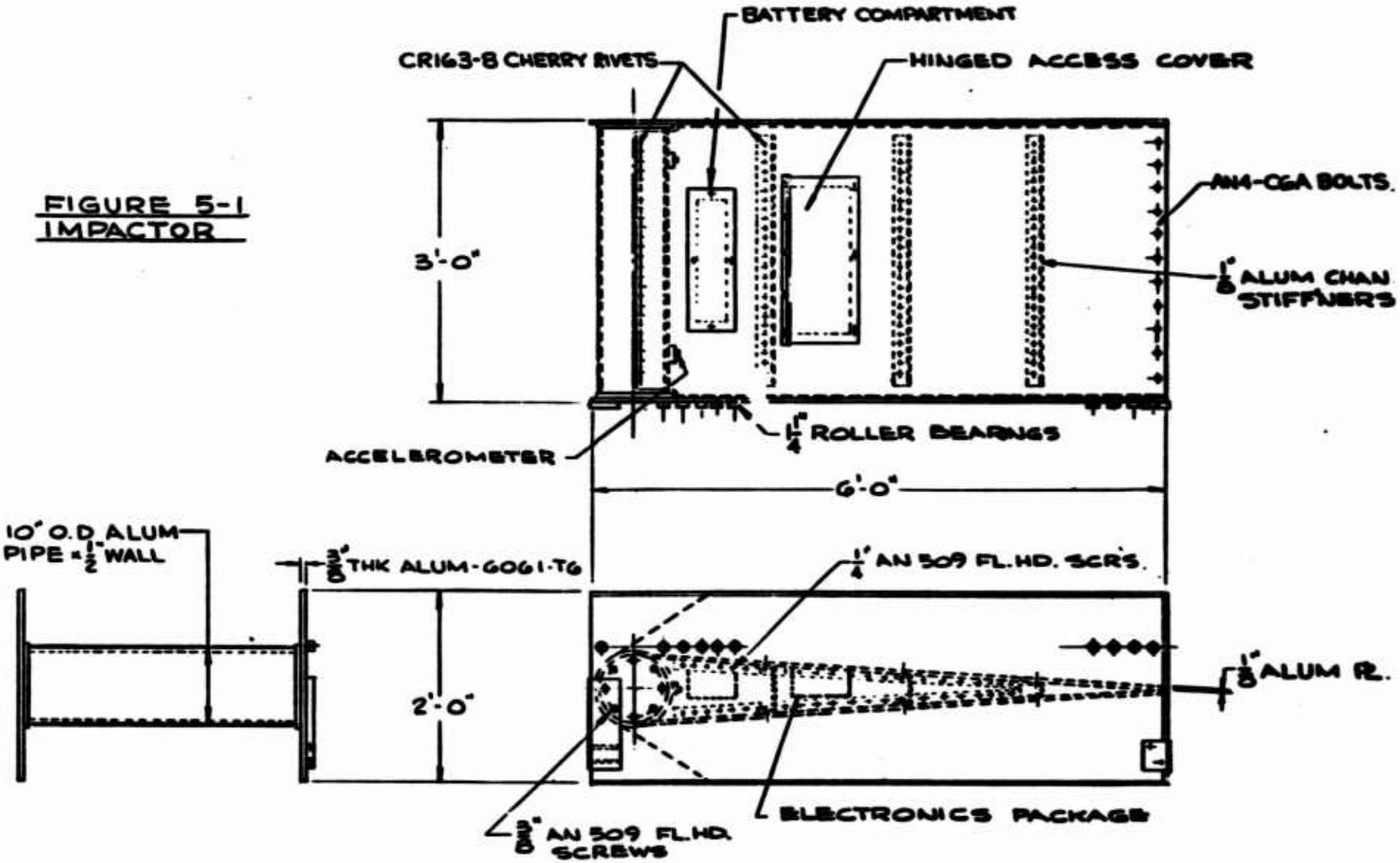

FIGURE 5-1
IMPACTOR

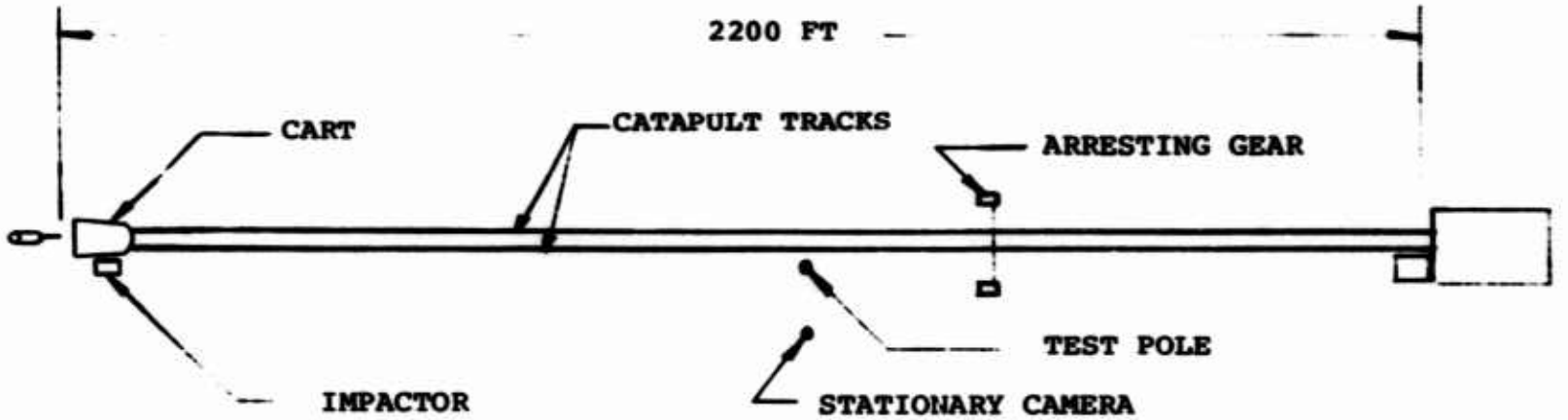

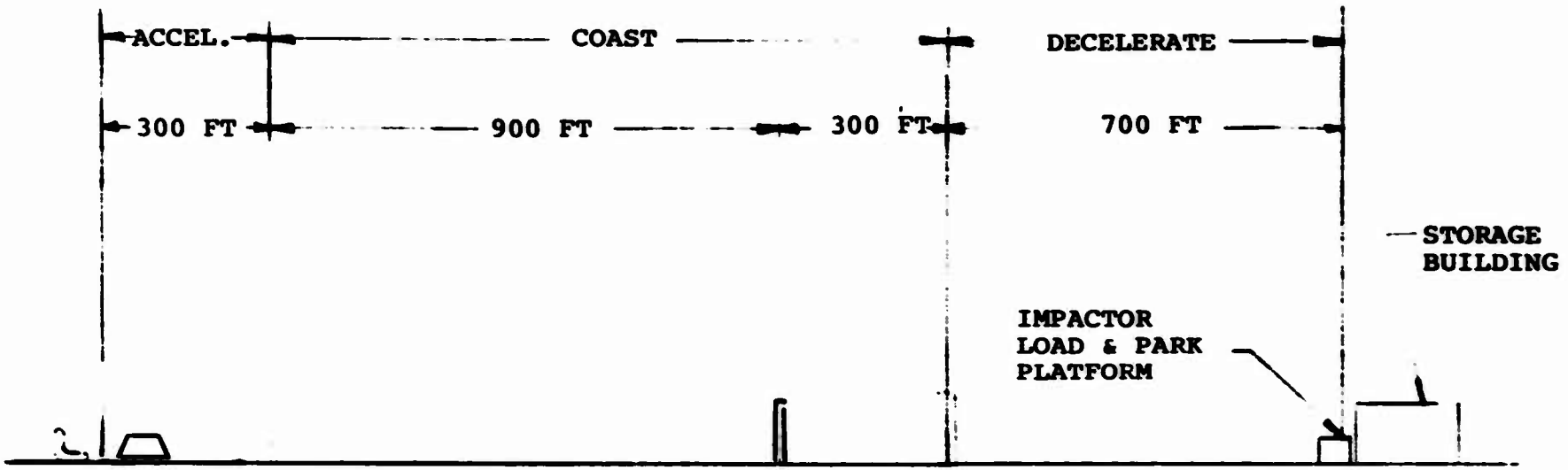

Figure 5-2 Test Facility at NASA Langley Research Center

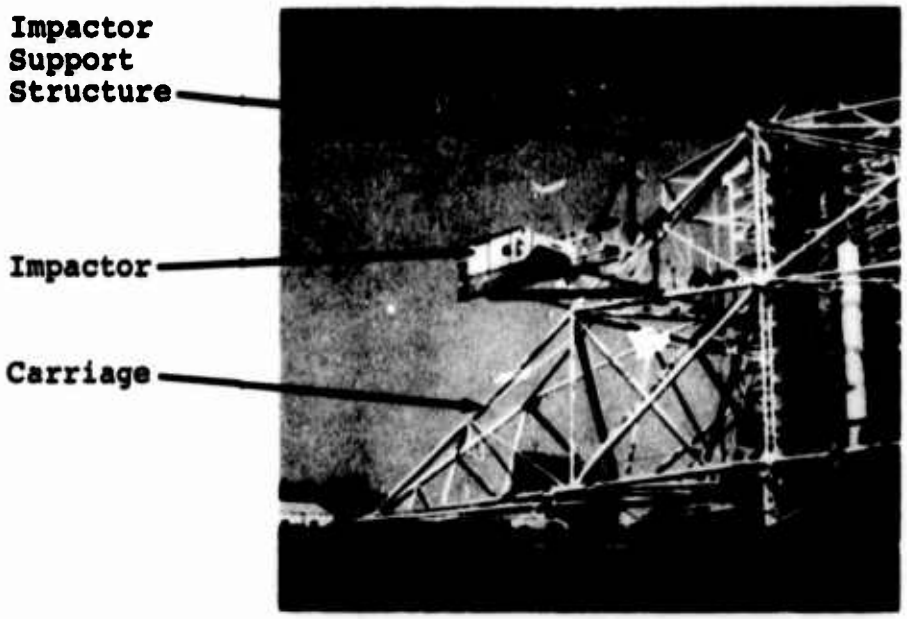

Figure 5-3 Impactor and Support Structure Mounted on Carriage

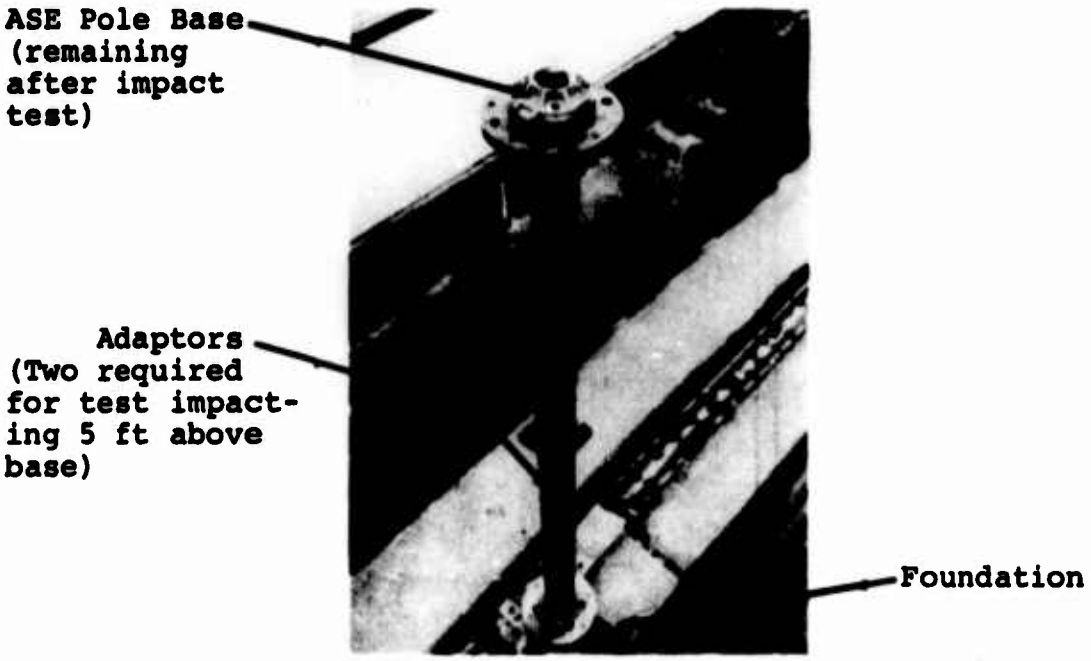

Figure 5-4 Foundation Set-up with Two Adaptors (After Impact TEst 5 Feet Above Base)

5.3.2.2 Test Structure Foundation

A steel foundation structure was designed, built, and anchored into the concrete foundation outboard of the catapult. The lamp support structures mount directly to this foundation structure and are thus located on the center line of the impactor. When mounted to this foundation structure, the lamp support structures will be struck by the impactor fifteen feet above the base of the pole. Special adaptors were designed and built which mount to the basic foundation support. These elevate the lamp support structures so that they can be struck by the impactor ten feet above the base or five feet above the base. Figure 5-4 shows two adaptors set up on the foundation for an impact test at 5 feet above the base.

To protect the impactor and the NASA carriage, should unexpectedly high forces be encountered during the impact tests, the test poles were mounted on the foundation base plate with fuse bolts. The fuse bolts consisted of a 3/4 - 10 Threaded rod with a 1/2 inch wide flat milled across the threads perpendicular to the centerline of the rod. See Figure 5-5. A hole was drilled through the flat to weaken the rod so that it would fail at a predetermined load. The hole in the fuse bolt was sized so it would fail at a load equivalent to 2 times the ultimate design wind load of the pole being tested. Table 5-1 indicates the hole size used for the different designs of light support structures.

Table 5-1 Fuse Bolt Safety Hole

Type of Light Support Structure	Dia. of Hole (inches)
ASE	25/64 (.391)
Belgian	23/64 (.359)
Canadian	25/64 (.391)

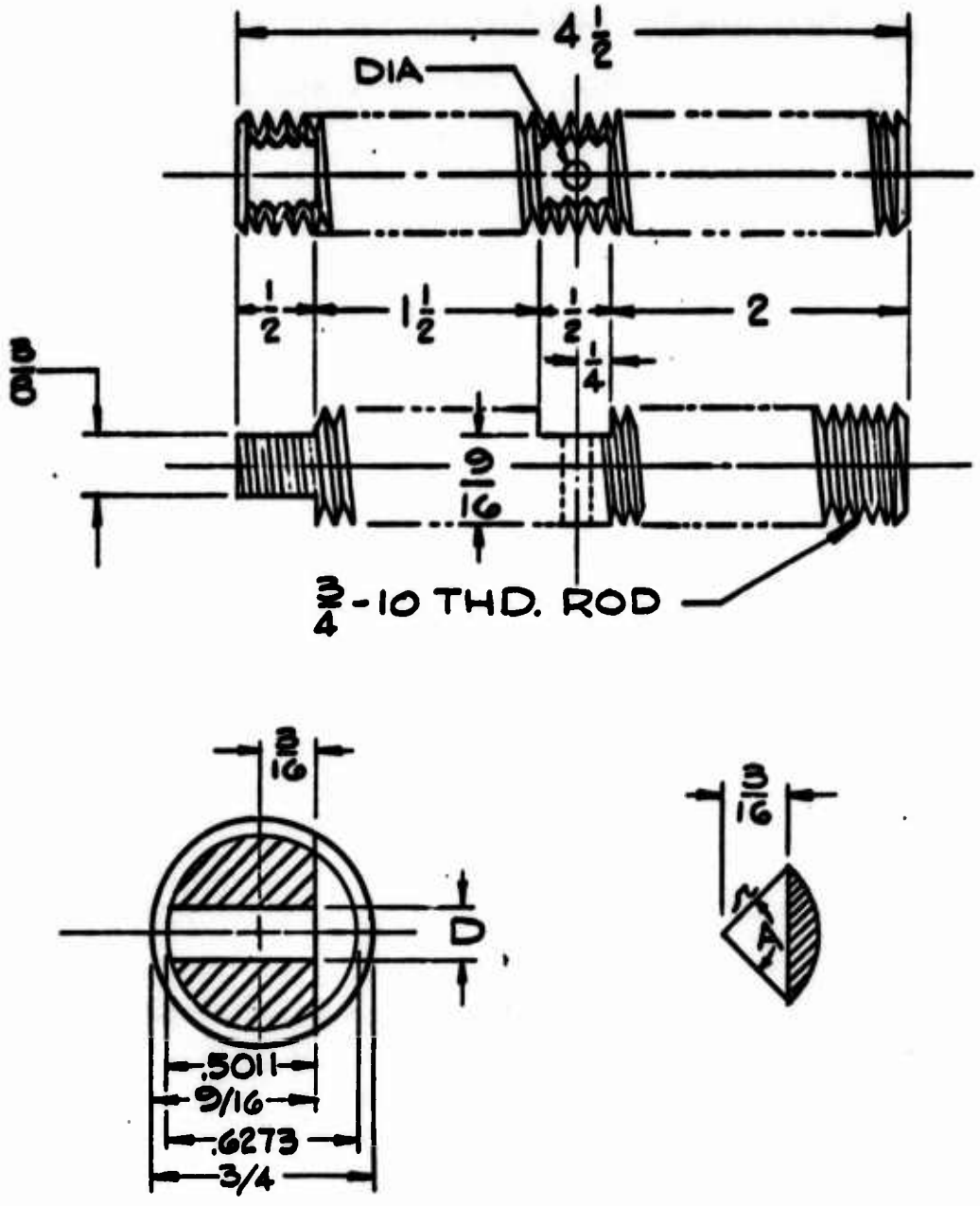

Note: All dimensions in inches.

Figure 5-5 Foundation Fuse Bolt

5.3.3 Instrumentation

Both optical and electronic instrumentation were used to obtain impact test data.

5.3.3.1 Optical Instrumentation

Two NASA high speed cameras were used with each of the impact tests conducted at Langley Field. One at 400 frames per second was placed on the ground opposite the impact site, as shown on Figure 5-2. The second, at 400 frames per second, was attached to the carriage on the support of the forward wheel and took continuous pictures of the vicinity of the impactor. A third high speed camera, placed on the ground, operated at 4000 frames per second, but after initial tests was not used because the 400 frames-per-second camera was considered to be adequate. Data reduction of the film record provided by these cameras is accomplished by using a special analytical projector, which allows timing and examination of each frame on an individual basis.

5.3.3.2 Electronic Instrumentation

Two channels were provided for obtaining data utilizing electronics. The primary channel system block diagram is shown in Figure 5-6. The secondary channel was provided for back-up purposes. Up to the integrator output, both channels use paralleled identical equipment. Each consists of a piezoelectric transducer selected as the accelerometer, because of excellent high frequency response, which is needed to obtain significant information from the first millisecond onward. The low pass filter, designed and provided by ASE, attenuates the higher harmonics and high frequency vibration or ringing of the impactor members excited by impact, and passes the signal with no appreciable loss. The preamp part of the accelerometer package amplifies the accelerometer output to usable levels of voltage and impedance. This signal, proportional to acceleration, is integrated by the integrator to yield velocity which,

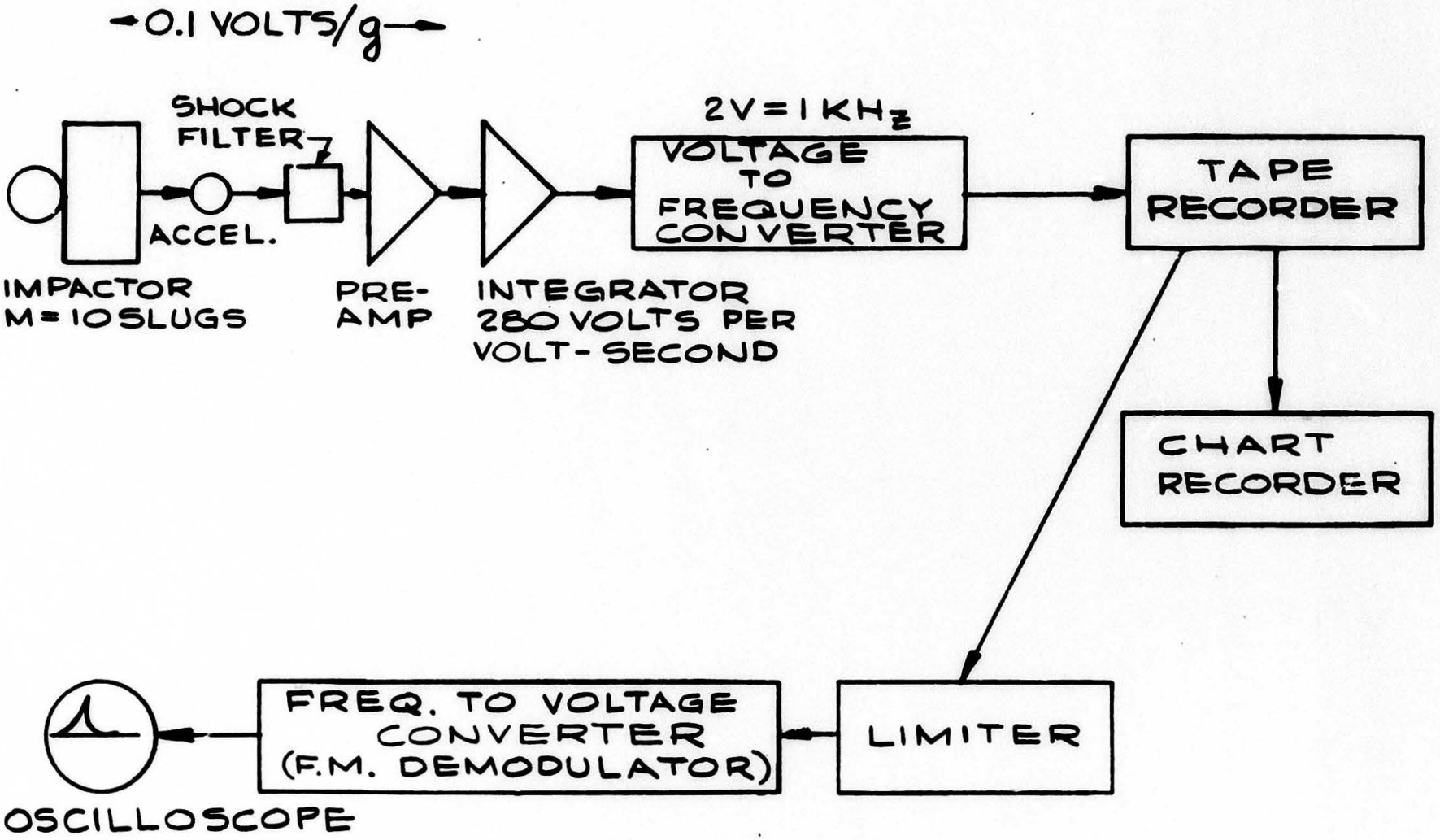

Figure 5-6 Primary Channel System Block Diagram

together with impact mass, gives a measure of energy, $(\frac{mv^2}{2})$.

At this point, both channels diverge. The primary channel uses a voltage-to-frequency converter and tape recorder to record the integrator output. Data reduction is accomplished by reversing the process and transmitting the converted signal as a voltage to an oscilloscope.

A second method of data reduction is to use the tape recorder output as input to a chart recorder with a 5 KHz frequency response.

The back-up channel used a different method to store the output voltage from the integrator. A sample-and-hold circuit digitizes the voltage, stores it digitally, and reads it out on demand through a digital-to-analog converter. This channel is protected from noise and other signals occurring outside the time slot of interest by a field-effect transistor (FET) gate. This gate is held open by a timing circuit for 30 milliseconds after arrival of the impact signal.

5.3.3.2.1 Power Supply

To satisfy the requirements of portability and constant voltage, a nickel-cadmium battery was used. Voltage regulation was not needed because of the extremely flat discharge characteristics of this type of battery. Also, the low impedance prevents any instabilities due to power supply coupling. The battery consists of 30 cells, each 1.2V, connected in series to give voltage of -12V, +12V, and +24V by appropriate taps. Load balancing resistors are added across the lightly loaded sections so that the entire battery will discharge at the same rate. The capacity of each cell is 4 ampere-hours, which at the normal load of about 0.2 amps gives 8 hours of operation, continuous or intermittent, and in practice required recharging only once a week.

5.4 Test Results

5.4.1 Test Schedule

Table 5-2 provides a record of the impact tests. It will be noted that there are two series of runs, the first extending from September 20, 1973 to September 27, 1973 and the second occurring on October 31, 1973 and November 1, 1973. The interregnum was occupied in repairing the damage caused to the impactor and electronics by the impact with the Canadian structure, the worst of both series. To prevent further disruption, Series II of the tests concentrated on the ASE and Belgian structures as the more frangible of the three types tested.

Table 5-2 Impact Test Schedule

Series	Run No.	Date (1973)	Pole Type	Cable Type	Impact Height (ft.)[3]	Impact Velocity (knots)
I	1	9-20	ASE	STD[1]	10	104
	2	9-21	Belgian		10	103
	3	9-25	ASE		10	53
	4	9-25	ASE		15	103
	5	9-26	ASE		15	53
	6	9-26	ASE		5	103
	7	9-27	Canadian		10	86
II	8	10-31	ASE	NONE	10	52
	9	11-1	ASE	Thin[2]	10	72
	10	11-1	Belgian	NONE	10	71
	11	11-1	Belgian	Thin	10	73

[1]Standard cable was a 2/C #10 Type SO cable.

[2]Thin cable was two single conductor #12 Type THHN or THWN cables.

[3]Height above the base of the pole.

5.4.2 Test Results

5.4.2.1 Electronic Test Data

The data resulting from the reduction of the electronic data output is given in Table 5-3. Where data is available from the back-up channel (#2), then the value given is the average of Channel #1 and Channel #2. The method of reducing the data is contained in Appendix F.

Table 5-3 Reduced Electronic Test Data

Run	Pole	Impact		Energy Inch Pounds	Remarks
		HT(FT	VEL(KTS)		
1	ASE I-1	10	104	48,000	Noisy Tape
3	ASE I-2	10	53	No Data	Tape Rec. Malfunction
4	ASE I-3	15	103	56,000	Std. Cable
5	ASE I-4	15	53	30,000	Std. Cable
6	ASE I-5	5	103	46,000	Std. Cable
2	Belgian I-I	10	103	200,000+[a]	Std. Cable
7	Canadian I-I	10	86	270,000+[a]	Std. Cable
8	ASE II-1	10	52	32,600	No Cable
9	ASE II-2	10	72	58.600	Thin Cable
10	Belgian II-I	10	71	189,500+[a]	No Cable
11	Belgian II-2	10	73	142,500+[a]	Thin Cable

[a] These values do not include the value of the vertical component of the energy extracted from the impactor, and are low by these indeterminate amounts.

5.4.2.2 Photographic Data

Photographs of interest obtained by the movie cameras and still cameras are reproduced below. The fracture phenomena recorded in these photographs provide significant qualitative and quantitative data.

5.4.2.2.1 Fracture Characteristics

When impacted, the ASE breakaway pole exhibited failure characteristics similar to those of a brittle structure - sections coming apart abruptly with little twisting, tearing, stretching or other ductile action to absorb energy. Figure 5-7 shows sections of an ASE pole immediately after impact. Three of the four sections in the air fell close to the base, indicating low energy transfer. Figure 5-8 shows components of the ASE pole after an impact test. The frangibility of the structure is illustrated by the separation of all sections by an impact in the center of the structure.

The structural differences between the Belgian and Canadian structures is shown in Figure 5-9. The Belgian structure is toward the left. It will be observed that the main difference between the two is that the Belgian structure has only horizontal members tying the legs together while the Canadian structure has diagonal shear members in addition to horizontal members. It would be expected and is a fact that the Canadian structure would act as a unit to a higher stress level than the Belgian structure, and would therefore be stronger, or, put another way, less frangible.

Both structures exhibited failure characteristics similar to each other when impacted at a height of 10 feet and at approximately 100 knots. On impact, the top of these

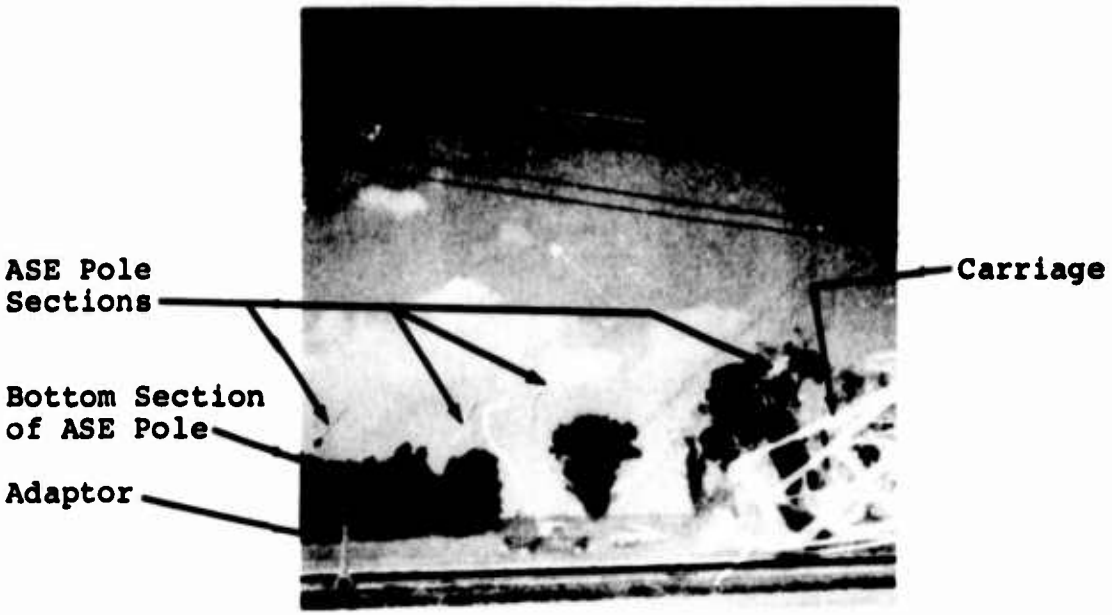

Figure 5-7 ASE Pole Immediately After Impact
(Impact Point- 10 Feet Above Base)

Figure 5-8 ASE POle After Impact

Figure 5-9 Belgian and Canadian Light Support Structures

structures whipped backward and slammed into the upper surface of the impactor. As the impactor continued to move forward, the top of the structures dragged across the top and nose of the impactor. The lower structure sections inclined forward with the impactor until tensile failure occurred. The effect on the impactor was an additional force with a horizontal component toward the rear and a vertical component downward toward the ground. This force operated until the tensile failure occurred, by tearing of the legs or by ripping the structure from the base and/or the foundation. Figure 5-10 illustrates this action.

A portion of the energy absorbed from the impactor by the Belgian structure, was transferred to a portion of the Belgian pole as kinetic energy. This was displayed by the propelling of the section in front of the impactor. An analysis, see Appendix G, indicates that the level of the combined translational and rotational energy is approximately 26,000 in. lbs., or 13% of the total energy absorbed.

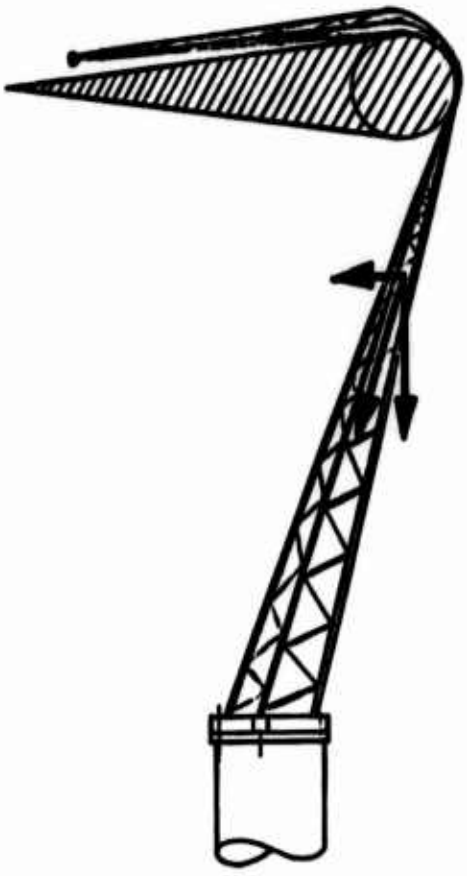

Figure 5-10 Forces Acting on Impactor During Impact With a Truss Structure

The difference between the Canadian and Belgian structures was that the Canadian structure maintained its structural integrity and acted essentially as a unit throughout the impact event. See Figure 5-11. This caused the energy absorbed from the impactor to peak at a higher value than from the Belgian structure. When the Belgian structure was impacted, a number of the horizontal members broke away and the legs of the structure acted subsequently as individual members breaking individually. Figure 5-12 shows a Belgian structure after impact. Two of the legs ruptured approximately in the center, while the third leg tore at the base and snapped into the bottom of the impactor. This leg wrapped around the impactor, rode with it until the end of the run.

Figure 5-11 Canadian Structure After Impact

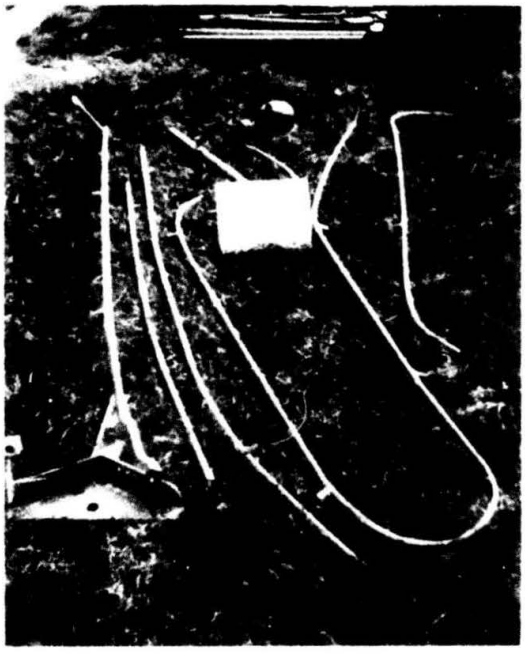

Figure 5-12 Belgian Structure After Impact

Figures 5-13A and 5-13B are photographs of another Belgian structure after impact. In this case the three legs ruptured in the vicinity of the impactor nose, and the top section rode with the impactor until the end of the run.

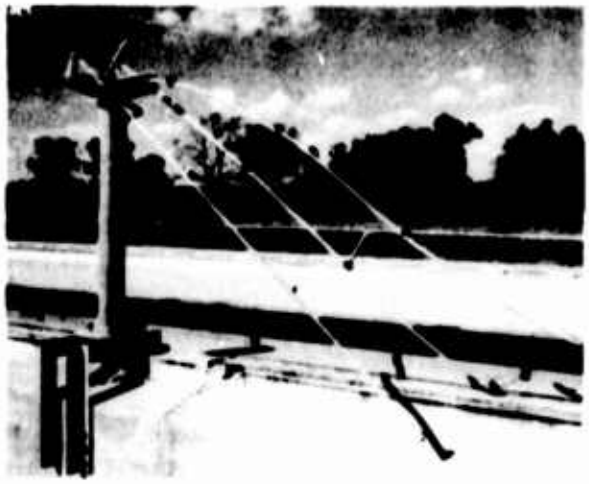

Figure 5-13A Another Belgian Structure After Impact

Figure 5-13B Same Belgian Structure After Impact

5.4.2.2.2 Impact Sequences

Figure 5-14 shows front views of typical impact sequences for the ASE, Belgian, and Canadian light support structures printed from the high speed motion pictures taken by the on-carriage camera. With the camera running at a nominal 400 frames per second, each frame is nominally 2.5 milliseconds (ms) apart. Figure 5-14 compares the impact events for the first 15 ms at 2.5 ms intervals, the next 85 ms at 10 ms intervals, and the next 100 ms at 25 ms intervals. Succeeding frames of interest are given with the appropriate times from moment of impact. The insets in the upper right hand corner of Figure 5-14 serve to identify the relationship of the impactor, carriage, test structures, on-carriage camera and the direction of travel of the impactor with respect to the test structure.

The fracture characteristics discussed in Section 5.4.2.2.1 are visible in these sequences. Of particular interest are the time taken for complete structural fracture and type of structural failure. See Section 7 for a discussion of these characteristics. Analysis of the motion pictures of all runs gives the following ranges of complete structural fracture times in milliseconds, exclusive of tearing of electric cable for all tests.

	Range	Average Value
ASE Pole	5-30	12.7
Belgian Structure	50-80	60.0
Canadian (1 test)	80	80.0

5.5 Data Evaluation

In this section, the data obtained both by the electronic instrumentation and the high speed cameras is examined from both the standpoint of possible errors and the effect of such errors upon final data and conclusions.

5.5.1 Electronic Data

Examination of the tape recorder records indicates that there was very likely an error in the data due to shock

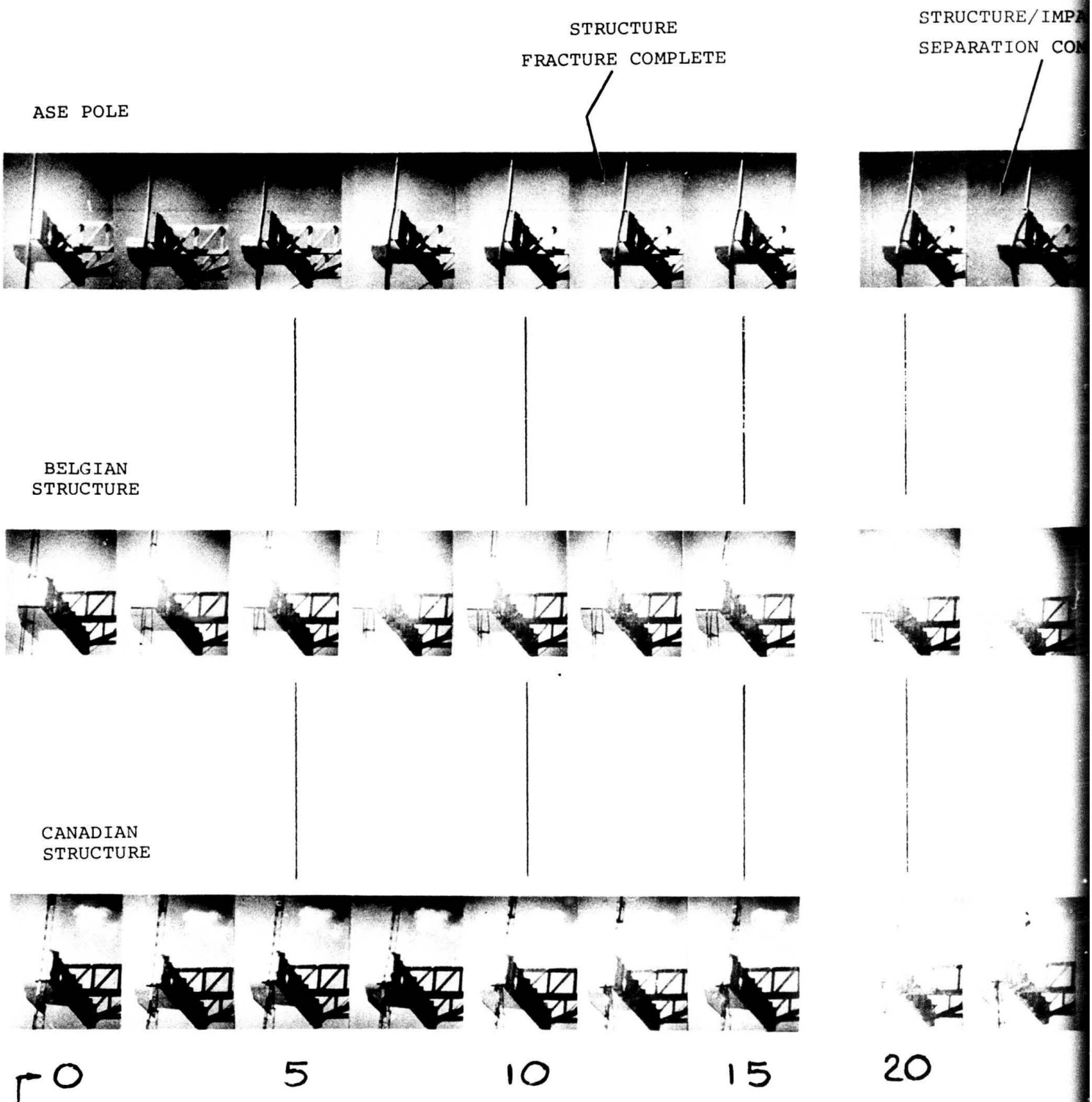

Figure 5-14 Impact Test Sequences - Three Different L

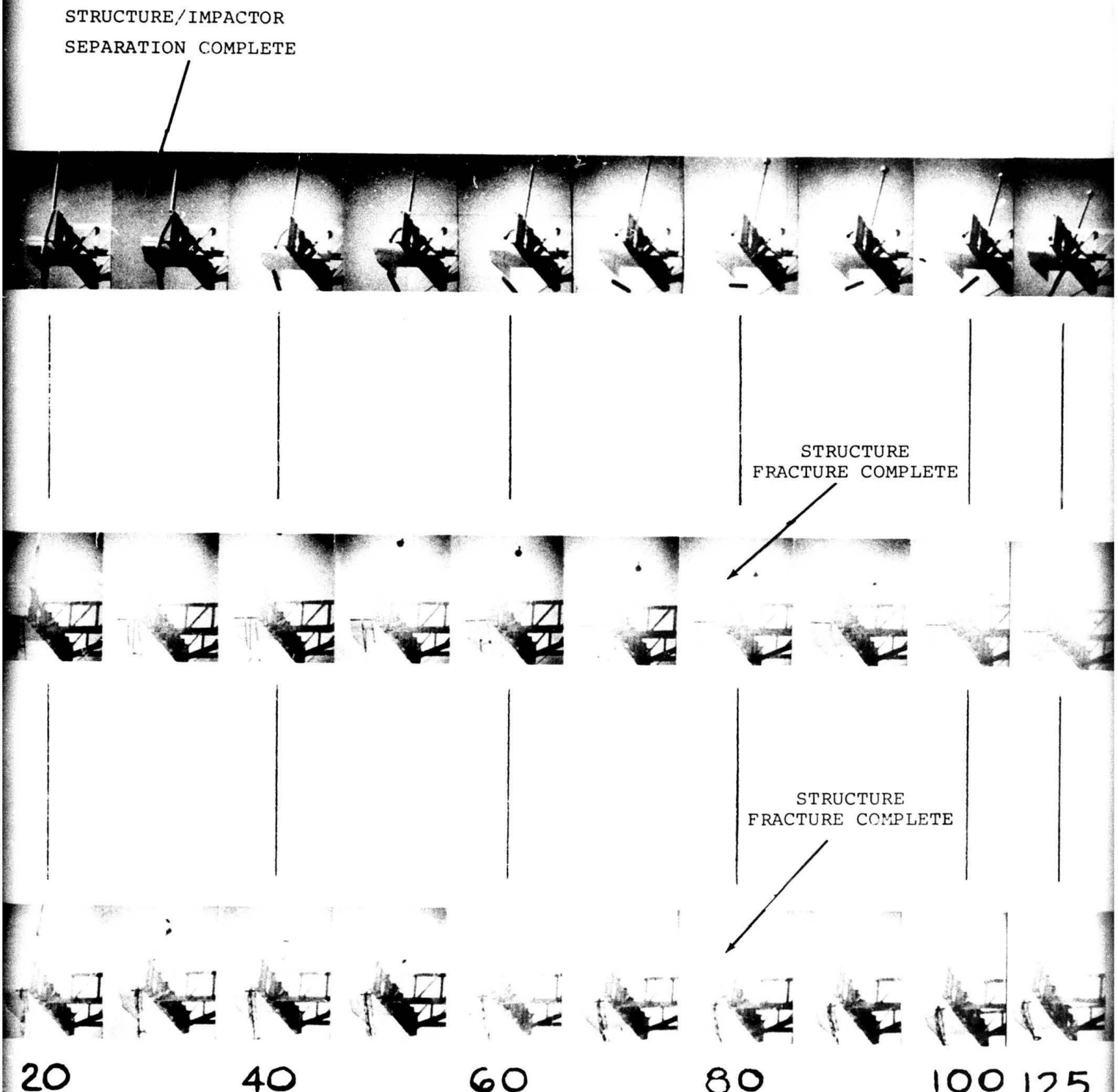

Three Different Light Support Structures

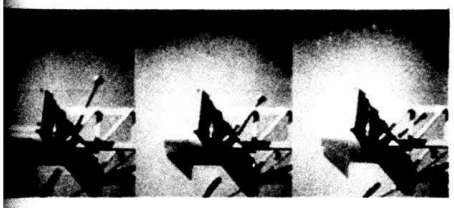

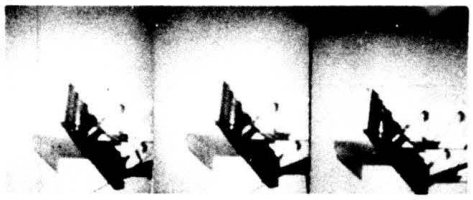

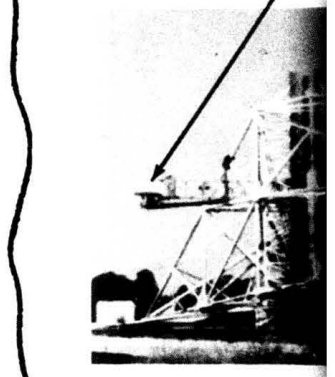

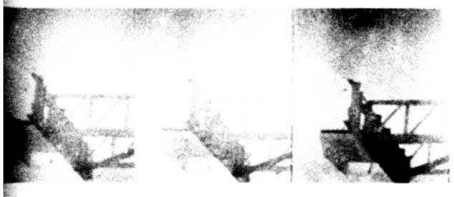

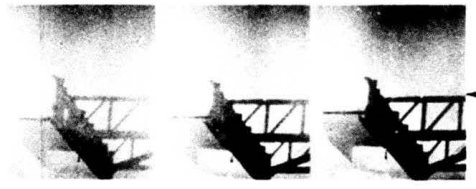

STRUCTURE/IMPACTOR
DO NOT SEPARATE

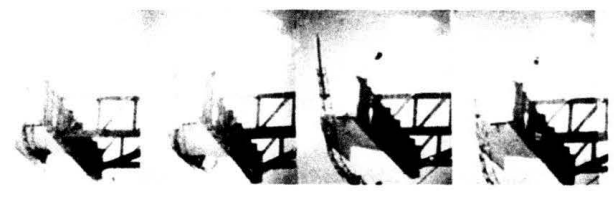

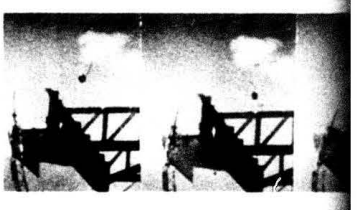

150 175 200 300 500 700 9

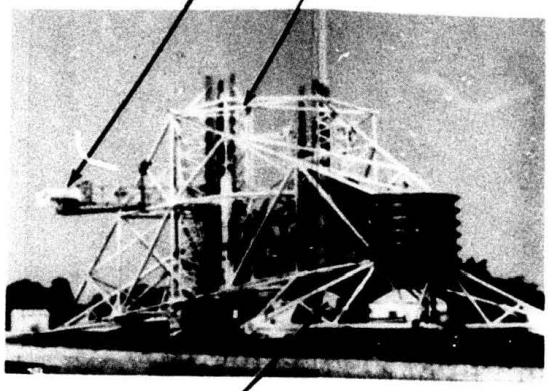

STRUCTURE/IMPACTOR
DO NOT SEPARATE

STRUCTURE/IMPACTOR
SEPARATION COMPLETE

excitation of the accelerometers by both impact and subsequent vibration. This effect would be more severe in the case of ASE poles because of the sudden impact and the short duration of the episode. In the case of Belgian poles, the force was applied more gradually over a much longer time, with less likelihood of shock excitation. However, as the record shows, vibration response was still quite large.

This shock susceptibility probably indicates that the readings are not as accurate as had been expected, with the error on the high side, and worst in the case of ASE poles. However, comparison with photographic records shows that the data is approximately correct. For example, it is calculated that 150,000 in. lbs. is required to bottom the springs, and the measured data for Belgian and Canadian poles is in the 150,000+ region. The same photographic records show relatively small deflection due to ASE impacts, and calculation indicates the energy should be in the 20,000 to 40,000 in. lb. region. Most of the measured data indicates considerably higher energies than this, leading to the suspicion that they are in error due to shock excitation.

5.5.2 High Speed Camera Data

The NASA high speed cameras discussed in Section 5.3.3.1 are driven by induction motors. As the speed of such motors is a function of their load, which in the case of a movie camera consists mainly of the friction, temperature and condition of the mechanisms, it is obvious that the accuracy of the camera speed is not well controlled. An additional factor to be considered is the time available for acceleration of the camera when the film of interest is exposed.

The fixed (broadside) camera was therefore calibrated by timing the velocities of known positions of the carriage past a reference point. The camera speed ranged from -6% to +9%. The maximum error in the data presented in Section 5.4.2.2.2 lies in the same range. The actual errors are

probably smaller, as the values from the on-carriage camera and the fixed camera were averaged. Insofar as relative values are concerned, since identical cameras were used and the conditions under which the cameras recorded the impact tests were very similar, the relative data is considered valid with an expected error of 6.5%. This data may therefore be used with confidence for comparing the performance of the different types of poles.

Section 6

NAFEC Runway 13 ALS Conversion from CAT I To CAT II

6.1 Installation Criteria

The original contract objectives of the R/W 13 conversion were to

(a) Update the ALS from CAT I to CAT II rating

(b) Install frangible light support structures that would be electromagnetically compatible with the ILS Localizer Antenna located within the ALS.

The original contract requirement was to convert the ALS as part of the Phase II effort after the frangible poles were developed and to install the frangible poles at all locations where the lamp height would be over 6 feet. However, because of other NAFEC commitments, the schedule for the R/W 13 conversion to CAT II was advanced ahead of the frangible pole development. Concurrently, it was decided to locate the ILS Localizer Antenna between Stations 8 and 9. Therefore, the conversion requirements were changed to:

(a) Modify the inner 900 feet of the ALS to result in a CAT II system

(b) Install light support structures that would be electromagnetically compatible with the ILS Localizer Antenna but would not necessarily be frangible.

6.2 R/W 13 Demolition

Prior to the start of new construction, the old center bars

were removed from Stations 1 through 9 including electrical components, support structures and foundations. Salvageable material was removed and stored for future use. Underground cable was cut off below ground. Demolition was performed in accordance with ASE Drawing 72003. Demolition started on 5 October 1972 and finished 3 November 1972.

6.3 Construction and Installation

The new construction and installation of the ALS is described in the following drawings:

2D027	-	ALS - R/W 13 Installation Details
2E029	-	ALS - CAT II ALS Installation
2D030	-	R/W 13 Wiring Diagram
2E031	-	R/W 13 Concrete Installation Plan
3E008	-	R/W 13 Station 1 Sidebar Extension

These drawings describe the installation of center bars and side bars at Stations 1 through 9, threshold using existing row of lamp bases, light support structures, all new wiring from the threshold to Station 9. The new wiring was interconnected with the existing wiring for Station 10 through 30 to achieve a balanced 3 loop system. Each lamp was installed on a single vertical member to be compatible with the horizontally polarized ILS Localizer Antenna.

The installation was started on 25 January 1973, the mechanical and electrical installation was completed on 11 April 1973. Grading and seeding was completed 14 May 1973.

SECTION 7

Conclusions and Recommendations

7.1 Conclusions

Phase I of Contract DOT-FA72WA-3043 is completed with the submission and approval of this Final Report.

Runway 13 at NAFEC has been successfully converted from a Cat I to a Cat II System per the contract requirements.

A frangible pole - the ASE Breakaway Pole - has been designed, developed, and tested. Analyses and tests have shown the pole to satisfy the survival and operational criteria specified in the contract. Superior electromagnetic compatibility with the ILS system is shown and discussed in Volume II of the Final Report.

7.1.1 Frangibility

The goal of this contract is to develop a light support structure that will extract the minimum amount of energy from an aircraft if accidentally struck by that aircraft and to thus minimize the damage to the aircraft and passengers. If extracted energy is used as a figure of merit, then this should be correlated with the velocity at which the structure is struck.

Another figure of merit which could be used is the time to fracture the support structure. As the impulse is $\int F dt$, it follows that the shorter that Δt can be made, then for equal force functions, the impulse and thus the energy will be decreased. If the force function is also decreased, then obviously the energy extracted will be minimized. Of course, even though the structure is

fractured, the fragments will continue to exert force on the aircraft (and extract energy) as long as the fragments are in contact with the impactor. This value is almost impossible to predict for any fragment, as its translational and rotational inertias, location of the center of gravity, and velocity at which struck are factors in the evaluation. The time for complete fracture of the structure alone is therefore a more amenable figure of merit.

The Canadian Light Support Structure in its initial test caused disabling damage to the impactor and the electronic instrumentation which required repairs. Since the Belgian structure was not as disabling in its effect, and more frangible, it was decided to limit further comparison to the ASE and Belgian structures. It should be noted, however, that the Belgian truss structure also damaged the impactor as it slammed down and attempted to wrap around the impactor. The top and bottom surfaces of the impactor were permanently distorted, and numerous high strength air-draft rivets were popped. The wrap around effect of both truss structures is considered undesirable because of the possible damage to the trailing edge of an aircraft wing and the control surfaces located there.

The pole developed under this contract exhibits frangibility in impact tests considerably superior to that of the Belgian light support structure. If fracture energy is used as a figure of merit, then for equal conditions and velocities, the ASE pole is superior to the Belgian structure by factors of 2.4 to 5.8. If time to fracture is the criterion, then for equivalent conditions, the ASE pole is superior by factors of 5.3 to 10.0.

Of the three designs tested, the R&D Section of the FAA selected the ASE design for installation in the ALS at Runway 31, NAFEC, that is to be installed as Phase II of this contract.

7.3 Recommendations for Future Effort

To further minimize possible damage, it is recommended that further work be done in the following areas:

a. Decrease the mass of the light fixture. The weight of a light fixture is 6-1/2 lbs. If impacted directly, it will be accelerated to the velocity at which struck. If, for example, it were struck at a velocity of 100 knots, from $KE = \frac{1}{2}mv^2$, it can be calculated that the energy absorbed will be 34,500 in. lbs., a sizeable value. Since the energy absorbed from an impacting body is a direct relationship to the mass struck, for increased safety, the mass of any structure exposed to impact should be as low as possible.

b. Reduce cable size and insulation to the greatest extent possible and provide waterproof connectors that disconnect under low forces.

APPENDIX A

DERIVATION OF EQUATIONS OF MOMENT, SLOPE AND DEFLECTION FOR A TAPERED CYLINDRICAL THIN WALL TUBE UNDER A UNIFORM LOAD

Charles W. Laible

The equations of moment, slope and deflection for a tapered cylindrical thin wall tube may be derived by reference to Figure A-1.

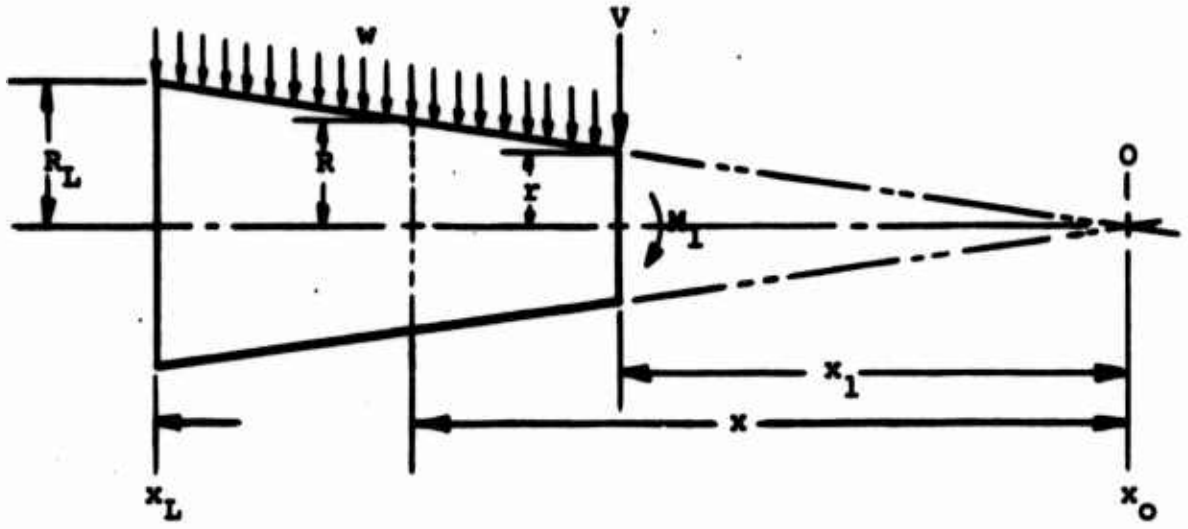

Figure A-1 Tapered Pole Parameters

This Appendix derives the equations which are used in calculating the stresses and deflection of the basic ASE pole

Notation

I = Moment of Inertia	- in^4
M = Moment	- lb in
V = Shear	- lbs
w = Uniform load	- $lbs/in^2/in$
x = Distance of a given section from origin	- in
R = Radius of a given section	- in
E = Modulus of Elasticity	- lbs/in^2
A = Slope of radii of pole = $\frac{r}{x_1}$	
y = Δ = Deflection of elastic curve of pole	- in
θ = Angle of tangent to elastic curve	- radians
t = thickness	- in

Moment of Inertia

To obtain the moment of inertia of any section (I_x) at a distance x from origin 0:

$$I_x = \pi R^3 t$$

$$R = Ax$$

$$I_x = \pi t A^3 x^3$$

Moment at any section x

To obtain the moment at any section, (M_x), at a distance x from 0:

$$M_x = M_1 + V(x - x_1) + w(x - x_1)(R + r)\left[\frac{1}{3}(x - x_1)\left(\frac{R + 2r}{R + r}\right)\right]$$

substituting $R = Ax$ and $r = Ax_1$, and simplifying,

$$M_x = M_1 + V(x-x_1) + \frac{wA}{3}(x-x_1)^2(x + 2x_1)$$

$$M_x = M_1 + V(x-x_1) + \frac{wA}{3}(x^3-3x_1^2x + 2x_1^3) \qquad \text{(A-2)}$$

Slope of Elastic Curve

The slope and deflection at the tip of the pole may be derived from the differential equation for the elastic curve:

$$EI \frac{d^2y}{dx^2} = M$$

Integrating once,

$$E \frac{dy}{dx} = \int \frac{M}{I} dx + C_1 \qquad \text{(A-3)}$$

but

$$\frac{M}{I} = \frac{1}{\pi t A^3}\left(\frac{M_1}{x^3} - \frac{Vx_1}{x^3} + \frac{V}{x^2} + \frac{wA}{3} - \frac{wAx_1^2}{x^2} + \frac{2wAx_1^3}{3x^3}\right)$$

Substituting in equation A-3, and separating variables,

$$E \frac{dy}{dx} = \frac{1}{\pi t A^3}\left[(M_1 - Vx_1 + \frac{2}{3}wAx_1^3)\int\frac{dx}{x^3} + (V - wAx_1^2)\int\frac{dx}{x^2} + \frac{wA}{3}\int dx\right] + C_1$$

let $B = (M_1 - Vx_1 + \frac{2}{3} wAx_1^3)$

$D = (V - wAx_1^2)$

Then $\pi t A^3 E \frac{dy}{dx} = -\frac{B}{2x^2} - \frac{D}{x} + \frac{wA}{3} x + C_1$

When $x = x_L$, $\frac{dy}{dx} = 0$

$C_1 = (\frac{B}{2x_L^2} + \frac{D}{x_L} - \frac{wAx_L}{3})$, and

$$\pi t A^3 E \frac{dy}{dx} = \frac{B}{2}\left(\frac{1}{x_L^2} - \frac{1}{x^2}\right) + D\left(\frac{1}{x_L} - \frac{1}{x}\right) + \frac{wA}{3}(x - x_L) \qquad \text{(A-4)}$$

Substituting for B and D, the slope of the elastic curve

$\frac{dy}{dx} = \theta_x$, may be found from

$$\pi t A^3 E \frac{dy}{dx} = \frac{1}{2}(M_1 - Vx_1 + \frac{2}{3} wAx_1^3)\left(\frac{1}{x_L^2} - \frac{1}{x^2}\right) + (V - wAx_1^2)\left(\frac{1}{x_L} - \frac{1}{x}\right) + \frac{wA}{3}(x - x_L) \qquad \text{(A-5)}$$

Deflection of Elastic Curve

The deflection of the elastic curve $y = \Delta$, may be found by integrating equation A-5:

$$\pi t A^3 E y = \frac{B}{2}\int\left(\frac{1}{x_L^2} - \frac{1}{x^2}\right) dx + D\int\left(\frac{1}{x_L} - \frac{1}{x}\right) dx + \frac{wA}{3}\int (x - x_L)\, dx$$

$$\pi t A^3 E y = \frac{B}{2}\left(\frac{x}{x_L^2} + \frac{1}{x}\right) + D\left(\frac{x}{x_L} - \ln x\right) + \frac{wA}{3}\left(\frac{x^2}{2} - x_L x\right) + C_2$$

when $x = x_L$, $y = 0$

$$C_2 = -\frac{B}{2}\left(\frac{1}{x_L} + \frac{1}{x_L}\right) - D\left(\frac{x_L}{x_L} - \ln x_L\right) - \frac{wA}{3}\left(\frac{x_L^2}{2} - x_L^2\right)$$

$$= -\frac{B}{2}\left(\frac{2}{x_L}\right) - D(1 - \ln x_L) - \frac{wA}{6}(x_L)^2$$

$$\pi t A^3 E y = \frac{B}{2}\left(\frac{x}{x_L^2} + \frac{1}{x} - \frac{2}{x_L}\right) + D\left(\frac{x}{x_L} \ln x - 1 + \ln x_L\right)$$

$$+ \frac{wA}{3}\left(\frac{x^2}{2^2} - x_L x + \frac{x_L^2}{2}\right)$$

simplifying,

$$\pi t A^3 E y = \left(\frac{B}{2 x x_L^2}\right)(x - x_L)^2 + \frac{wA}{6}(x - x_L)^2 + D\left(\frac{x}{x_L} + \ln\frac{x_L}{x} - 1\right)$$

substituting for B and D,

$$\pi t A^3 E y = \left(\frac{1}{2 x x_L^2}\right)\left(M_1 - V x_1 + \frac{2}{3} wA x_1^3\right)(x - x_L)^2 + \frac{wA}{6}(x - x_L)^2$$

$$+ (V - wA x_1^2)\left(\frac{x}{x_L} + \ln\frac{x_L}{x} - 1\right) \qquad \text{(A-6)}$$

Summary

The above equations for a tapered thin wall tube are summarized below:

Moment of Inertia at any Section:

$$I_x = \pi t A^3 x^3 \qquad \text{(A-1)}$$

Moment at any Section:

$$M_x = M_1 + V(x - x_1) + \frac{wA}{3}\left[x^3 - 3x_1^2\, x + 2x_1^3\right] \qquad \text{(A-2)}$$

Slope of elastic curve:

$$\pi t A^3 E\theta_x = \left(\frac{1}{2}\right)\left(M_1 - Vx_1 + \frac{2}{3}\, wAx_1^3\right)\left(\frac{1}{x_L^2} - \frac{1}{x^2}\right)$$

$$+ \left(V - wAx_1^2\right)\left(\frac{1}{x_L} - \frac{1}{x}\right) + \frac{wA}{3}(x - x_L) \qquad \text{(A-5)}$$

Deflection of elastic curve:

$$\pi t A^3 E\Delta_x = \left(\frac{1}{2xx_L^2}\right)\left(M_1 - Vx_1 + \frac{2}{3}\, wAx_1^3\right)(x - x_L)^2 + \frac{wA}{6}\,(x - x_L)^2$$

$$+ \left(V - wAx_1^2\right)\left(\frac{x}{x_L} + \ln\frac{x_L}{x} - 1\right) \qquad \text{(A-6)}$$

APPENDIX B

ALTERNATE IMPACT TEST METHODS

John Lazarin

and

Charles W. Laible

1. Introduction

Several alternate impact test methods were considered and rejected for reasons of greater technical complexity, and/or higher costs. These methods, all satisfying the test parameters in Section 5.2.1, are:

a - An impactor towed by an airplane
b - A dropping weight
c - A Pendulum
d - Flywheel Machines
e - Other Catapults

2. Impactor Towed by an Airplane

The impactor, essentially the same as that described in Section 5.4.1, would be towed by an airplane at the end of a long cable to impact the test structures at a given height and velocity. The impactor would have servo controlled drag brakes added to provide fine control of its height. Data from the instrumentation would be recorded on an on-board recorder or telemetered to the ground. The impactor is aerodynamically smooth, hence the drag coefficient, C_d, is on the order of 0.15. The drag force on the impactor, F_I in pounds is

$$F_I = C_d \times A_I \times q \times \left(\frac{V_t}{100}\right)^2$$

Where A_I = frontal area, ft.^{2}

q = dynamic force of air at 100 mph = 25.6 psf.

V_t = test velocity, 140 mph

$$F_I = .15 \times \frac{10" \times 36"}{144"^2} \times 25.6 \text{ psf} \times \left(\frac{140}{100}\right)^2 = 18.81 \text{ pounds}$$

In this Appendix, alternate methods for conducting the dynamic impact tests are considered and evaluated.

Assume the towing cable to be 3/16" diameter, 300 feet long. For a round cable the drag coefficient, C_d, is 1.2.

The cable drag $F_c = 1.2 \times \frac{3"}{16} \times 300' \times 25.6 \times \left(\frac{140}{100}\right)^2 = 282.24$ pounds

The following analysis will determine the approximate angle θ during the towing condition:

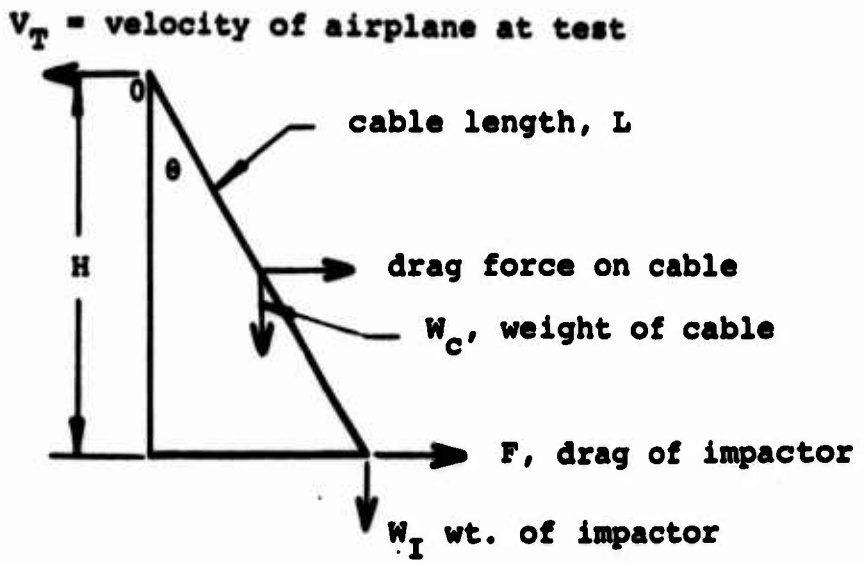

Figure B-1 Forces on Impactor Towed by Airplane

The simplified analysis assumes:

a. that the drag coefficient of the cable remains constant, independent of the angle θ, (actually it will decrease as θ increases because the slanted cable will be more streamlined)

b. that the towing cable weight is negligible compared to the magnitude of the drag forces on the cable and the weight of the impactor, and

c. that the cable between the impactor and the airplane is straight, (although it will be somewhat curved).

The cable weight W_C = .06 lbs/ft. x 300 ft. = 18 pounds

For equilibrium at 140 mph:

$$\sum F_o = 0$$

$$W_1 \times L \sin \theta = F_I \times L \cos \theta + F_c \times .5L \cos \theta$$

$$\frac{\sin \theta}{\cos \theta} = \tan \theta = \frac{F_1 + .5 F_c}{W_I} = \frac{18.81 + 141.12}{325} = .49$$

$$\theta = 26.1^{\circ}$$

The airplane height H will be about 269 feet.. A way to fine control the height of the impactor while the towing airplane flies at constant altitude, would be to vary the drag of the impactor. This can be readily accomplished by adding servo controlled drag brakes. The above equation can be modified by making the drag of the impactor, F_I, variable as follows:

$$W_I \, L \sin \theta = (F_I + \Delta F_I) \, L \cos \theta + F_c \times .5 \, L \cos \theta$$

Flat plates could be used, $C_d \approx 1.5$

For 4 plates, each with an area of 3" by 3", the drag at 140 mph will be:

$$\Delta F_I = 1.5 \times \frac{3" \times 3"}{144"^2} \times 4 \times 25.6 \text{ psf} \times \left(\frac{140}{100}\right)^2$$

ΔF_I = 18.81 pounds, for brakes fully extended.

If we set the neutral setting at 1.5" extended, then we can add or subtract as much as 9.4 pounds of drag to the impactor plus increase the drag of the impactor to (18.81 + 9.40) = 28.21 pounds.

At neutral setting the angle $\theta = 27.46^{\circ}$

and

H = 266.2 feet

The altitude adjustment allowed will be:

$$\theta = \tan^{-1} \frac{(28.21 + 141.12) \pm 9.40}{325} = 26.474^{\circ} \begin{matrix} + 1.135^{\circ} \\ - 1.176^{\circ} \end{matrix}$$

The fine adjustment will be about ± 3 feet. It may be that the better way of doing this is to have the brakes full out and have the airplane come in a little high. The fine adjustment would then be achieved by retracting the drag brakes, thereby allowing a fine adjustment of about 5.5 feet in the impactor altitude. The force in the towing cable will be about 350 pounds. A 3/16" diameter 7 x 19, stainless steel cable of aircraft quality will have a minimum breaking strength of 4,700 pounds. In addition, a weak link will be used near the top of the towing cable for purpose of assuring safety of the airplane at all times.

3. Dropping Weight

A dropping weight, see Figure B-2, of 325 to 500 pounds could be instrumented so that the velocity just before impact and the change in velocity could be measured. In this way, the change in kinetic energy could then be calculated.

The required free fall height H, in feet can be calculated as follows:

$$H = \frac{V^2}{2g}$$

Where
V is velocity in feet per second
g = 32.2 ft. per sec.^{2}

For V = 88 feet per sec. (60 mph), H = 120 feet
For V = 205 feet per sec. (140 mph), H = 650 feet

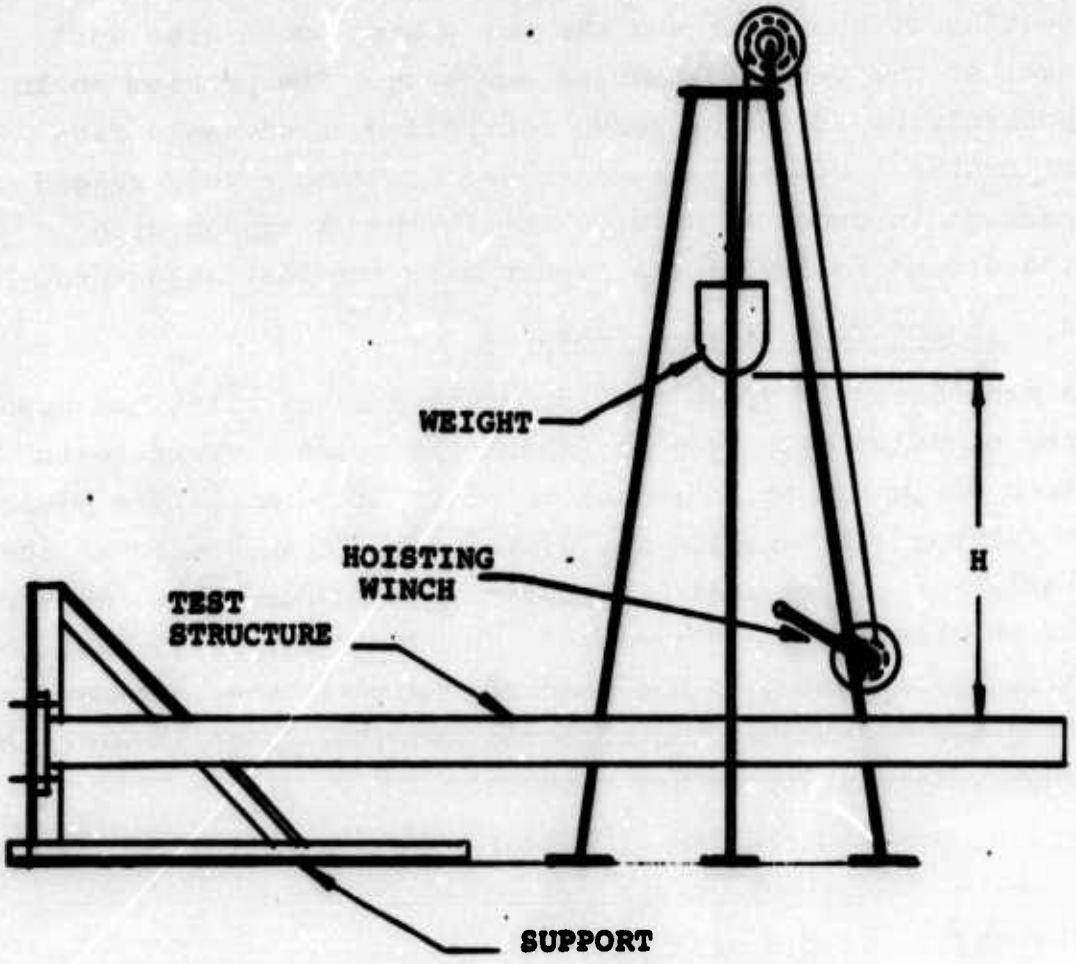

Figure B-2 Dropping Weight Impact Test

An additional height needs to be added to the nominal height to compensate for losses incurred due to wind drag, friction of guide rails, etc. The technical difficulties associated with this method become formidable when one considers the fact that even if such a tall tower or structure were available, the aiming is almost impossible. The time of fall for an object falling 650 feet is about 6.3 seconds. The least side force due to structure sway and lack of perfect aerodynamic symmetry will make the weight drift off the intended course. A tower 650 feet high would sway as much as 10 feet due to wind. Differential

heating of the tower and the guy cables would also work against the required bombing accuracy. The problem could possibly be solved by servo controlled aerodynamic fins or brakes. However, we would need to have a very rugged package in order to survive the forces at impact with the ground following the impact with the test structure.

4. Impact Test Using a Pendulum

A manufacturing group testing highway light poles has used the pendulum technique to impact the poles. Their tests were conducted at an impact velocity of 20 mph. The pivot point for the pendulum was at the top of two towers 65 feet tall. The impact mass was suspended by cables from the top of the towers, see Figure B-3. A second tower was used to lift the impactor to the required height. The instrumentation was mounted on the impactor and the change in kinetic energy during impact was measured.

The simple equation for a pendulum is:

$$V = \sqrt{2gH} \quad \text{or} \quad H = \frac{V^2}{2g}$$

V = velocity in fps

g = gravity = 32.2 ft/sec^2

H = height of pendulum fall in feet.

The impact velocity range for the airport approach light supports is 60 to 140 mph. If friction and wind drag are neglected, the pendulum height required for these speeds are:

(a) For V = 60 mph = 88 fps

$$H = \frac{(88)^2}{2x32.2} = 120 \text{ feet}$$

(b) For V = 140 mph = 205 fps

$$H = \frac{(205)^2}{2x32.2} = 550 \text{ feet}$$

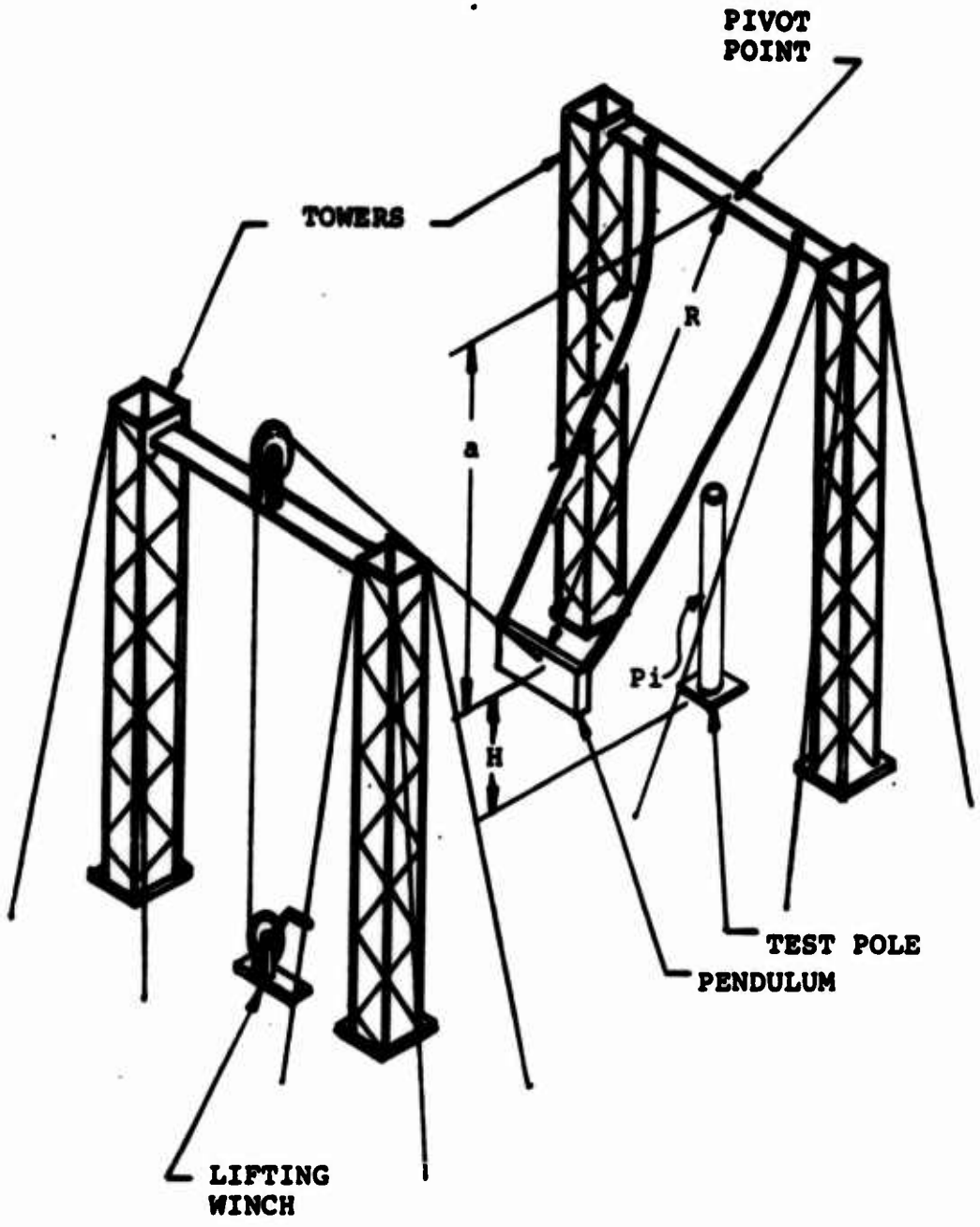

Figure B-3 Pendulum Impact Test

For the realistic condition where drag and friction are included, the height H would have to be increased to obtain the required impact velocity. As a general comparison, the highway test group used towers 65 feet tall to impact test at 20 mph. The pendulum fall, H, was:

$$V = 20 \text{ mph} = \frac{88}{3} \text{ fps}$$

$$H = \frac{(88/3)^2}{2 \times 32.2} = 13.3 \text{ feet}$$

The above calculations indicate that a scaled up structure in excess of 1,000 ft. high would be required to perform similar tests on the airport light supports, if we use the pendulum approach. As a frame of reference, a thousand foot tower would be as tall as a 100-story building. This size structure appears impractical. In addition, the accuracy of a free falling pendulum from these heights would be impaired by cross winds, imperfect aerodynamic stability of the impactor and the support cables, and the sway of the support towers. In addition, the problem of measuring the amount of impact energy transferred to the test structure becomes very difficult due to the losses in vibration of the support cables, towers, and the necessary tower guying cables.

5.0 Flywheel Machines

The requirements for flywheel machines are similar to those for pendulum machines, except that the mechanical details are different.

A machine could be built with a suitable flywheel, such that the energy of the blow is determined by the change in velocity of a rotating flywheel, before and after impact. The device could have a retractable striker arm which would be carried with the flywheel until the wheel is brought up to speed. Controls and activators would be required to release the striker arm from its stowed position to its impacting position.

Consider a required energy transfer at impact of 4,000 inch-pounds plus a suitable reserve for the case where we may test a structure that is 3 or 4 times as strong as required. Also, the flywheel should be sized so that the speed change during an impact is on the order of 10% of the flywheel operating speed. The reason for this is that we expect an impacting aircraft to continue on through the structure with essentially the same or only slightly reduced speed. The kinetic energy of a rotating wheel can be expressed with the following formula.

$$K.E. = \frac{I\omega^2}{2}$$

Where I = rotary mass moment of inertia, slug - ft^2

ω = angular velocity, radians per second

Let the flywheel striker act at a three foot radius arm, then to get a striker velocity of 140 mph (205 fps) the flywheel velocity will be $\frac{205}{3} = 68.3$ radians per second or 650 rpm.

The flywheel could be made of a high strength steel rim on a spoked hub. The rim dimensions could be 2" by 2".

$$I = \frac{\pi\rho t r^4}{2g}$$

Let $r = 3'$

$t = .167'$ (2")

$g = 32.2$ ft/sec^2

$\rho = 518$ pounds/ft^3 for steel

$I = 341$ slug ft^2

At a speed of 650 rpm, the flywheel kinetic energy,

$$K.E. = \frac{1}{2} \times 341 \times (68.3)^2 = 800{,}000 \text{ ft. lbs.}$$

which is more than adequate.

The stress in the rim would be

$$\sigma = \frac{V_R^2}{10}$$

Where V = velocity of rim, fps

σ = stress, psi

$$\sigma = \frac{(205)^2}{10} = 4200 \text{ psi}$$

The design and construction of a flywheel machine does not appear to present insurmountable technical problems. The reason for discarding this approach is that the cost for design and construction of this machine would be more than the selected method.

6.0 Other Catapults

A catapult/sled could be used to impact the light support structures. The prime mover for the catapult could be:

a. Spring (sling-shot)
b. Jet sled
c. Carrier type steam catapult

6.1 Spring Powered Catapult

To approximate the spring required to achieve a velocity of 140 mph, assume the strain energy of the spring stored in a solid mass of steel.

The strain energy, E_s, is 1/2 PΔ where

$$\Delta = \frac{PL}{AE}$$

$$\text{therefore} \quad E_s = 1/2 \times P \times \frac{PL}{AE} \times \frac{A}{A}$$

$$E_s = 1/2 \times \frac{S^2}{E} \times L \times A$$

where S = maximum stress = 60,000 psi

LxA = volume of spring

E = modulus of steel = 30×10^6 psi

P = total load, pounds

The kinetic energy imparted to the impactor is $1/2\ MV^2$ where

M = 500 lb - mass of impactor

V = 140 mph = 205 ft/sec - velocity of impactor

As a first approximation, ignore the velocity of the spring itself and assume all of the strain energy of the spring is transferred to the impactor.

$$1/2 \times \frac{s^2}{E} \times (L \times A) = 1/2\ MV^2$$

$$\text{Volume} = LxA = M \times E \times \frac{V^2}{s^2}$$

$$\text{Volume} = \frac{500}{32.2} \times 30 \times 10^6 \times \left(\frac{205}{60{,}000}\right)^2 \times \frac{12\ \text{in}}{\text{ft}} = 65{,}000\ \text{in}^3$$

$$\text{Weight} = 65{,}000 \times 0.3 = 19{,}500\ \text{lbs.}$$

For the second approximation assume that half of the spring mass is accelerated to the same velocity of the impactor. Then

$$M' = 9{,}750 + 500 = 14{,}750\ \text{lbs.}$$

and

$$\frac{M'}{M} = \frac{14{,}750}{500} = 30$$

Then the volume and weight of the required spring would also be tripled and the spring weight would be 19,500 x 3 = 60,000 lbs.

A third and fourth approximation, using one half the new weight each time, shows the weight of the spring to be 140,000 lbs, then 300,000 lbs. and still increasing.

The above analysis is presented so that one can readily conclude that the cost and complexity of this approach is prohibitive for this problem.

6.2 Jet Engine Propelled Sled

A sled being propelled by jet engines could achieve the 140 mph velocity required. Such vehicles are used for testing at the Lakehurst Naval Air Station. The disadvantages of this system are the costs involved to:

(a) fabricate the sled
(b) procure the jet engines
(c) operation of the test facility which includes the track, propulsion ignition systems, arresting gear to stop the sled and fuel.

In addition, the weight of the sled, propulsion system and propulsion system support structure would add significantly to the weight of the sled. This extra weight would complicate the measurement of the velocity change during impact because ΔV is inversely proportional to the mass of the impactor. It is calculated that for a sled mass of 500 lbs. the ΔV during impact is 1.46 in/sec. If the sled plus propulsion system weighed 1,500 lbs. the ΔV at impact would be approximately 0.5 in/sec.

6.3 Steam Powered Catapults

Steam catapults at the Lakehurst Naval Air Station can accelerate carts weighing several thousand pounds up to speeds of 140 mph. The catapult tracks are equipped with an arresting gear to capture the cart after impact. This equipment seems well suited to the test requirements of the impact test. The only apparent disadvantage is the availability of the facility, the cost of the cart and the operating cost of the facility.

The catapult at NAFEC was considered, however, the maximum speed of this machine is 80 mph which is not adequate for our requirements.

APPENDIX C

IMPACTOR SUPPORT STRUCTURE AND CARRIAGE MODIFICATIONS

John Lazarin

and

Charles W. Laible

APPENDIX C

TABLE OF CONTENTS

This Appendix provides an analysis of the forces and stresses acting on the impactor support structure and the catapult carriage at NASA Langley Research Center during an impact test. Effects on carriage performance are also evaluated.

APPENDIX C

LIST OF FIGURES

APPENDIX C

Impactor Support Structure and Carriage Modifications

1.0 Introduction

An impactor weighing about 300 lbs. is designed to impact with three different designs of light support structure for the purpose of comparing the frangibility of each of the structures under varying conditions. The impactor weight may be increased up to 500 pounds to act as a heavier unit, if necessary, by adding weights to the basic impactor. The impactor rode piggyback on the catapult test facility at NASA Langley Research Center at Hampton, Va. The impactor is supported and guided by a structure shown schematically in Figure C-1. Figure 5-3 is a photograph of the impactor mounted on the support structure and the carriage. It is desired to ascertain the forces and induced stresses which will act on the carriage and support structure, and the drag which will be added to that of the carriage. The impactor is supported by rails on Truss 3C012-1 and is centered by a spring system. In this way the impactor can move relative to the main carriage. Figure C-1 should be referred to in conjunction with the other figures that follow in this Appendix.

The expected forces applied to the carriage are primarily due to the weight of the added structure and the wind forces encountered during a test run. Although the maximum speed of the carriage is estimated as 120 knots, the analysis will be based on 150 mph relative wind on the ASE impactor support structure.

The forces have been analyzed and member stresses are included for ease in the proposed design.

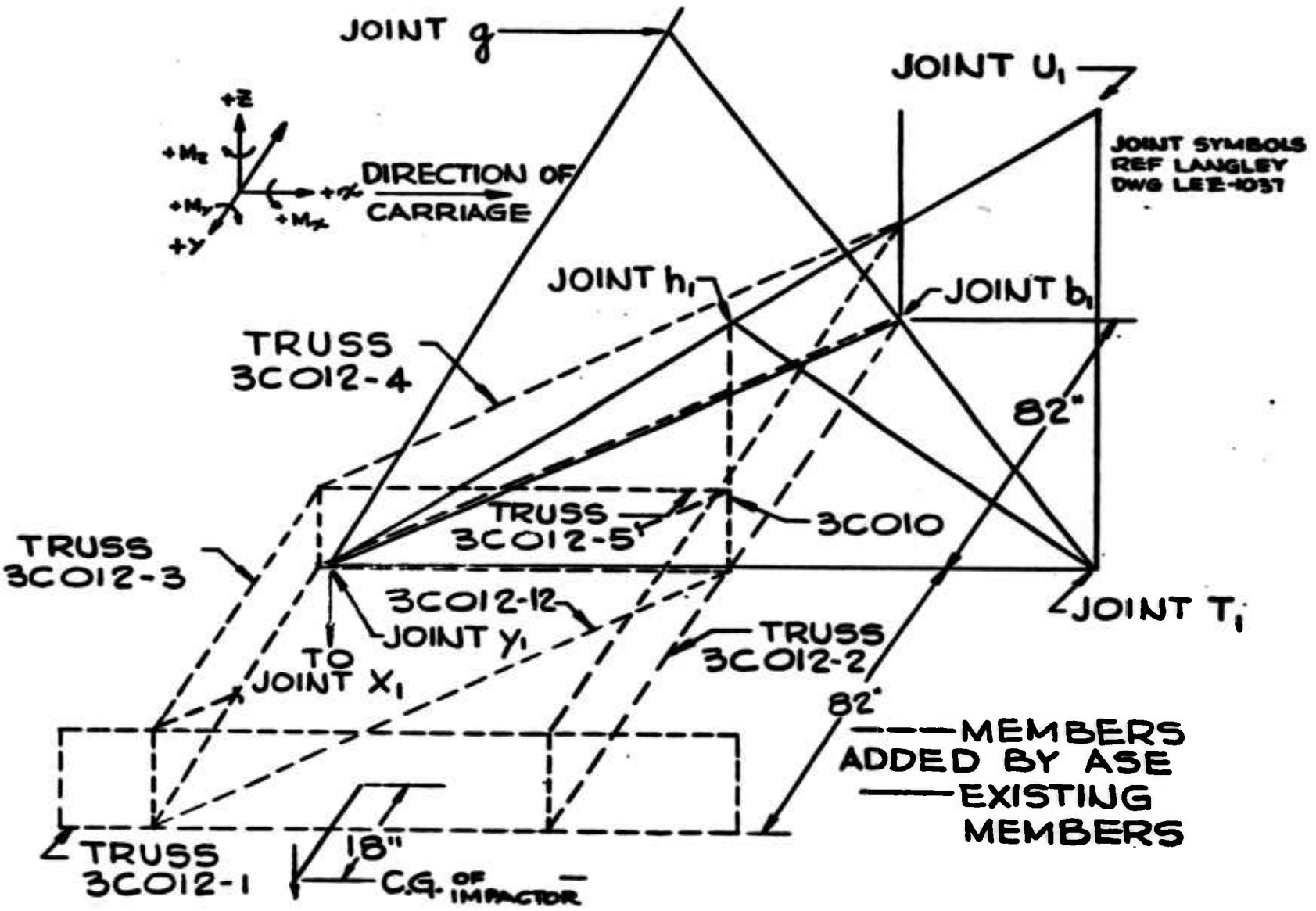

Figure C-1 Impactor Support Structure Schematic

Reference Drawings

ASE Drawing 3E012 Sheets 1 and 2, Impactor Support Structure
Langley Drawing LEZ-1037, Main Carriage.

2.0 Summary

The analysis shows that the additional stresses added to the Langley carriage members during the ASE/FAA impact test are negligibly small and should cause no damage to the carriage.

The maximum calculated stresses due to the impact test and the percent of the allowable stress are tabulated below. The allowable stress is 55,000 psi for 4130 annealed steel, the carriage material.

Table C-1: Maximum Stresses on Carriage Members Due to Impact Test

Member	Stress	% of Allowable
$Y_1 - T_1$	3310 psi	6%
$g - b_1 - T_1$	1800 psi	3%
$b_1 - a_1$	2100 psi	4%
$Y_1 - \textcircled{h_1}$	1925 psi	3.5%
$T_1 - \textcircled{h_1}$	7700 psi	14%
$Y_1 - X_1$	2200 psi	4%

Total Weight Added

The total estimated weight of impactor and support structure attached to the Langley Carriage - - - - - - - - - - - 1300 lbs.

Total Drag Force Added

The total estimated drag force added to the Langley Carriage by the impactor and support structures - - - - - - - - 4500 lbs.

3.0 Load Conditions

1. During the acceleration and deceleration modes, the

maximum level of 7 g's in the x direction occurs for the high velocity runs. The impactor will also see a load of about 7 g's.

It is anticipated that the vertical load during this mode will be less than 1.5 g's at the carriage and less than 2.0 g's at the impactor.

2. The anticipated peak loads, when the impactor strikes the test pole, are 10 g's in the x direction and 5 g's in the z direction. The impactor is floating in the x direction during this mode and will not transmit the 10 g's to the support structure.

A conservative assumption for the analysis is:

$\ddot{x}$ = 10 g's on impactor and the support structure
$\ddot{z}$ = 5 g's on the impactor
1.5 g's on the impactor support structure
$\ddot{y}$ = negligible

Maximum wind drag will be additive to the x loads.

4.0 Impact Test Stresses

4.1 "X" Reactions on Carriage (See Figure C-2)

Load = 10 g's + Wind Drag

F = Wt x 10 + Drag Force

F_i = (500)(10) + 21 = 5021#

F_{-1} = (240)(10) + 460 = 2860#

F_{-2} = (167)(10) + 1510 = 3180#

F_{-3} = (83)(10) + 715 = 1545#

F_{-4} = (133)(10) + 1190 = 2520#

F_{-5} = (91)(10) + 370 = 1280#

$F_{s.b.}$ = (90)(10) + 200 = 1100# (Fwd. support beam)

17,500#

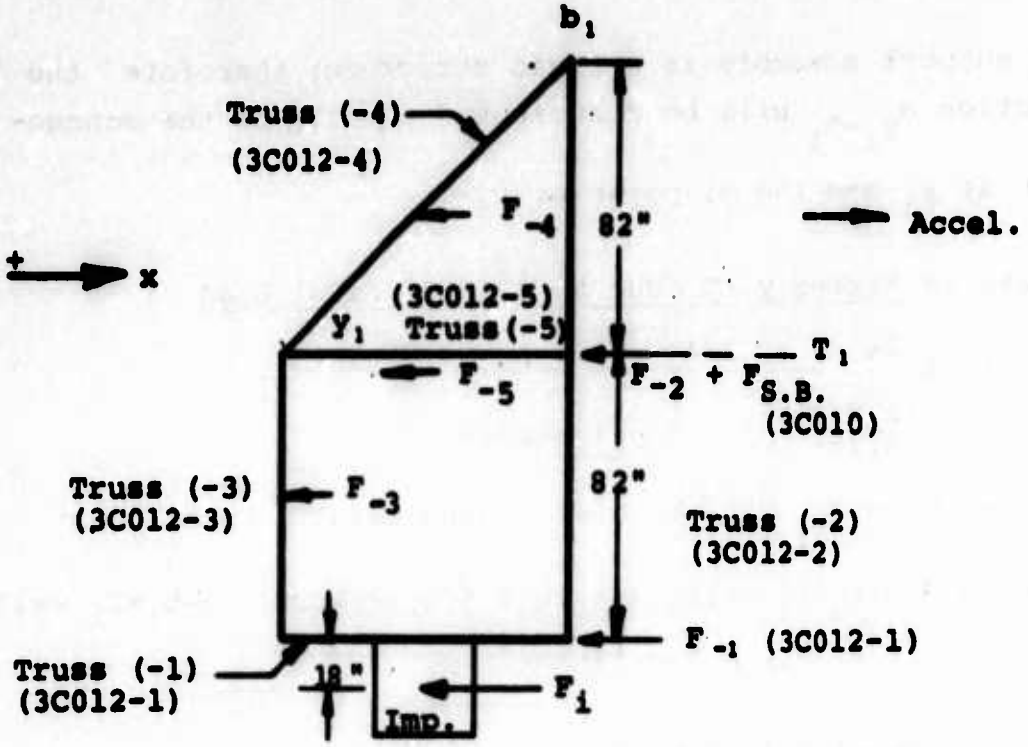

Figure C-2 Horizontal Plane T_1-y_1-b_1, Line Diagram

$$\Sigma M_{R_{b_1}} = 0$$

$$82\ R_{y_1-T_1} = (41)(2520) + (3180)(82) + (1100)(82) + (1545)(123) + (2860)(164) + (5021)(182)$$

$$82\ R_{y_1-T_1} = \begin{array}{r} 103,300 \\ 260,700 \\ 90,200 \\ 190,000 \\ 469,000 \\ \underline{913,800} \\ 2,027,000 \text{ in. lbs.} \end{array}$$

$$R_{y_1-T_1} = \frac{2,027,000}{82} = 24,700^{\#}$$

$$R_{b_1} = 24,700 - 17,500 = 7,200^{\#}$$

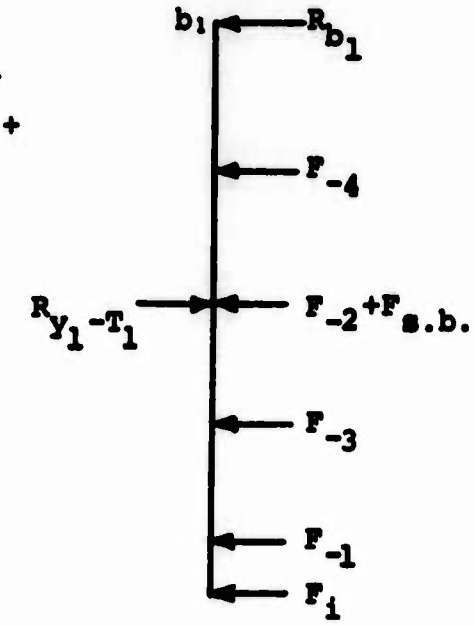

Figure C-3 Moment Diagram

The support assembly is a rigid structure; therefore the reaction $R_{y_1-T_1}$ will be distributed equally to the connection at y_1 and the midpoint of y_1-T_1.

Stress in Member y_1-T_1 Due to 12,350# Axial Load

y_1-T_1 is 5" ϕ, 1/4" wall, A = 3.73 in.^{2}

$$\sigma_A = \frac{12,350}{3.73} = 3,310 \text{ psi stress}$$

The reaction R_{b_1} will be distributed equally to members y_1-b_1 and $g-b_1-T_1$ which are both 5"ϕ members. $g-b_1-T_1$ wall thickness = 3/16", A = 2.83 in.^{2}

4.2 "Z" Reactions on Carriage

The impactor will be pre-positioned on Truss (-1) but to be conservative, assume the impactor will be located adjacent to Truss (-2) and all of the impactor vertical loads are reacted by Truss (-2). Truss (-3) is similar to Truss (-2) and if the impactor were located adjacent to Truss (-3) the reactions on the carriage would be similar.

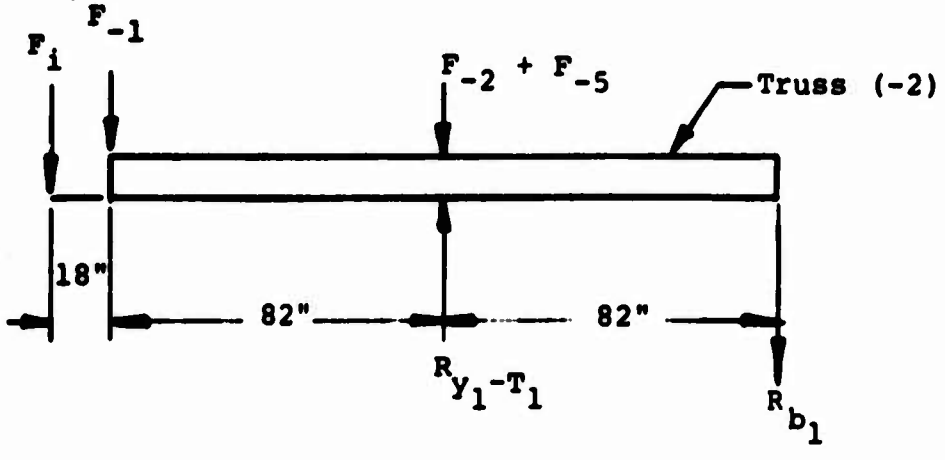

Figure C-4 "Z" Reactions on Carriage

Load

5 g's on the impactor

1.5 g's on the support structure

1/2 the wt. of Truss (-1) & (-5) are supported by Truss (-2)

$F_i = (500)(5) = 2500^{\#}$

$F_{-1} = (\frac{240}{2})(1.5) = 180^{\#}$

$F_{-2} = (167)(1.5) = 250^{\#}$

$F_{-5} = (\frac{91}{2})(1.5) = 70^{\#}$

$3000^{\#}$

$\Sigma M_{R_{b_1}} = 0$

$82R_{y_1-T_1} = (82)(320) + (164)(180) + (182)(2500) = 510,000$

$R_{y_1-T_1} = 6220^{\#}$

$R_{b_1} = 6220 - 3000 = 3220^{\#}$

Reactions From Trusses (-3)&(-4)

Load

1.5 g's on the support structure

1/2 the wt. of Truss (-1) & (-5) are supported by Truss (-3)

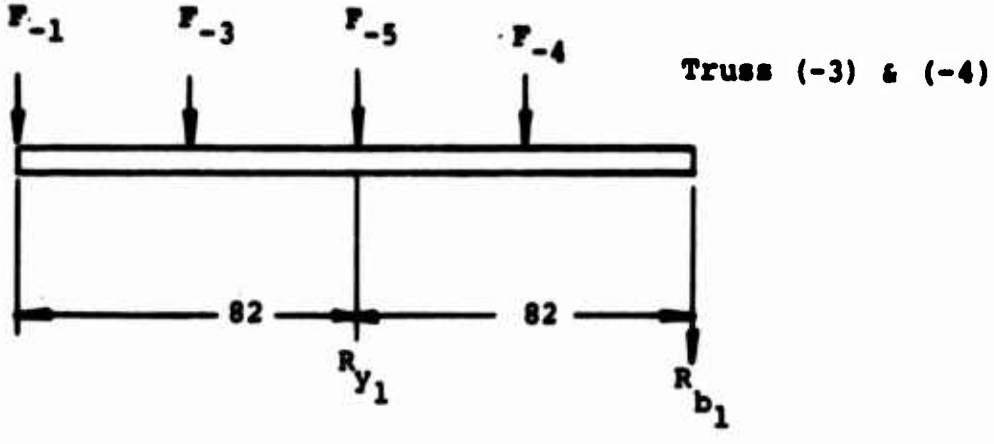

Figure C-5 Reactions from Trusses (-3) & (-4)

$$F_{-1} = \left(\frac{240}{2}\right)(1.5) = 180^{\#}$$

$$F_{-3} = (83)(1.5) = 125^{\#}$$

$$F_{-5} = \left(\frac{91}{2}\right)(1.5) = 70^{\#}$$

$$F_{-4} = (133)(1.5) = \frac{200^{\#}}{575^{\#}}$$

$$\Sigma M_{R_{b_1}} = 0$$

$$82\ R_{y_1} = (200)(41) + (70)(82) + (125)(123) + (180)(164)$$

$$82\ R_{y_1} = 8200 + 5740 + 15,375 + 29,520 = 58,800$$

$$R_{y_1} = 720^{\#}$$

$$R_{b_1} = 720 - 575 = 145^{\#}$$

The total reaction at R_{b_1} is the sum of the (-2) & (-4) reactions.

$$R_{b_1} = 3220 + 145 = 3365^{\#}$$

The maximum vertical reactions are

$R_{y_1\text{-}T_1} = 6220^{\#}$ (depending on location of impactor. Max. vert. reactions do not occur simultaneously)

$R_{b_1} = 3365^{\#}$

R_{b_1} is reacted by member b_1-a_1 which is 3"ϕ tube, 1.80" wall, $A = 1.6$ in.^{2}

$$\sigma = \frac{3365}{1.6} = 2100 \text{ psi stress}$$

$R_{y_1\text{-}T_1}$ is reacted by the forward support beam 3C010 which is connected to member U_1-Y_1 at Joint (h_1)

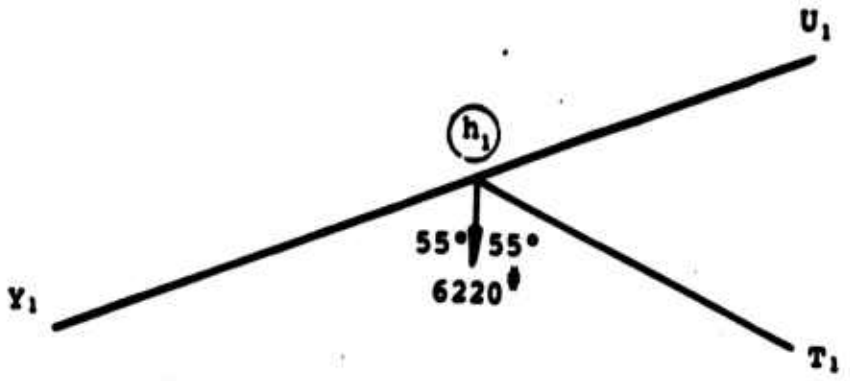

Figure C-6 Forces on Joint h_1

Reaction in Y_1-h_1 = Reaction in T_1 - h_1 = $\frac{3110}{\cos 55^\circ} = \frac{3110}{.57}$

$R = \frac{3110}{.57} = 5450^{\#}$ COMP.

Member Y_1-h_1 is 5"ϕ Tube, 3/16" wall, A = 2.83 in.^{2}

$\sigma = \frac{5450}{2.83} = 1925$ psi stress (COMP.)

Member T_1- h_1 is 2"ϕ Tube, .120 wall, A = .71 in.^{2},

r = .666 in. (rad. of gyro), l = 8 ft.

$\sigma = \frac{5450}{.71} = 7700$ psi (COMP.)

Allowable stress = $\sigma_{all} = \frac{\pi^2 x E}{(K\frac{l}{r})^2}$

T_1- h_1 is fixed at both ends $\therefore K = 0.5$

$\sigma_{all} = \frac{\pi^2 x 30 x 10^6}{(.5x\frac{96}{.666})^2} = \frac{30 \times 10^7}{5195} = 57{,}757$ psi

σ_y = 55,000 psi for 4130 annealed

Safety Margin = $\frac{55{,}000}{7{,}700} - 1 = 7$

R_{y_1} is reacted by member Y_1-X_1 which is 5"ϕ Tube, 3/16" wall, A = 2.83 in.^{2}

$\sigma = \frac{6220}{2.83} = 2200$ psi

Loading on Truss 3E012-2

See Section 4.2 for load calculations,

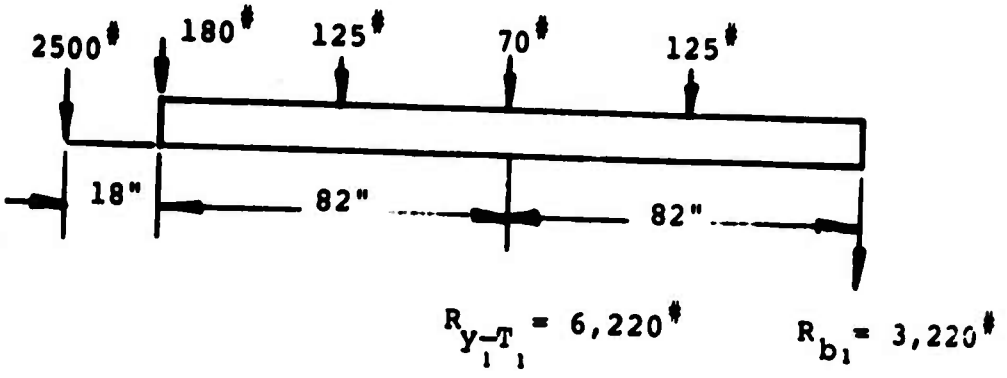

Figure C-7 Loading on Truss 3E012-2

Max. moment and shear occurs at $R_{y_1-T_1}$

$$M_{y_1-T_1} = (2500)(100) + (180)(82) + (125)(41)$$

$$M_{y_1-T_1} = 250,000 + 15,000 + 5,000 = 270,000 \text{ in. lbs.}$$

$$V_{y_1-T_1} = 2500 + 180 + 125 = 2800\#$$

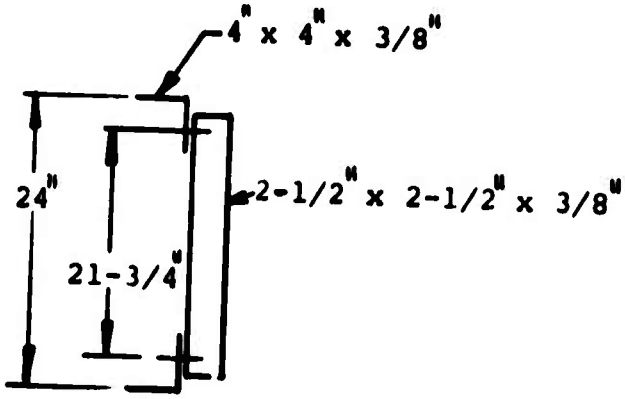

Figure C-8 Cross Section of Truss

From Figure C-8,

CAPS

$A = 2.86 \text{ in.}^2$

$I = Ad^2 = (2)(2.86)(10.88)^2$

$I = 677 \text{ in.}^4$

Bending Stress

$$\sigma_B = \frac{Mc}{I} = \frac{270{,}000 \times 12}{677}$$

$\sigma_B = 800$ psi

Shear Transfer to Diagonals

A of Diag. $= 1.37 \text{ in.}^2$

$$\sigma = \frac{2800 \times 1.4}{1.37} = 2800 \text{ psi}$$

Connections

All bolted connections to have a minimum of two 3/8 inch diameter bolts and secured with locknuts. Shear capacity of 3/8 inch bolts (AN-6) is $8280^{\#}$.

Edge distance of bolt holes to be 1.5 x dia.

Loads on Drag Shear Member 3C012-12

See Section 4.1 for force calculations.

$F_i = 5021^{\#}$-Load from impactor

$F_{-1} = 2860^{\#}$-Load from Truss (-1)

$F_{-2} = 800^{\#}$-1/4 of the total load from Truss (-2)

$F_{-3} = 800^{\#}$-1/2 of the total load from Truss (-3)

$9481^{\#}$

Total load in Member 3C012-12 $= \frac{9481}{.707} = 13{,}410^{\#}$

3C012-12 is 4 x 4 x 3/8, $A = 2.86 \text{ in.}^2$

$$\sigma = \frac{13{,}410}{2.86} = 4690 \text{ psi stress}$$

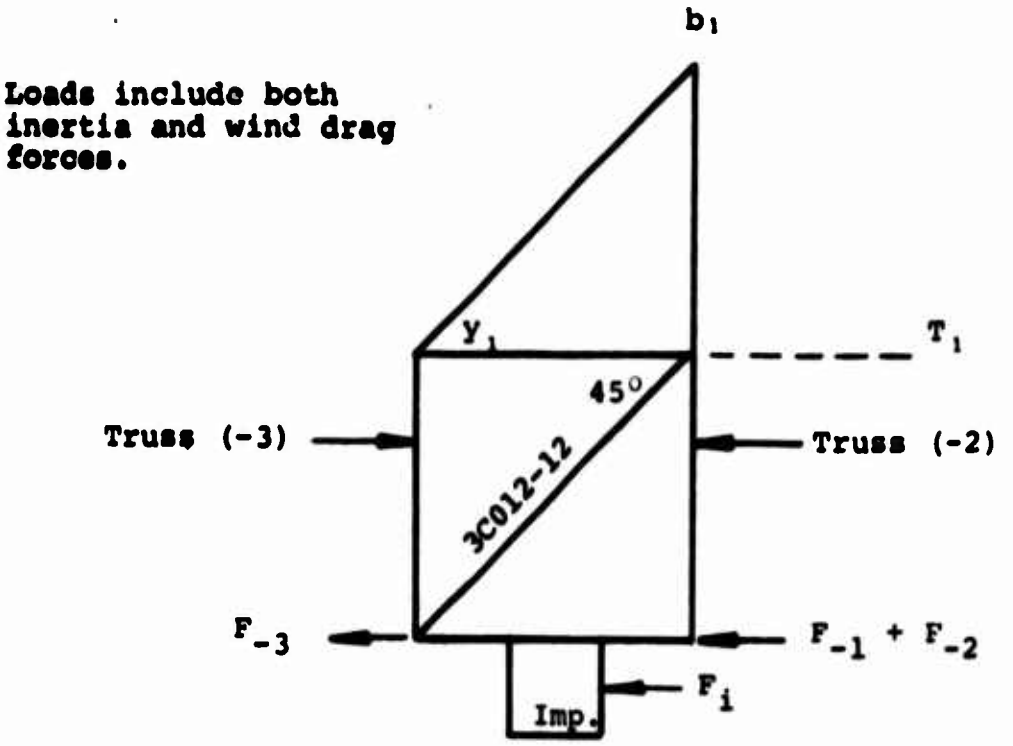

Figure C-9 Loads on Drag Shear Member 3C012-12

5.0 Weight Estimate

5.1 Weight of Impactor Support Structure (Dwg. 3E012)

Truss 3E012-1

W = weight in lbs.

Top and bottom caps - 4 x 4 x 3/8 aluminum angle @ 3.46#/ft. - 12 ft. long

W = 3.46 x 12 x 2 = 83#

Vertical members 4 x 4 x 3/8 aluminum angle on 27" centers - 2 ft. long - 6 required

W = 3.46 x 2 x 6 = 42#

Bars - 1-1/2 x 2 alum. @ 3.53#/ft. 12 ft. long - 2 required

W = 3.53 x 12 x 2 = 85#

Est. Hardware = 30#

Total wt. = 83 + 42 + 85 + 30 = 240 lbs.

$$w = \frac{240}{12} = 20^{\#}/ft.$$

Truss 3E012-2

Top & bottom caps - 4 x 4 x 3/8 aluminum angle
@ 3.46#/ft. - 13.7 ft. long
W = 3.46 x 13.7 x 2 = 95#

Vertical members - 2-1/2 x 2-1/2 x 3/8 alum. angle
@ 2.11#/ft. on 22" centers - 2 ft. long,
6 required
W = 2.11 x 2 x 6 = 25#

Diagonal members - 2-1/2 x 2-1/2 x 3/8 alum. angle
@ 2.11#/ft. - 2.5 ft. long - 6 required
W = 2.11 x 2.5 x 6 = 32#

Est. Hardware = 15#

Total wt. = 95 + 25 + 32 + 15 = 167#

$$w = \frac{167}{13.7} = 12.2\#/\text{ft.}$$

Truss 3E012-3

Top & bottom caps - 4 x 4 x 3/8 aluminum angle
@ 3.46#/ft. - 6 ft. long
W = 3.46 x 6 x 2 = 42#

Vertical members - 2-1/2 x 2-1/2 x 3/8 alum. angle
@ 2.11#/ft. on 24" centers - 2 ft. long
4 required
W = 2.11 x 2 x 4 = 17#

Diagonal members - 2-1/2 x 2-1/2 x 3/8 alum. angle
@ 2.11#/ft. - 2.5 ft. long - 3 required
W = 2.11 x 2.5 x 3 = 16#

Est. hardware = 8#

Total wt. = 42 + 17 + 16 + 8 = 83#

$$w = \frac{83}{6} = 13.8\#/\text{ft.}$$

Truss 3E012-4

Top & bottom caps - 4 x 4 x 3/8 aluminum angle
@ 3.46#/ft. - 10 ft. long
W = 3.46 x 10 x 2 = 70#

Vertical members - 2-1/2 x 2-1/2 x 3/8 alum. angle
@ 2.11#/ft. on 2' centers - 2 ft. long - 6 required
W = 2.11 x 2 x 6 = 25#

Diagonal members - 2-1/2 x 2-1/2 x 3/8 alum. angle
@ 2.11#/ft. - 2.5 ft. long - 5 required
W = 2.11 x 2.5 x 5 = 26#

Est. hardware = 12#

Total wt. = 70 + 25 + 26 + 12 = 133#

$$w = \frac{133}{10} = 13.3\#/ft.$$

Truss 3E012-5

Top & bottom caps - 4 x 4 x 3/8 aluminum angle
@ 3.46#/ft. - 6.75 ft. long
W = 3.46 x 6.75 x 2 = 47#

Vertical members - 2-1/2 x 2-1/2 x 3/8 alum. angle
@ 2.11#/ft. on 2'3" centers - 2 ft. long
4 required
W = 2.11 x 2 x 4 = 17#

Diagonal members - 2-1/2 x 2-1/2 x 3/8 alum. angle
@ 2.11#/ft. - 3 ft. long - 3 required
W = 2.11 x 3 x 3 = 19#

Est. hardware = 8#

Total wt. = 47 + 17 + 19 + 8 = 91#

$$w = \frac{91}{6.75} = 13.5\#/ft.$$

Fwd. Truss Support Beam 3C010

Vertical member - 4 x 4 x 3/8 steel angle
@ 9.8#/ft. - 5.25 ft. long
W = 5.25 x 9.8 = 52#

Bent plate - 4 x 7 x 3/8 steel plate - 2 required

$W = 4 \times 7 \times 3/8 \times .3 \times 2 = 6^{\#}$

Lower plate - 10 x 6 x 3/8 steel plate

$W = 10 \times 6 \times 3/8 \times .3 = 7^{\#}$

Upper plate - 10 x 22 x 3/8 steel plate

$W = 10 \times 22 \times 3/8 \times .3 = 25^{\#}$

Total wt. = 52 + 6 + 7 + 25 = $90^{\#}$

5.2 Total Weight Added to Carriage

	Est. Wt.
Truss 3C012-1	240
Truss 3C012-2	167
Truss 3C012-3	83
Truss 3C012-4	133
Truss 3C012-5	91
Fwd. Supt. Beam 3C010	90
Impactor 72005	500
	1304 lbs.

6.0 Wind Drag Estimate

Wind Pressure at 150 mph

q = pressure in $\#/ft.^2$ (psf)

$q = 25.6 \times (\frac{150}{100})^2 = 57.6\ \#/ft.^2$

Drag Force

$F = C_D qA$ = drag force in lbs.

C_D = drag coefficient = 2 for angles & plates

A = projected area in $ft.^2$

Drag Force on Truss 3E012-1 (x direction)

Projected area is the face of vertical members 4" x 2' - qty. of 6

$A = \frac{4}{12} \times 2 \times 6 = 4.0\ ft.^2$

$F = (2)(57.6)(4.0) = 460^{\#}$

Drag Force on Truss 3E012-2 (x direction)

Projected area is the face of the truss; caps, vertical & diagonal members

Caps: $A = \frac{4}{12} \times 13.7 \times 2 = 9.1 \text{ ft.}^2$

Vert.: $A = \frac{2.5}{12} \times \frac{16}{12} \times 6 = 1.7 \text{ ft.}^2$

Diag.: $A = \frac{2.5}{12} \times \frac{22}{12} \times 6 = 2.3 \text{ ft.}^2$

Total A = 13.1 ft.^2

$F = (2)(57.6)(13.1) = 1510^{\#}$

Drag Force on Truss 3E012-3 (x direction)

Projected area is the face of the truss; caps, vertical & diagonal members

Caps: $A = \frac{4}{12} \times 6 \times 2 = 4.0 \text{ ft.}^2$

Vert.: $A = \frac{2.5}{12} \times \frac{16}{12} \times 4 = 1.1 \text{ ft.}^2$

Diag.: $A = \frac{2.5}{12} \times \frac{22}{12} \times 3 = 1.1 \text{ ft.}^2$

Total A = 6.2 ft.^2

$F = (2)(57.6)(6.2) = 715^{\#}$

Drag Force on Truss 3E012-4 (x direction)

Projected area is the face of the truss; caps, vertical & diagonal members

Caps: $A = \frac{4}{12} \times 10 \times 2 = 6.7 \text{ ft.}^2$

Vert.: $A = \frac{2.5}{12} \times \frac{16}{12} \times 6 = 1.7 \text{ ft.}^2$

Diag.: $A = \frac{2.5}{12} \times \frac{22}{12} \times 5 = 1.9 \text{ ft.}^2$

Total A = 10.3 ft.^2

$F = (2)(57.6)(10.3) = 1190^{\#}$

Drag Force on Truss 3E012-5 (x direction)

Projected area is cross-section of truss; vertical & diagonal members

Vert.: $A = \frac{2.5}{12} \times 2 \times 4 = 1.7$ ft.^{2}

Diag.: $A = \frac{2.5}{12} \times \frac{28}{12} \times 3 = 1.5$ ft.^{2}

Total A = 3.2 ft.^{2}

$F = (2)(57.6)(3.2) = 370^{\#}$

Drag Force on Fwd. Truss Support Beam - 3C010

Projected area is vertical 4 x 4 angle

$A = \frac{4}{12} \times 5.25 = 1.8$ ft.^{2}

$F = (2)(57.6)(1.8) = 200^{\#}$

Drag Force on Impactor

Impactor is an airfoil shape with $C_D = .15$
Projected area is nose of airfoil - 10" x 36"

$F = (.15)(\frac{10 \times 36}{144})(57.6) = 21^{\#}$

Estimate of Total Drag Added

	Est. Drag Force
Truss 3C012-1	460
Truss 3C012-2	1510
Truss 3C012-3	715
Truss 3C012-4	1190
Truss 3C012-5	370
Fwd. Supt. Beam 3C010	200
Impactor 72005	21
	$4466^{\#}$

APPENDIX D

STRESS AND DEFLECTION ANALYSES AND TESTS OF ASE BREAKAWAY POLE

Charles W. Laible

TABLE OF CONTENTS

This appendix provides analyses which prove the compliance of the basic ASE pole with the survival and deflection requirements. Also contained herein is a description of the bend tests conducted to determine the characteristics of the joints of the sectionalized pole and to enable the selection of joint dimensions to optimize the overall performance.

APPENDIX D

LIST OF FIGURES

APPENDIX D

Stress and Deflection Analyses and Tests of ASE Breakaway Pole

1.0 Introduction

This appendix is divided into two general sections. The first - Section 2 - provides stress and deflection analyses of the basic ASE pole design as a unit. The second - Section 3 - considers the effect of sectionalizing this pole to provide frangibility. Optimized joint dimension ratios are selected, and it is shown that the sectionalized pole acts linearly beyond the moments imposed by the survival wind criteria. The results of the analyses and tests are summarized in Table D-1.

Table D-1 Summary of ASE Pole Analyses and Tests

Survival Wind	
100 mph - no ice	
Pole Stress, psi	10,180
Factor of Safety	3.2
75 mph - ½" ice	
Pole Stress, psi	7,636
Factor of Safety	4.3
Operational Wind - 45 mph	
Lamp Deflection, inches	1.84
Slope of Lamp, degrees	0.71

2.0 Stress and Deflection Analyses

The analyses which follow are based on the structure of the basic pole, which is shown in Figure D-1.

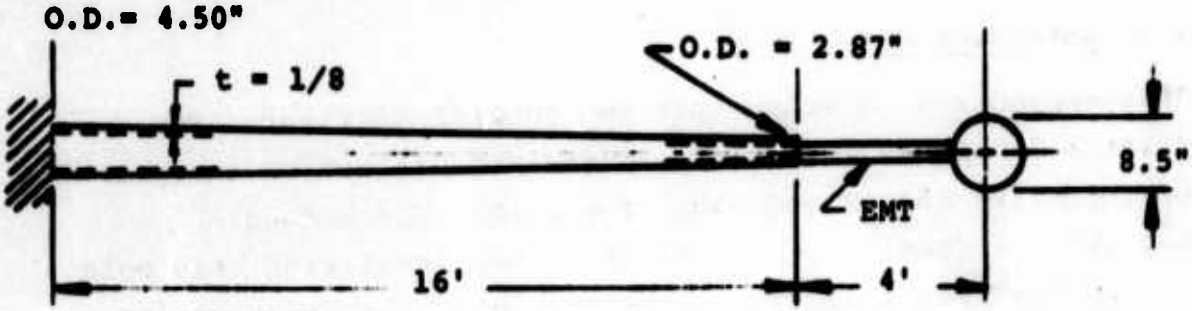

EMT: O.D. + 2.197", ID = 2.067", I = .248 in^4
Coefficient of Drag, C_D: Lamp = 1.0, Pole = 1.2

Figure D-1 Basic ASE Pole Structure

The structural criteria contained in Section 3.1 are repeated for convenience:

Survival Wind - 75 mph with ½" radial ice
Operational Wind - 45 mph wind shall cause no more than 3" deflection of the lamp.

ASE recommends that the structure be able to withstand 100 mph winds with no ice on structure. The structure is therefore analyzed for this condition as well as the specified condition.

2.1 Survival Conditions - 100 mph Wind with No Ice

At 100 mph wind, stagnation pressure q = 25.6 psf.

Lamp w = (25.6) (1.0) = 25.6 psf
Pole w = (25.6) (1.2) = 30.7 psf

For EMT Section

Wind Load on lamp = $\pi R^2 w = \frac{\pi(4.25)^2}{144}(25.6) = 10.1$ lbs.

Wind Load on EMT = $wDL = (30.7)(\frac{2.2}{12})(3\text{-}2/3) = 20.6$ lbs.

At Base

$V = 10.1 + 20.6 = 30.7$ lbs.

$M = (10.1)(4) + (20.6)(\frac{11}{6}) = 40.4 + 37.8 = 78.2$ ft.lbs.

$\sigma = \frac{Mc}{I} = \frac{(78.2)(12)(1.1)}{.248} = 4160$ psi

For Tapered Section

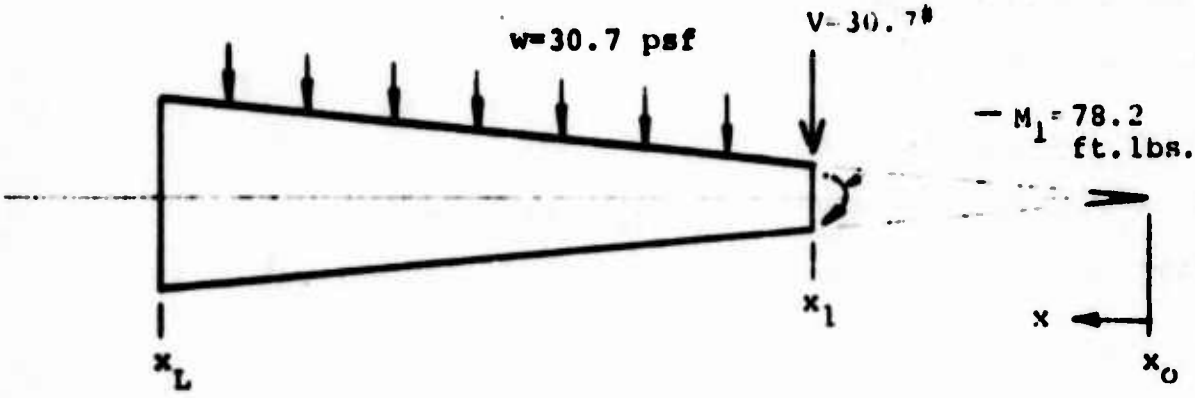

Figure D-2 Forces on Tapered Section @ 100 mph Wind

Slope = $A = (1/2)\left[\frac{4.50 - 2.87}{16 \times 12}\right] = \frac{1.63}{16 \times 24} = .004245 \frac{in}{in}$

$x_1 = \frac{1.435}{.004245} = 338$ in.

$x_L = 338 + (16 \times 12) = 530$ in.

at x_L, from Appendix A, Equation A-2,

$$M = M_1 + V(x_L - x_1) + \frac{WA}{3}(x_L^3 - 3x_1^2 x_L + 2x_1^3)$$

$$M = (78.2 \times 12) + (30.7)(192) + \frac{(30.7)(.004245)}{(144)(3)}\left[(530)^3 - 3(338)^2(530) + 2(338)^3\right] = 20{,}241 \text{ in. lbs.}$$

$z = \pi R^2 t = \pi(2.25)^2\ (1/8) = 1.988\ in^3$

$\sigma = \frac{M}{z} = \frac{20,241}{1.988} = 10,180\ psi$

Factor of Safety in Yielding

Information from ALCOA indicates that aluminum alloy 6005-T5, the material selected for the pole, has expected minimum yield values (for design) of 33 ksi in tension and 35 ksi in compression for thickness of less than 0.5 inches.

The factor of safety then is $\frac{33}{10.2} = 3.2$

2.2 **Survival Conditions - 75 mph Wind with ½" Radial Ice**

Lamp $w = 25.6\ (\frac{75}{100})^2 = 14.4$ psf

Pole $w = 30.7\ (\frac{75}{100})^2 = 17.3$ psf

For EMT Section

Wind load on lamp $= \pi r^2 w = \frac{\pi(4.75)}{144}(14.4) = 7.1^{\#}$

Wind load on EMT $= wDl = (17.3)(\frac{3.2}{12})(3\text{-}2/3) = 16.9^{\#}$

At Base

$V = 7.1 + 16.9 = 24.0^{\#}$

$M = (7.1)(4)' + (16.9)(\frac{11}{6})' = 28.4 + 31.0 = 59.4$ ft.lbs.

$\sigma = \frac{Mc}{I} = \frac{(59.4)(12)(1.1)}{.248} = 3162$ psi

For Tapered Section

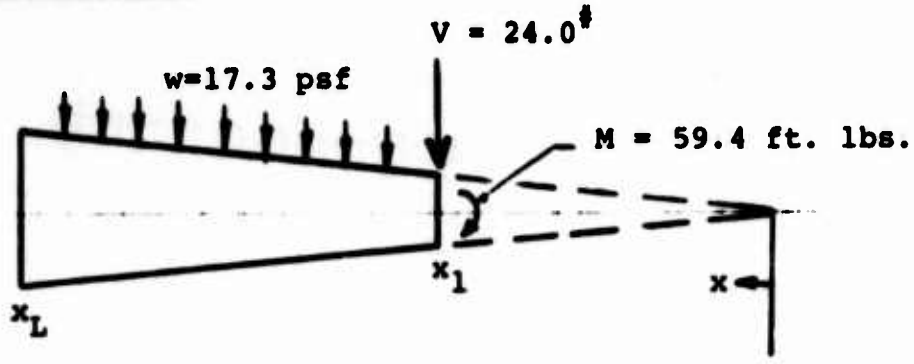

Figure D-3 Forces on Tapered Section @ 75 mph Wind, 1/2" Ice

D at x_L = 4.50 + 1.00 = 5.50 in.

D at x_1 = 2.87 + 1.00 = 3.87 in.

Slope = A = $(\frac{1}{2})\left[\frac{5.50 - 3.87}{16x12}\right] = \frac{1.63}{16x24} = .004245 \frac{in}{in}$ (on radius)

$x_L = \frac{r}{A} = \frac{2.75}{.004245} = 648$ in.

$x_1 = \frac{r}{A} = \frac{1.935}{.004245} = 456$ in.

<u>at x_L</u>, from Appendix A, Equation A-2,

$$M = M_1 + V(x_L - x_1) + \frac{WA}{3}(x_L^3 - 3x_1^2 x_L + 2x_1^3)$$

$$M = (59.4 \times 12) + (24)(192) + \frac{(17.3)(.004245)}{(144)(3)}\left[(648)^3 - 3(456)^2(648) + 2(456)^3\right]$$

M = 15,181 in lbs.

$z = 1.988$ in.^{3}

$\sigma = \frac{M}{z} = \frac{15,181}{1.988} = 7,636$ psi

Factor of safety in yielding = $\frac{33}{7.6} = 4.3$

2.3 Deflection under 45 mph Wind

For information and ease in calculation, deflections are calculated first for 100 mph wind, and are then factored to give the 45 mph wind deflections.

Slope at End of Tapered Section, x_1

From Appendix A, Equation A-5, and at 100 mph,

$$\pi t A^3 E\theta_{x_1} = 1/2\ (M_1 - Vx_1 + 2/3\ wAx_1^3)\left(\frac{1}{x_L^2} - \frac{1}{x_1^2}\right) + (V - wAx_1^2)\left(\frac{1}{x_L} - \frac{1}{x_1}\right) + \frac{WA}{3}(x_1 - x_L)$$

$$\pi t A^3 E = \pi(\tfrac{1}{8})(.004245)^3(10^7) = .3004 \frac{\#}{in.}$$

$$\text{1st term} = 1/2\ (78.2 \times 12 - 30.7 \times 338 + 2/3 \times \frac{30.7}{144} \times .004245 \times 338^3)$$

$$= 6{,}930\ (\frac{1}{530^2} - \frac{1}{338^2}) = -.03599\ ^{\#}/\text{in.}$$

$$\text{2nd term} = (30.7 - \frac{30.7}{144} \times .004245 \times 338^2)\ (\frac{1}{530} - \frac{1}{338})$$

$$= +\ .07793\ ^{\#}/\text{in.}$$

$$\text{3rd term} = (\frac{30.7}{144})\ (\frac{.004245}{3})\ (338 - 530) = -.05792$$

$$\theta_{x_1} = (\frac{1}{.3004})\ (-.03599 + .07793 - .05792)$$

$$\theta_{x_1} = \frac{-.01598}{.3004} = -.0532 \text{ radians (100 mph wind)}$$

<u>At 45 mph Wind</u>

$$\theta_{x_1} = (\frac{45}{100})^2\ (.0532) = .0108 \text{ radians (45 mph wind)}$$

<u>Deflection at End of Tapered Section, x_1</u>

From Appendix A, Equation A-6, and at 100 mph,

$$\pi t A^3 E \Delta_{x_1} = (\frac{1}{2\ x_1 x_L^2})\ (M_1 - V x_1 + \frac{2}{3}\ wA x_1^3)\ (x_1 - x_L)^2 + \frac{wA}{6}\ (x_1 - X_L)^2 + (V - wA x_1^2)\ \left[\frac{x_1}{x_L} + \ln \frac{x_L}{x_1} - 1\right]$$

$$\pi t A^3 E = .3004\ ^{\#}/\text{in.}$$

$$\text{1st term} = \left[\frac{1}{(2)\ (338)\ (530)^2}\right]\ (13{,}859)\ (-\ 192)^2 = +2.6905\#$$

$$\text{2nd term} = (\frac{30.7}{144})\ (\frac{.004235}{6})\ (192)^2 = +5.5604\#$$

$$\text{3rd term} = (-72.7)\ (\frac{338}{530} + \ln \frac{530}{338} - 1) = (72.7)\ (-.3622 + \ln 1.568) = -6.3685\#$$

$$\Delta x_1 = \left(\frac{1}{.3004}\right)(+ 2.6905 - 6.3685 + 5.5604) = \frac{+1.8824}{.3004}$$

$\Delta x_1 = 6.2663$ inch (100 mph wind)

At 45 mph Wind

$$\Delta x_1 = \left(\frac{45}{100}\right)^2 (6.2663) = 1.27 \text{ inch}$$

Deflection of Lamp with Respect to EMT Base

At 100 mph Wind

$$\Delta(\text{wind on lamp}) = \frac{Pl^3}{3EI} = \frac{(10.1)(4 \times 12)^3}{(3)(10^7)(.248)} = .150$$

$$\Delta(\text{wind on EMT}) = \frac{wl^3}{8EI} = \frac{(20.6)(4 \times 12)^3}{(8)(10^7)(.248)} = .115$$

$\Delta = .265$ inch

At 45 mph Wind

$$\Delta = \left(\frac{45}{100}\right)^2 (.265) = .054 \text{ inch}$$

Total Deflection at Lamp (at 45 mph Wind)

Tapered section Δx_1 =	1.27
Tapered section slope (at EMT base)	
θ_{x_1} x 4' = (.0108)(48") =	.52
EMT Δ =	.05
	1.84 inch

Total Slope of Lamp (at 45 mph Wind)

Lamp Drag, $\theta = \frac{Pl^2}{2EI} = \left(\frac{45}{100}\right)^2 \left(\frac{10.1 \times 48^2}{2 \times 10^7 \times .248}\right)$ .00095 rad.

EMT Drag, $\theta = \frac{wl^2}{6EI} = \left(\frac{45}{100}\right)^2 \left(\frac{20.6 \times 48^2}{6 \times 10^7 \times .248}\right) = .00065$

Tapered section slope (at EMT base), $\theta_{x_1} = .0108$

$\theta = .01240$ rad.

$\theta = 0.71$ deg.

3.0 Breakaway Joints

The analyses contained in earlier portions of this Appendix were predicated on a single tapered section and a single straight portion, the EMT. To provide the desired frangibility or breakaway characteristics, the tapered pole is comprised of four sections wedged together. These joints are not readily amenable to linear analysis, as in providing their desired function the metal is stressed beyond the elastic limit. Bend tests were therefore conducted on pole sections with varying socket depth ratios (L/D), with the test fixture shown in Figure D-4. The tests show that the selected joint acts linearly beyond the moments calculated for maximum (survival) conditions. The segmented pole with the appropriate (L/D) ratio will therefore act like the basic pole insofar as stress and deflection are concerned.

Wind loading moments at each of the joints of the sectional pole are calculated in Section 3.1 while the tests are discussed in Section 3.2.

3.1 Joint Moment Calculations

Table D-2 gives a summary of the moments at each point of the sectional pole. See Figure D-5.

Table D-2 Wind Moments (in. lbs.) at Joints of Sectional Pole

Joint	75 MPH Wind 1/2 Radial Ice	100 MPH Wind No Ice
A	713	938
B	2,545	3,151
C	5,397	6,971
D	9,609	12,600
E	15,181	20,242

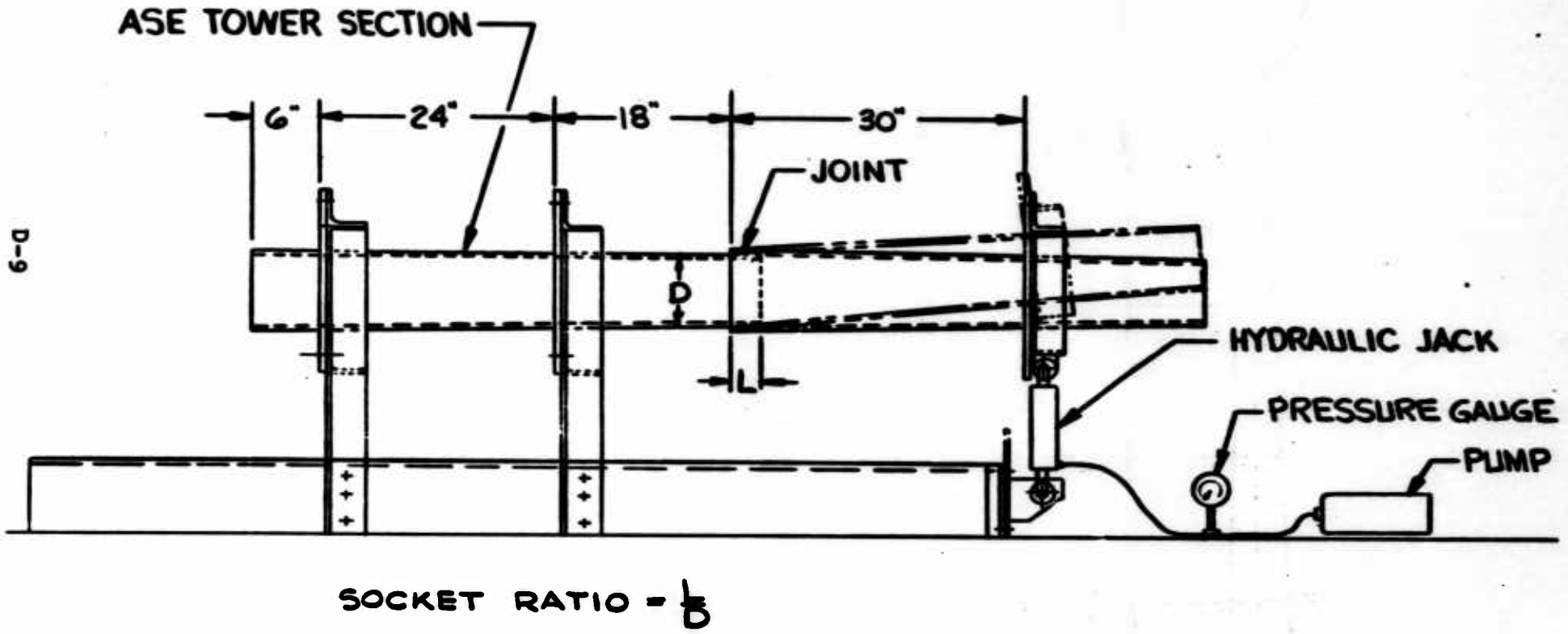

Figure 4-4 Breakaway Joint Test Fixture

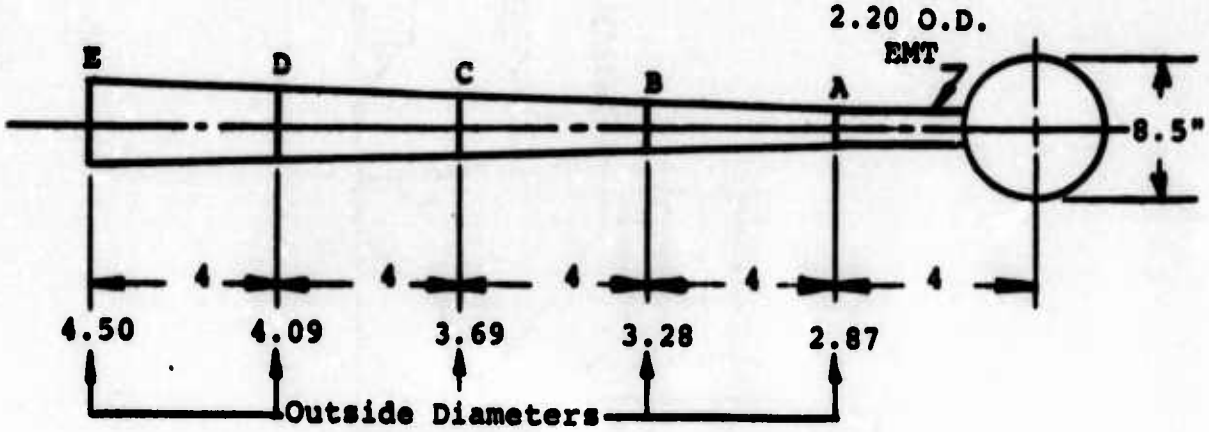

Figure D-5 Sectional ASE Pole Dimensions

Pole Parameters

$Dia._A = 2.87"$

$Dia._E = 4.50"$

$$Slope = \frac{4.50 - 2.87}{16 \times 12} = \frac{1.63}{192} = .00849 \frac{in.}{in.} \quad (dia.)$$

$Dia._B = 2.87 + .00849 \times 48 = 2.87 + .41 = 3.28$

$Dia._C = 2.87 + .00849 \times 96 = 2.87 + .82 = 3.69$

$Dia._D = 2.87 + .00849 \times 144 = 2.87 + 1.22 = 4.09$

Coefficient of Drag, C_d: Lamp = 1.0, Pole = 1.2

3.1.1 For 100 mph Wind, stagnation pressure q = 25.6 psf.

lamp w = (25.6)(1.0) = 25.6 psf

pole w = (25.6)(1.2) = 30.7 psf

For EMT Section

Wind load on lamp = $\pi r^2 w = \frac{\pi(4.35)^2}{144}(25.6) = 10.1^{\#}$

Wind load on EMT = $wD1 = (30.7)(\frac{2.2}{12})'(3\text{-}2/3)' = 20.6^{\#}$

At Base

$V = 10.1 + 20.6 = 30.7^{\#}$

$M_1 = (10.1)(4)' + (20.6)(\frac{11}{6})' = 78.2$ ft. lbs.

For Tapered Section

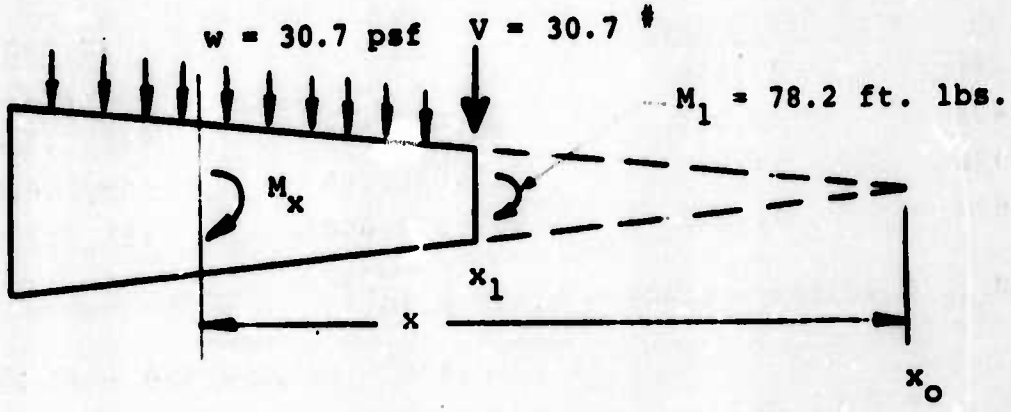

Figure D-6 Forces on Tapered Section at 100 mph Wind

Slope = $A = (\frac{1}{2})(.00849) = .004245 \frac{in}{in}$ (radius)

$x_1 = \frac{1.435}{.004245} = 338$ in.

$x_B = 338 + 48 = 386$ in.

$x_C = 338 + 96 = 434$ in.

$x_D = 338 + 144 = 482$ in.

$x_E = 338 + 192 = 530$ in.

From Appendix A, Equation A-2, the moment at any section x,

$M_x = M_1 + V(x-x_1) + \frac{wA}{3}(x^3 - 3x_1^2 x + 2x_1^3)$

$M_1 - Vx_1 = (78.2)(12) - (30.7)(338) = -9,438.2$ in. lbs.

$x_1^2 = (338)^2 = 114,244 \text{ in.}^2$

$3x_1^2 = 342,732 \text{ in.}^2$

$x_1^3 = 38,614,472 \text{ in.}^3$

$2x_1^3 = 77,228,944 \text{ in.}^3$

$\frac{wA}{3} = \frac{(30.7)(.004245)}{(3)(144)} = .0003016 = 3.016 \times 10^{-4} \frac{\#}{in^2}$

$M_x = 30.7(x) - 9,438 + 3,016 \times 10^{-4}$

$$\left[(x^3 - (342,732)\ x + 77,228,944)\right]$$

x	30.7 (x)	x^3	342,732 x
386	11,850	57,512,456	132,294,550
434	13,324	81,746,504	148,745,680
482	14,797	111,980,160	165,196,820
530	16,271	148,877,000	181,647,960

$M_{386} = 11,850 - 9,438 + 3.016 \times 10^{-4}$

$(57,512,456 - 132,294,550 + 77,228,944)$

$M_{386} = 3151 \text{ in lbs.}$

$M_{434} = 13,324 - 9,438 + 3.016\ (8175 - 14,875 + 7,723)$

$= 6971 \text{ in lbs.}$

$M_{482} = 14,797 - 9438 + 3.016\ (11,198 - 16,520 + 7723)$

$= 12,600 \text{ in lbs.}$

$M_{530} = 16,271 - 9,438 + 3.016\ (14,888 - 18,165 + 7723)$

$= 6833 + 3.016\ (4446) = 6,833 + 13,409$

$= 20,242 \text{ in lbs.} = 1687 \text{ ft. lbs.}$

Shear at Joint

$V_x = V_1 + 30.7(x - x_1)(\frac{1}{2})(D_{x_1} + D_x)$

$V_x = 30.7 + \frac{15.35}{144}(x - 338)"(2.87 + D_x)"$

$V_{386} = 30.7 + (.1066)(386 - 338)(2.87 + 3.28) = 62.2$ lbs.

$V_{434} = 30.7 + (.1066)(434 - 338)(2.87 + 3.69) = 97.8$ lbs.

$V_{482} = 30.7 + (.1066)(482 - 338)(2.87 + 4.09) = 137.5$ lbs.

$V_{530} = 30.7 + (.1066)(530 - 338)(2.87 + 4.50) = 181.5$ lbs.

3.1.2 For 75 mph Wind, 1/2" Radial Ice

Moment Calculations

$Dia._A = 3.87$

$Dia._B = 4.28$

$Dia._C = 4.69$

$Dia._D = 5.09$

$Dia._E = 5.50$

$Dia._{EMT} = 3.20$

$Dia._{Lamp} = 9.50$

Lamp $w = (25.6)(1.0)(\frac{75}{100})^2 = 14.4$ psf

Pole $w = (25.6)(1.2)(\frac{75}{100})^2 = 17.3$ psf

For EMT Section

Wind load on lamp = $r^2w = \frac{\pi(4.75)^2}{144} = 7.1^{\#}$

Wind load on EMT = $wD1 = (17.3)(\frac{3.2}{12})'(3\text{-}2/3)' = 16.9^{\#}$

At Base

$V = 7.1 + 16.9 = 24.0^{\#}$

$M_1 = (7.1)(4)' + (16.9)(\frac{11}{6})' = 59.4$ ft. lbs.

For Tapered Section

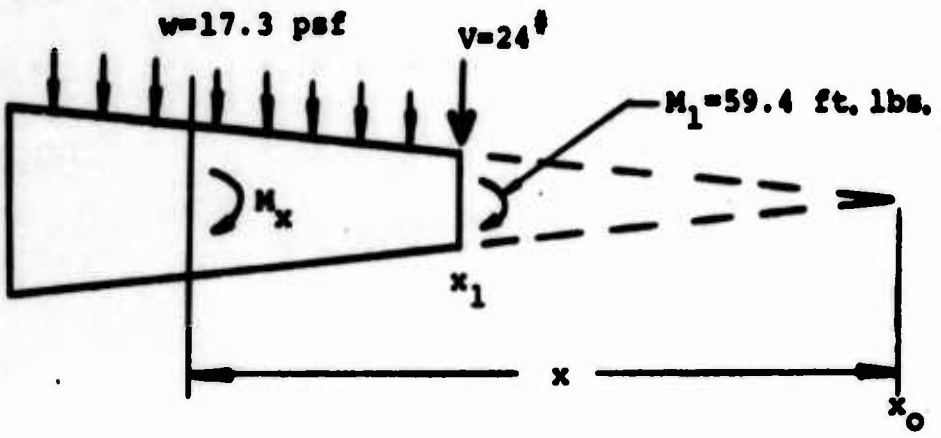

Figure D-7 Forces on Tapered Section at 75 MPH Wind with 1/2" Radial Ice

Slope = A = .004245 $\frac{in}{in}$ (on radius)

$x_1 = x_A = \frac{r}{A} = \frac{1.935}{.004245} = 456$ in.

$x_B = \frac{2.14}{.004245} = 504$ in.

$x_C = \frac{2.345}{.004245} = 552$ in.

$x_D = \frac{2.545}{.004245} = 600$ in.

$x_E = \frac{2.75}{.004245} = 648$ in.

From Appendix A, Equation A-2, the moment at any section x,

$$M_x = M_1 + V(x-x_1) + \frac{wA}{3}(x^3 - 3x_1^2 x + 2x_1^3)$$

$$M_1 - Vx_1 = (59.4 \times 12) - (24 \times 456)$$

$$M_1 - Vx_1 = -10,231 \text{ in lbs.}$$

$$\frac{wA}{3} = \frac{(17.3)(.004245)}{3(144)} = .00017 = 1.7 \times 10^{-4} \frac{\#}{in^2}$$

$3x_1^2 = (3)(456)^2 = 624 \times 10^3 \text{ in}^2$

$2x_1^3 = (2)(456)^3 = 190 \times 10^6 \text{ in}^3$

$$M_x = (24)(x) - 10{,}231 + (1.7 \times 10^{-4}) \left[x^3 - (624 \times 10^3)\, x + 190 \times 10^6\right]$$

Joint	x	24(x)	x^3	$624 \times 10^3 (x)$
B	504	12,096	128×10^6	314×10^6
C	552	13,248	168×10^6	344×10^6
D	600	14,400	216×10^6	374×10^6
E	648	15,552	272×10^6	404×10^6

$M_B = 12{,}096 - 10{,}231 + (1.7 \times 10^{-4})(128 - 314 + 190)(10^6)$

$M_B = 1865 + (170)(4)$

$M_B = 2{,}545$ in. lbs.

$M_C = 13{,}248 - 10{,}231 + (1.7 \times 10^{-4})(168 - 344 + 190)(10^6)$

$M_C = 3017 + (170)(14)$

$M_C = 5{,}397$ in. lbs.

$M_D = 14{,}400 - 10{,}231 + (1.7 \times 10^{-4})(216 - 374 + 190)(10^6)$

$M_D = 4169 + (170)(32)$

$M_D = 9{,}609$ in. lbs.

$M_E = 15{,}552 - 10{,}231 + (1.7 \times 10^{-4})(272 - 404 + 190)(10^6)$

$M_E = 5321 + (170)(58)$

$M_E = 15{,}181$ in. lbs.

3.2 Bend Tests of Breakaway Joints

As previously described, joints of the segmented pole were subjected to bend tests to: 1) verify the viability of the segmented pole under survival conditions and 2) to determine an optimized L/D ratio, i.e., that ratio which would survive under the specified environment and yet extract the minimum energy from a colliding object. Figure D-4 is a diagram of the test set-up, together with pertinent dimensions.

Tests were conducted for two sizes of joint, 3-1/4" diameter and 3-9/16" diameter. Three sets of L/D ratio, L/D = .40", .46", and 0.79", were tested for the 3-1/4" diameter joint. The 3-9/16" diameter joint was tested at L/D = .49". The results of the tests are shown in Figure D-8. The reference moments shown on Figure D-8 are the wind moments calculated for the joint diameter shown under the maximum loading conditions:

(a) 75 mph wind with 1/2" radial ice
(b) 100 mph wind with no ice

The performance of the joint can now be assessed against the design moments.

It will be seen that all joints exhibit similar characteristics within the limits of the data. Initially there is a linear relationship between the deflection and the applied moment up to a "yield moment" at which point it is hypothesized that yielding starts within the joint. From this point the joint again deflects linearly with the applied moment, but at a higher rate. The L/D = .40 has a "yield moment" less than the survival moment, and is deemed unsatisfactory for that reason. The L/D = .78 has a yield moment far in excess of the survival moment, and is thus not optimized for minimum energy extraction. The L/D ratio of .46 and .49 "yield" at a moment which provides a small margin against the maximum survival moment. The L/D ratio selected is 0.50, which provides margin for manufacturing tolerances.

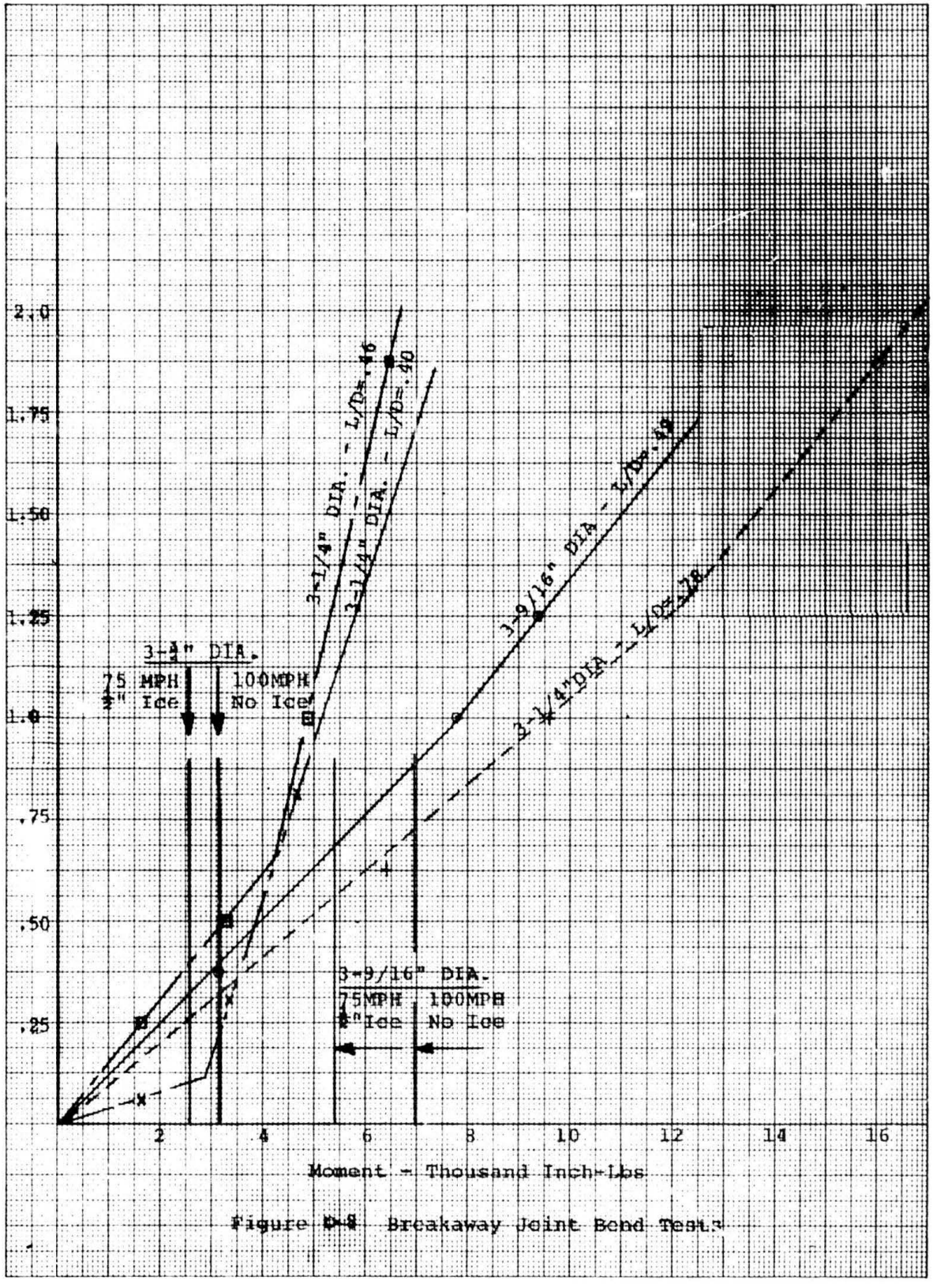

Figure D-8 Breakaway Joint Bend Test

APPENDIX E

STRESS ANALYSIS AND LOAD/DEFLECTION TEST OF CANADIAN LIGHT SUPPORT STRUCTURE

Charles W. Laible

APPENDIX E

TABLE OF CONTENTS

This Appendix provides an analysis which proves the compliance of the Canadian Light Support Structure with the survival and deflection requirements. Also included is a description of a Load/Deflection Test which was conducted to prove the analyses results, and to ascertain the action of the structure under static loads.

APPENDIX E

Stress Analyses and Load/Deflection Tests of Canadian Light Support Structure

1.0 Introduction

The Canadian Light Support Structure was analyzed for stress levels and tested for load and deflection to verify compliance with the survival and deflection criteria. The survival mode was tested for buckling of a vertical leg at the base of the structure for the 100 mph wind with no ice, and for 75 mph wind with 1/2" radial ice, as for the ASE Breakaway Pole, see Appendix D. The results of the analyses and test are that the Canadian structure satisfies the survival and deflection criteria. Results of these efforts are summarized in Table 4-1.

2.0 Stress Analysis

The Canadian structure is of open truss construction and is shown in Figure E-1. It consists of three sections, a lower constant cross-section 7' long, an upper constant cross-section 10' long, and a 2" EMT section approximately 3' long to the center of the lamp assembly, fastened together at assembly in the field. The chord members are solid 9/16" diameter solid aluminum alloy rods, while the diagonals are solid 5/16" diameter aluminum rods.

Dimensional Parameters

Vertical Legs

Dia. = .570 in., $A = .255$ in.^{2} $I = .00515$ in.^{4}

Lacing Rods

Dia. = .310 in.

Coefficient of Drag, $C_D = 1.2$ (for cylinders)

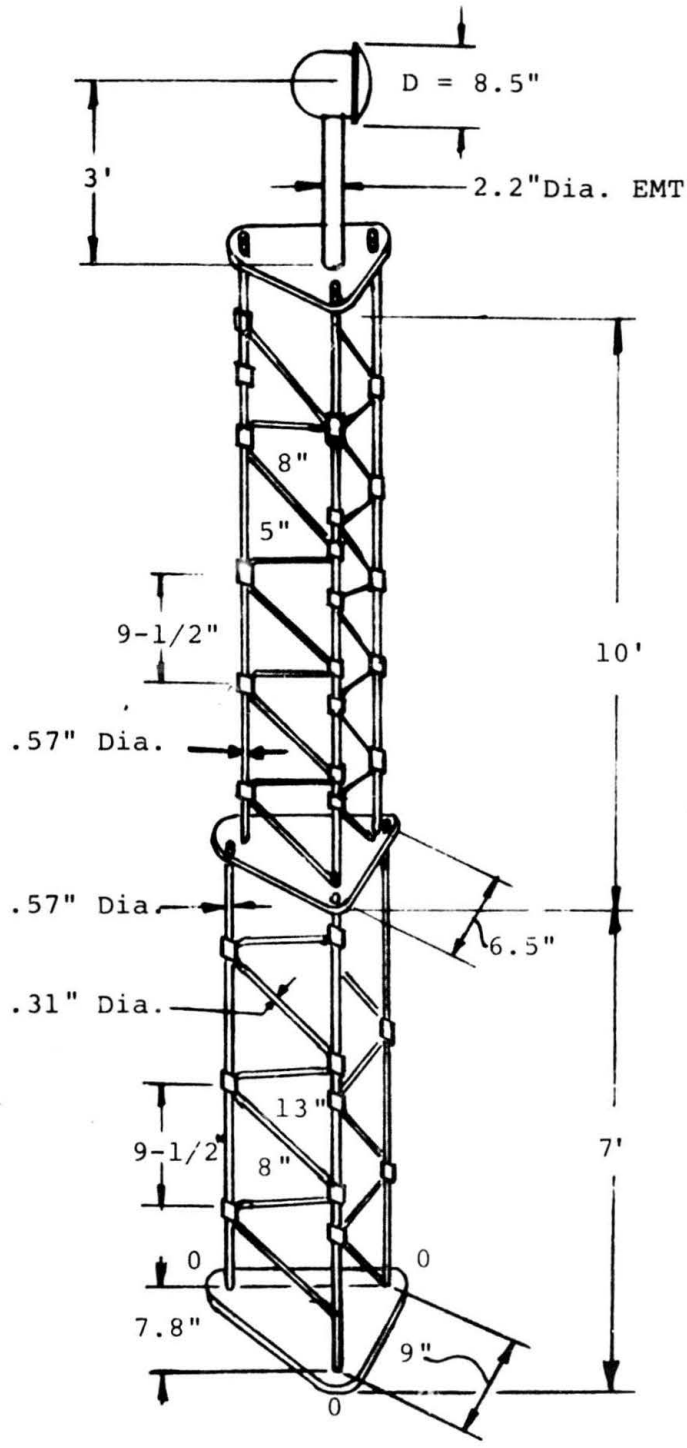

Figure E-1 Canadian Light Support Structure

2.1 Survival Conditions - 100 mph Wind with No Ice

Wind loading = $w = (q)(C_D)$

$w = (25.6)(1.2) = 30.7$ psf/unit projected area

Projected Area

EMT = $(\frac{2.2}{12})'(3)' = .55$ ft.^{2}

Upper Section (U.S.)

3 legs = $3 \times 10' \times \frac{.57}{12}$ = 1.43 ft.^{2}

3 trusses = $22(\frac{.31}{12})(\frac{13}{12} \times \frac{120}{9.5})$ = .71 ft.^{2}

2.14 ft.^{2}

Lower Section (L.S.)

3 legs = $3 \times 7 \times \frac{.57}{12}$ = 1.0 ft.^{2}

3 trusses = $2(\frac{.31}{12})(\frac{19}{12} \times \frac{84}{9.5})$ = .725 ft.^{2}

1.725 ft.^{2}

Drag on Lamp = $wC_D\pi r^2 = (25.6)(1.0)(\pi)(\frac{4.25}{12})^2 = 10.1^{\#}$

Moment at base

Lamp	(10.1)(20)'	= 202
EMT	(.55)(30.7)(18.5)'	= 312
U.S.	(2.14)(30.7)(12)'	= 788
L.S.	(1.725)(30.7)(3.5)'	= 185
		1487 ft. lbs.

Compression load on vertical member at base

$P = \frac{(1487)(12)}{7.8} = 2,288$ lbs.

$\sigma = \frac{2288}{.255} = 8,973$ psi

Factor of Safety

For pin-pin compression member,

$P_{critical} = \frac{\pi^2 EI}{l^2} = \frac{\pi^2(10^7)(.00515)}{(9.5)^2} = 5640$

fos = $\frac{5640}{2288} = 2.4$

2.2 Survival Conditions - 75 mph Wind with 1/2" Radial Ice

Wind loading = $w = (q)(C_D)$

$$w = (25.6)\left(\frac{75}{100}\right)^2(1.2) = 17.3 \text{ psf/unit projected area}$$

Projected Area

$$\text{EMT} = (.55)\left(\frac{3.2}{2.2}\right) = 0.80 \text{ ft.}^2$$

Upper Section

$$\text{3 legs} = (1.43)\left(\frac{1.57}{.57}\right) = 3.94$$

$$\text{3 trusses} = (.71)\left(\frac{1.31}{.31}\right) = \underline{3.00}$$

$$6.94 \text{ ft.}^2$$

Lower Section

$$\text{3 legs} = (1.0)\left(\frac{1.57}{.57}\right) = 2.75$$

$$\text{3 trusses} = (.725)\left(\frac{1.31}{.31}\right) = \underline{3.06}$$

$$5.81 \text{ ft.}^2$$

$$\text{Drag on Lamp} = (10.1)\left(\frac{75}{100}\right)^2\left(\frac{4.75}{4.25}\right)^2 = 7.1 \text{ lbs.}$$

Moment at Base

Lamp	(7.1)(20)'	= 142
EMT	(.80)(17.3)(18.5)'	= 256
U.S.	(6.94)(17.3)(12)'	= 1,441
L.S.	(5.81)(17.3)(3.5)'	= 352
		2,191 ft. lbs.

Compression load on vertical member at base

$$P = \frac{2191 \times 12}{7.8} = 3{,}371 \text{ lbs.}$$

$$\sigma = \frac{3{,}371}{.255} = 13{,}220 \text{ psi}$$

Factor of Safety

$$\text{fos} = \frac{P_{\text{critical}}}{P} = \frac{5640}{3{,}371} = 1.67$$

3.0 Load/Deflection Tests

The test set up for the Canadian Light Support Structure, also known as the Canadian Tower, is shown in Figure E-2. Two structures were mounted back-to-back on a fixture on a support bracket and loaded equally with 5.5 lb. incremental weights on 12" centers. This procedure counterbalanced the load equally about the support bracket, simplifying its design and construction. Deflection was measured at Stations 7 and 17. Results of the deflection test are shown on Figure E-3.

Procedure

1. (a) Load was applied to 7 foot section - see line "a" on Figure E-3. Deflection was measured at Stations 7 and 17.
   (b) Load was applied to 10 foot section - see line "b" on Figure E-3. Deflection was measured at Stations 7 and 17.
2. Line "c" on Figure E-3 is drawn parallel to line "b" and intersects line "a" at the load equal to the wind load at 100 mph on the 7 foot section.
3. Line "d" on Figure E-3 is drawn parallel to line "b" and intersects line "a" at the load equal to the wind load at 75 mph with 1/2" ice on the 7 foot section.
4. Maximum load applied - 215 lbs. There was no permanent set in the structure.
5. The load/deflection measurements of the test procedure, 1.(a) above, on the seven foot section were used in an attempt to determine the bending characteristics of the seven foot section.

   Using the deflection at Station 7, an equivalent moment of inertial I_δ was determined using the equation of a uniform beam

$$\delta = \frac{wl^4}{8EI} \quad \text{or} \quad I_\theta = \frac{wl^3}{6E\theta}$$

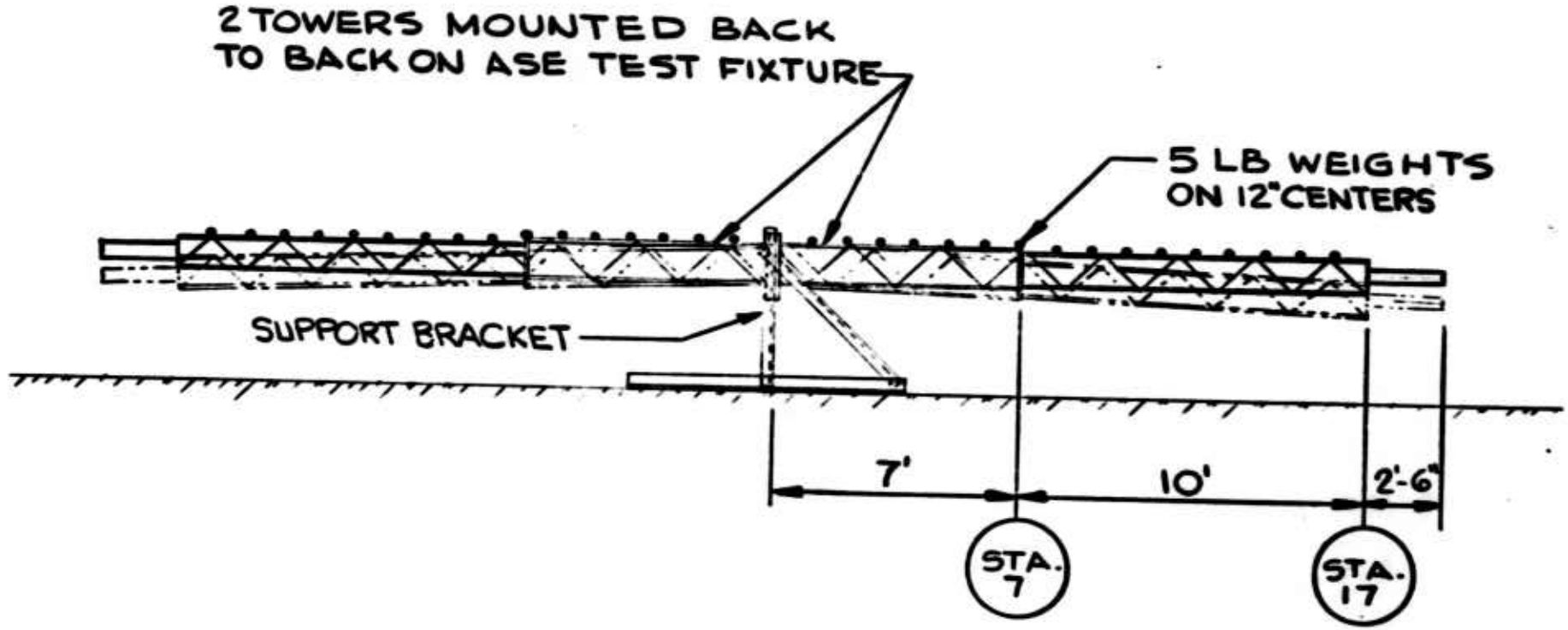

Figure E-2 Canadian Tower Deflection Load Test

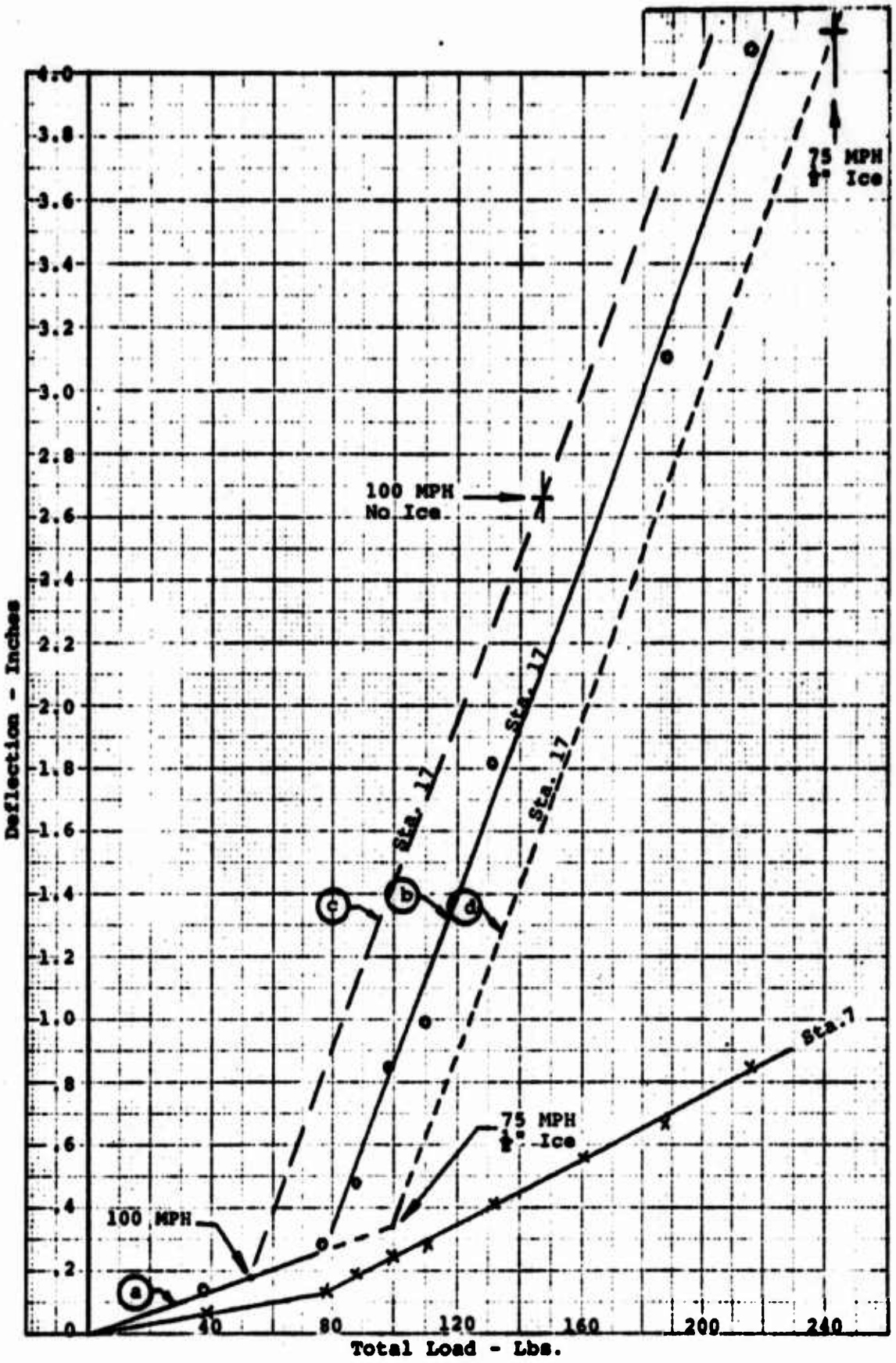

Figure E-3 Canadian Structure Deflection Test Results

Load #/ft	I_δ	I_θ
5.5	4.53	42.5
11.0	4.05	46.6

From the inconsistent values above, it appears that the Canadian pole does not behave as a uniform beam during bending.

4.0 Discussion

From the results of the analyses and test, the Canadian structure satisfies the survival wind and deflection criteria. The deflection at Station 17 for 100 mph wind with no ice, factored for 45 mph and added to the anticipated slope and deflection of the EMT yields a value of approximately 0.80 inches.

It will be noted, in contradistinction to the ASE pole, that the 75 mph wind with 1/2" radial ice is the governing survival criterion, i.e., the factor of safety is lower for the 75 mph wind with ice than for 100 mph wind with no ice. This is explained by the fact that due to the multiplicity of members, the increase of area due to icing is greater for the Canadian structure than for the ASE pole. This is reinforced by comparison of the total wind drag for the Canadian structure under 100 mph wind and 75 mph wind with 1/2" ice.

Total Wind Drag (100 mph wind - no ice)

Lamp		= 10.1
EMT	(.55)(30.7)	= 16.9
U.S.	(2.14)(30.7)	= 65.7
L.S.	(1.725)(30.7)	= 53.0
		145.7 lbs.

Total Wind Drag (75 mph - 1/2" radial ice)

Lamp	=	7.1
EMT (.80)(17.3)	=	13.9
U.S. (6.94)(17.3)	=	120.0
L.S. (5.81)(17.3)	=	100.5
		241.5

APPENDIX F

ELECTRONIC INSTRUMENTATION

Robert Harralson

TABLE OF CONTENTS

This Appendix provides the rationale for selecting the electronic instrumentation, the derivation of equations underlying the data reduction, descriptions of circuit operation and calibration procedures.

APPENDIX F

LIST OF FIGURES

APPENDIX F

Electronic Instrumentation

1.0 Introduction

This program was designed to measure the energy required to break a frangible pole designed under conditions which would simulate impact by a small plane making a landing approach. The pole under study was designed by ASE for the FAA to be used in approach light supports. For comparison, two other poles were also tested: one, the Belgian pole, and the other a pole used in Canada, in this Appendix referred to as the Canadian pole.

The technique was to use a structure, called the Impactor, which simulated a section of airplane wing, instrument it for acceleration measurement, and "fly" it into the poles.

The instrumentation used derived from the original concept of the test program in which the impactor was to be flown under a helicopter and the data telemetered to a ground station. This operation involved setting and resetting the electronics by remote control from the ground necessitating telemetry equipment, and the use of accelerometers and integrators to measure the velocity change.

When the program concept was modified and the impactor was "flown" by a ground-based carriage, consideration was given to a new system of measurement which would record the displacement of the impactor relative to the carriage, giving a simpler system and a more nearly direct measurement of kinetic energy. However, by that time the electronic system was operating in bench test, and was considered to be good enough that a redesign was not warranted. Accord-

ingly, the program went ahead as originally planned, but with the addition of an on-board tape recorder to replace the telemetry system. See Figure F-1.

2.0 Tabulation of Data

Table F-1 provides a tabulation of the reduced data for two series of runs. See Table 5-2 for a chronological tabulation of the Impact Test Schedule, and additional information.

Table F-1 Data Tabulation

Series	Date	Pole	Inch Pounds Channel 1[a]	Inch Pounds Channel 2[b]
I	20 Sept	ASE 1	48,000	No Data
	20 Sept	ASE 2	No Data[c]	No Data
	25 Sept	ASE 3	56,000	56,000
	26 Sept	ASE 4	28,000	32,000
	26 Sept	ASE 5	46,000	No Data
	21 Sept	Belg 1	200,000[d]	No Data
	27 Sept	Canadian 1	270,000[d]	No Data
II	31 Oct	ASE 1	32,600	No Data
	1 Nov	ASE 2	58,600	No Data
	1 Nov	Belg 1	189,500[d]	No Data
	1 Nov	Belg 2	142,500[d]	No Data

(a) Channel 1 Recorded on tape and is more reliable.

(b) Channel 2 Used Sample-and-Hold with a fixed 30 millisecond gate

(c) No data obtained for this run due to tape recorder malfunction.

(d) These values do not include the value of the vertical component of the energy extracted from impactor and are low by these indeterminate amounts.

3.0 Instrumentation

Purpose

The purpose of the instrumentation was to give a quantitative measure of the energy extracted from the impactor when the pole is struck.

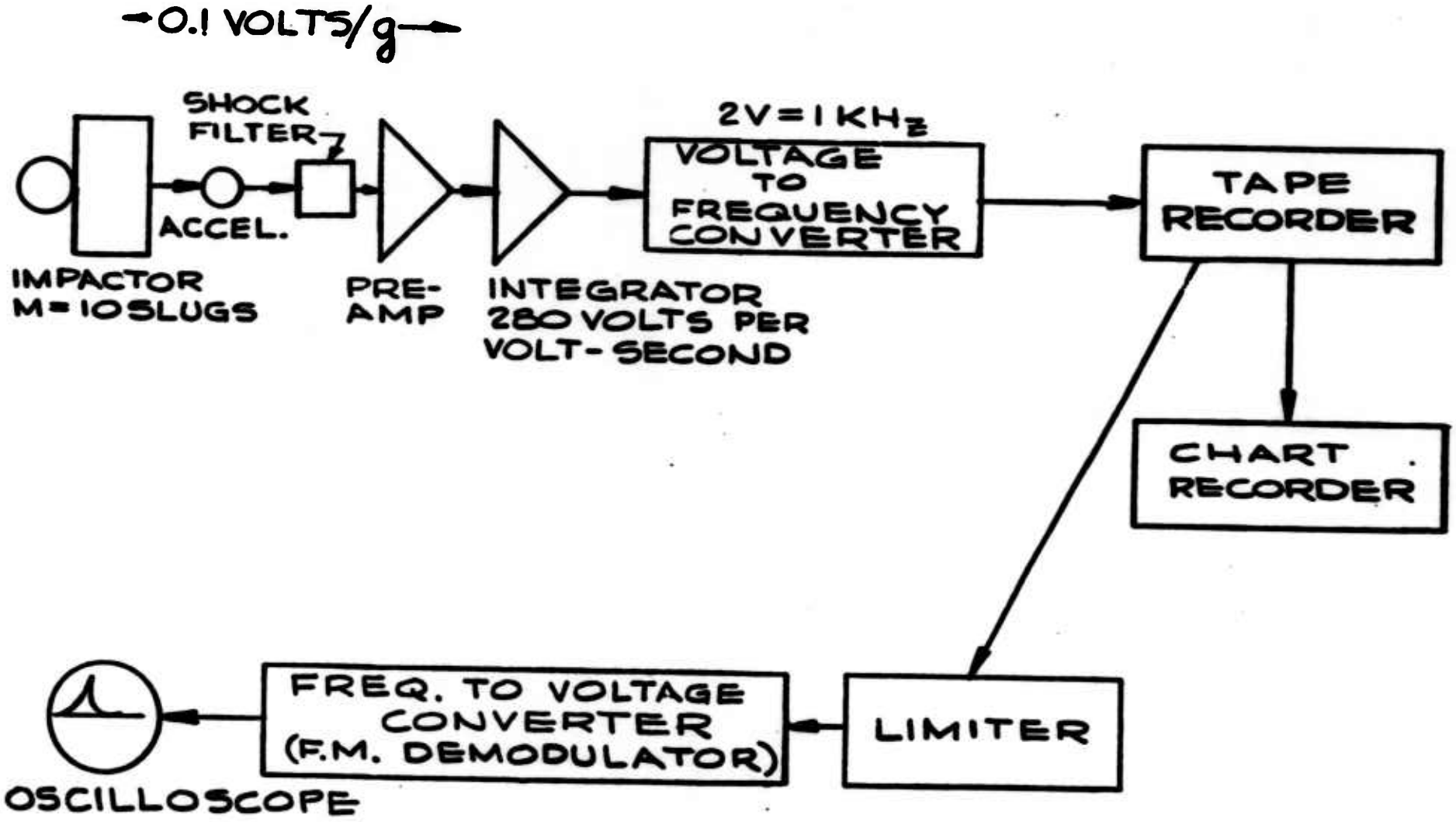

Figure F-1 Primary Channel System Block Diagram

Impact Configuration

The original concept of the impact episode was that it would last only a few milliseconds (probably less than 10) and would contain significant information in the first one millisecond.

Transducer Selection

For this reason, piezoelectric transducers were selected as pickup elements because of their excellent high frequency response and good performance for periods up to 20 milliseconds.

Type of Signal

The crystal transducer produces a signal proportional to acceleration. This signal must then be integrated to yield velocity which, together with impactor mass, gives a measure of energy ($\frac{mv^2}{2}$).

Electronics

The integration of the accelerometer output and its recording for future use was the function of the electronics package consisting of preamplifier, integrator, sample-and-hold, voltage to frequency converter, and tape recorder.

Shock Excitation Problem

During subsystem test, it was discovered that the accelerometer was sensitive to shock excitation, and would also give the same reading almost independently of the direction of the initial impact. None of these was a correct reading of either acceleration or velocity. Also, for rather moderate impacts, the preamplifier (part of the purchased accelerometer package) would overload, producing additional errors. During these tests, the impact used was such as to produce velocities equivalent to those that would result from 4000 in. # as mentioned in the contract. The resonances excited by shock were in the 3000 Hz region for the first impactor

structure, representing vibration of the body of the structure at its natural frequency.

The attack on this problem was by means of a low pass filter between the accelerometer and its preamplifier so proportioned that it attenuated the high frequency body resonances, but did not cause appreciable loss of signal. Impact test equivalent to 6000 in. # at 50 to 100 knots showed the electronics giving the correct readouts for frontal impacts.

4.0 Data Presentation

Figures F-2 through F-5 show data plotted for the second series of runs, and the method used for calculation of the energy absorbed. The method used for the first series of runs is identical, aside from the values of the correction factors, see Figures F-7 and F-8.

In comparing the performance of ASE and Belgian poles, it is important to note that the ASE pole exerts almost entirely horizontal force on the impactor, the vertical component due to severing the wire being quite small. However, in the case of the Belgian pole, the downward pull approximates, and probably exceeds, the horizontal force. This is apparent from the geometry of the situation at the moment the pole is ruptured as shown in Figure F-6 where the vertical force is $\frac{12}{9}$ or 4/3 the horizontal force. Thus, in addition to the more than 150,000 in. lbs. horizontal work done on the impactor, there is an equal or greater amount of work pulling the impactor downward.

Spurious Responses

It will be noted that the data presented in Figures F-2 to F-5 shows accelerometer response after the separation of the structure and the impactor is observed on the motion picture record of the run. This is attributed to vibration of the impactor and support structure after impact.

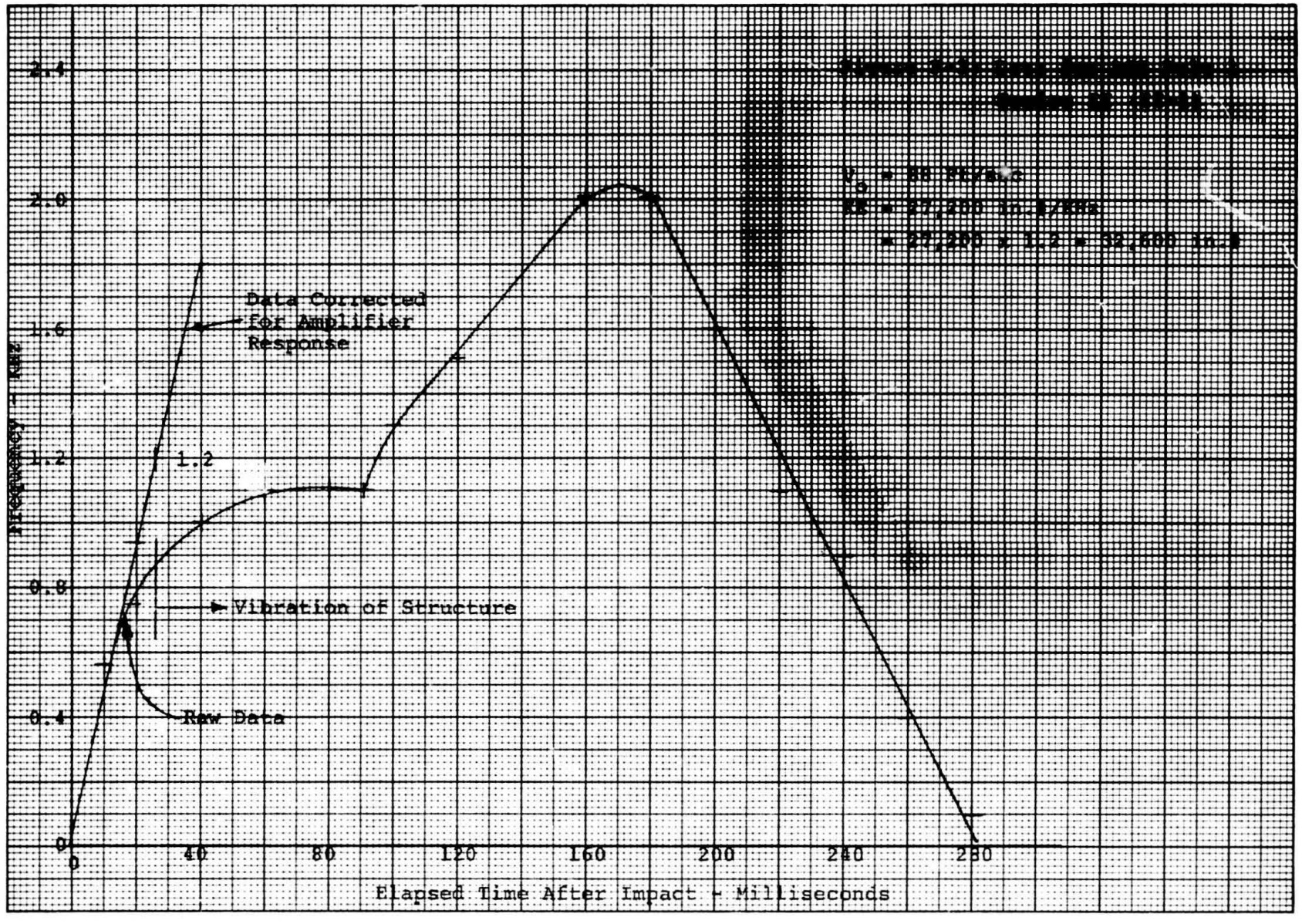
2.4
2.0
1.6
1.2
0.8
0.4
0
Frequency - Kez
1.2
Data Corrected for Amplifier Response
Vibration of Structure
Raw Data
0
40
80
120
160
200
240
280
Elapsed Time After Impact - Milliseconds

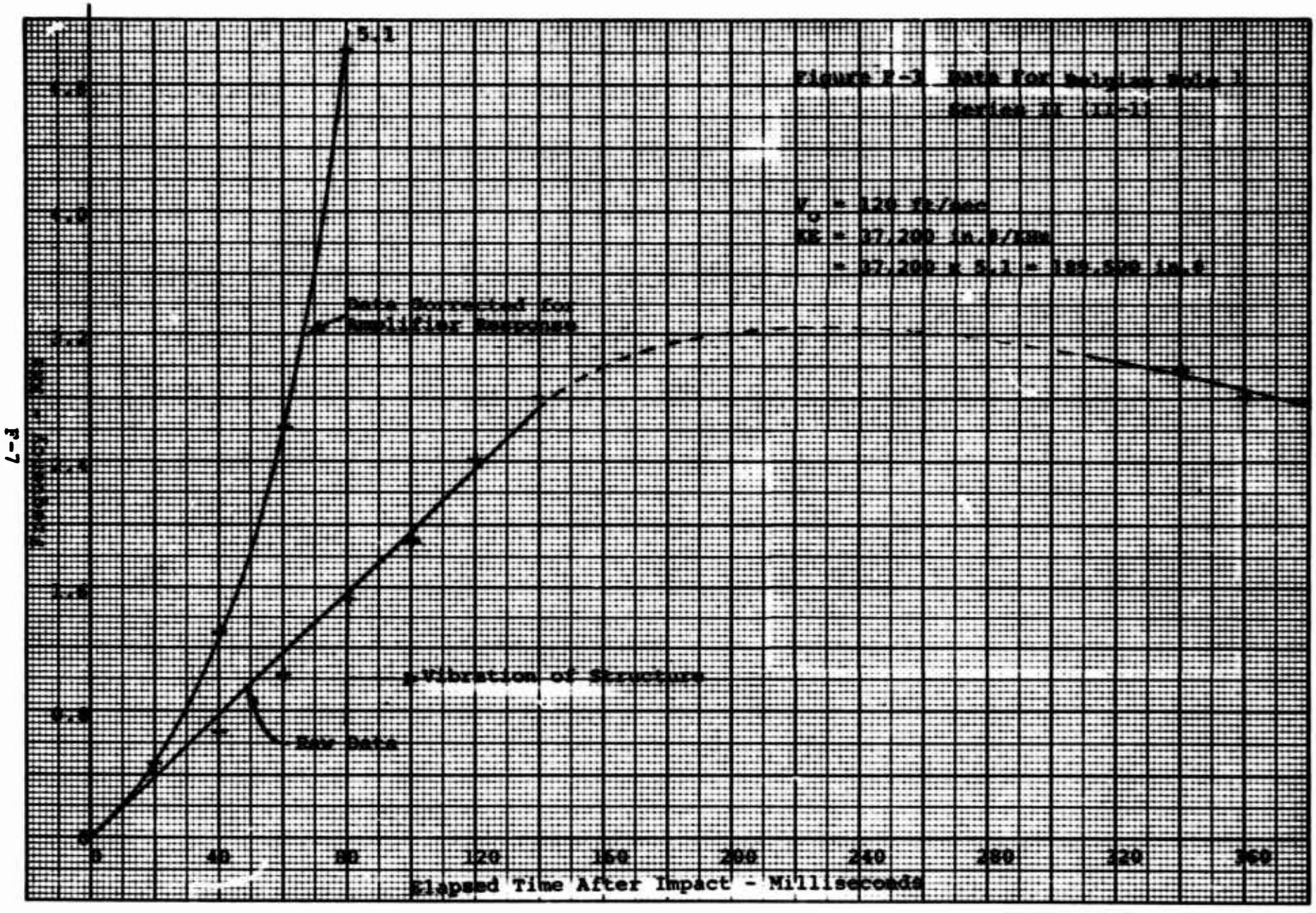

Figure F-3 Data for Belgian Style 1 Series II (II-1)

V_o = 120 ft/sec

KE = 37,200 in.#/cm

= 37,200 x 5.1 = 189,500 in.#

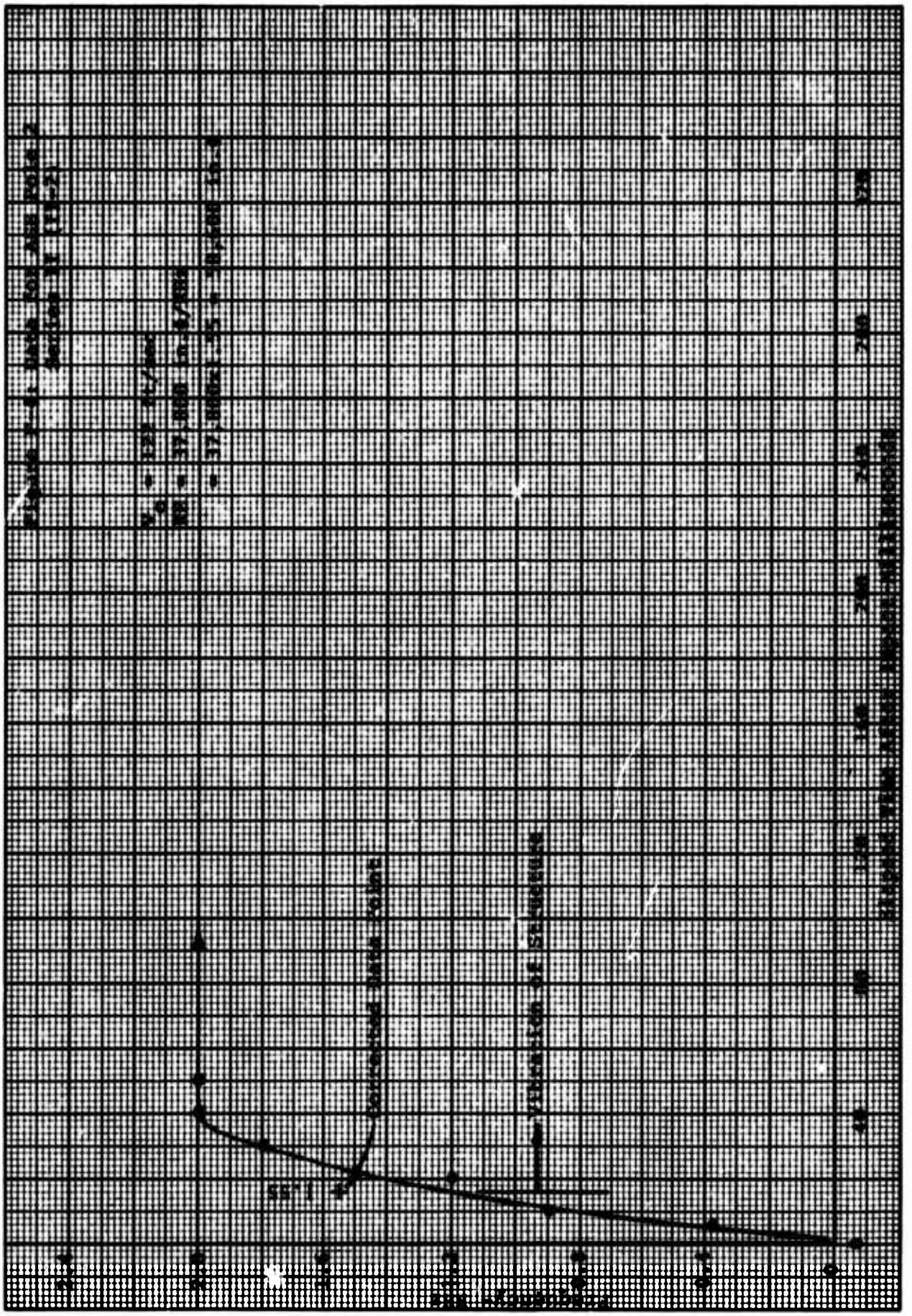

F-9

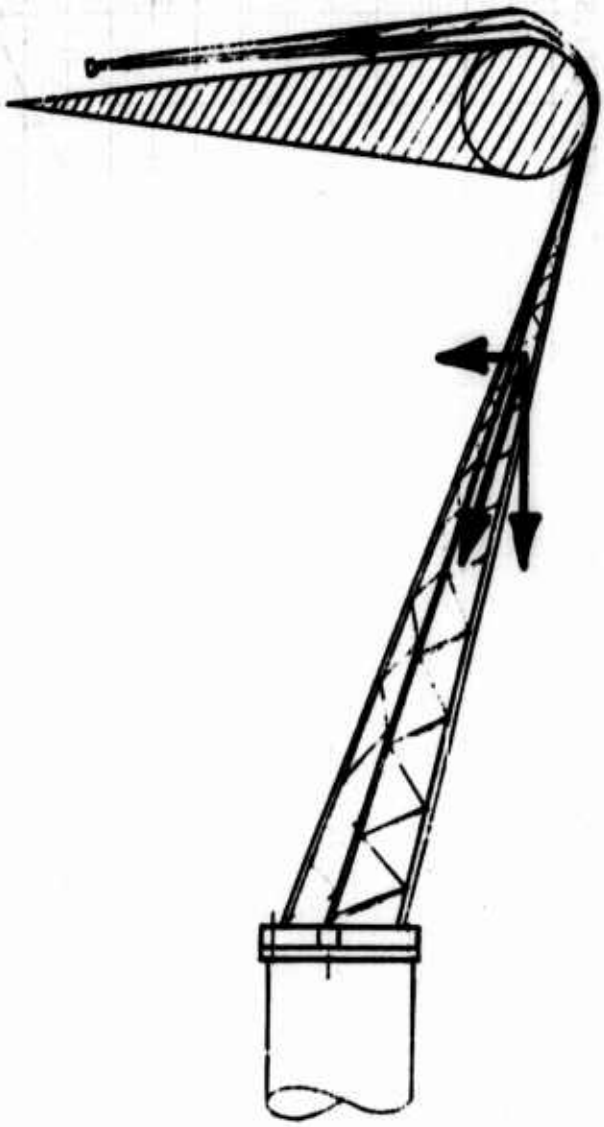

Figure F-6 Forces Acting on Impactor During Impact with a Truss Structure

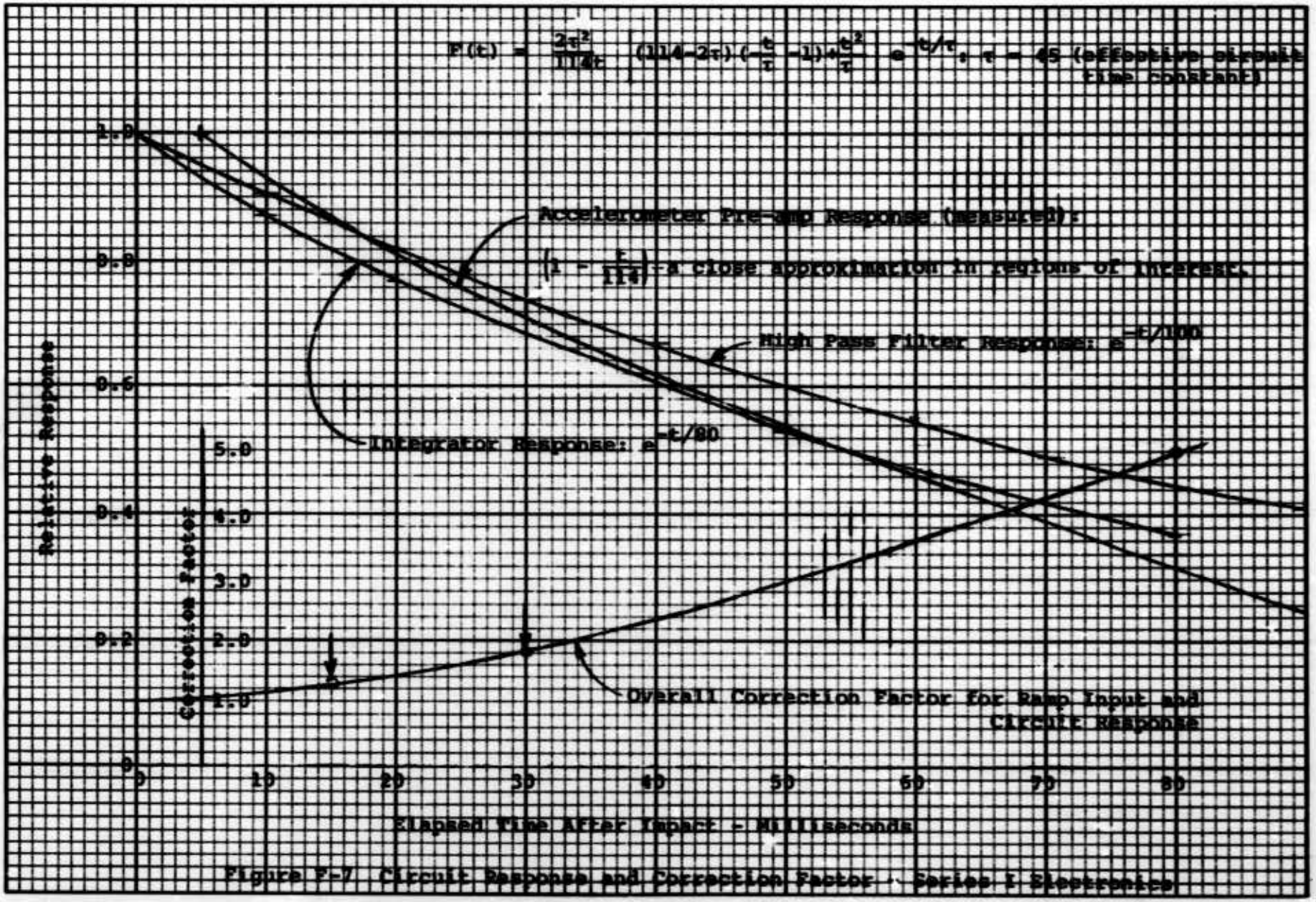

Figure F-7 Circuit Response and Correction Factor - Series I Electronics

F-12

This type of excitation was not anticipated, but does not impair the value of the data.

5.0 Data Evaluation

Examination of the tape recorder records indicates that there was very likely an error in the data due to shock excitation of the accelerometers by both impact and subsequent vibration. This effect would be more severe in the case of ASE poles because of the sudden impact and the short duration of the episode. In the case of Belgian poles, the force was applied more gradually over a much longer time, with less likelihood of shock excitation. However, as the record shows, vibration response was still quite large.

This shock susceptibility probably indicates that the readings are not as accurate as had been expected, with the error on the high side, and worst in the case of ASE poles. However, comparison with photographic records shows that the data is approximately correct. For example, it is easily calculated that 150,000 in. lbs. is required to bottom the springs, and the measured data for Belgian and Canadian poles is in the 150,000+ region. The same photographic records show relatively small deflection due to ASE impacts, and calculation indicates the energy should be in the 20,000 to 40,000 in. lb. region. Most of the measured data indicates considerably higher energies than this, leading to the suspicion that they are in error due to shock excitation.

6.0 Mathematical Background

Systems Constants

Mass of Impactor (M)

a.	Original	9.5 slug	305 pounds
b.	Rebuilt	10.0 slug	325 pounds

Spring constant (K), Impactor Assembly - 240 pounds per foot
Time of oscillation of Impactor - Spring Assembly: T = 1.28 Sec.

Velocity of Carriage, V_o

a.	50 knots	85 feet per second
b.	75 knots	127 feet per second
c.	100 knots	170 feet per second

Accelerometer and pre-amp scale factor v_a = 0.1 volts per g
Integrator gain:

a.	Series I (original)	270 volts per volt-second
b.	Series II (revised)	250 volts per volt-second

Symbols Used

A	Amplifier Gain
d	Distance
F	Force
g	Acceleration of gravity, 32.2 ft. per sec.^{2}
h	Height
K	Spring Constant
l	Length
M	Mass, Slugs = $\frac{\text{weight}}{32.2} = \frac{w}{g}$
T	Period of oscillation
t	Time
τ	Time constant
V	Velocity
v	Voltage, volts mv = millivolts = volts x 1000
v_a	Accelerometer output
v_o	Integrator output
W	Weight, pounds
KE	Kinetic Energy, foot pounds or inch pounds
in	Inch
lb, #	Pound
ft	Foot
sec	Second

6.1 Derivation of Formulas

6.1.1 Basic Kinetic Energy Equation

When a mass M is decelerated from V_1 to V_2, the kinetic energy required is

$$KE = \frac{1}{2} M_1 V_1^2 - \frac{1}{2} M_1 V_2^2 = \frac{1}{2} M (V_1^2 - V_2^2)$$

$$= M \frac{(V_1 + V_2)}{2} (V_1 - V_2)$$

$V_1 - V_2 = \Delta V_1$ the change in velocity,

$\frac{V_1 + V_2}{2}$ = Average Velocity

If the velocity change is small, $\frac{V_1 + V_2}{2} \doteq V_1$

for the present application, V_1 is about 150 and ΔV about 10 for Belgian poles, and less for ASE poles. Therefore, the error involved in using the simple formula $KE = MV_o \Delta V$ is about 3%. Therefore, we use the equation:

$$KE = MV_o \Delta V \qquad \text{(F-1)}$$

6.1.2 Accelerometer Scale Factors

The accelerometer and its companion preamplifier have a gradient of 0.1 volts per g of acceleration.

$$v_a = 0.1\ g = .1 \frac{dV}{dt} \times \frac{1}{32.2} = \frac{dV}{dt} \times \frac{1}{322}$$

then $\frac{dV}{dt} = 322\ v_a$, or

$$\Delta V = 322\ v_a\ t \qquad \text{(F-2)}$$

This says that the velocity change in ft/sec = 322 times the volt second product out of the accelerometer preamp.

Integrator

In order to get volts from Volt-seconds, an integrator is used. This one had a gain of 280 volts per volt-second. (Series I).

$v_o = 280\ v_a t$, or $v_a t = \frac{v_o}{280}$ (F-3)

substituting in (F-2) above,

$\Delta V = 322\ \frac{v_o}{280}$, v_o = integrator output volts

$\Delta V = 1.15\ v_o$ ft. per second (F-4)

Voltage to Frequency Converter

This device had a scale factor of 1 KHz per volt input, but the output had to be passed through a scale-of-two circuit to make the waveform symmetrical. The combination scale factor was therefore

F = .5 KHz per volt

$f\ (KHz) = .5\ v_o$

combining with Equation (F-4)

$\Delta V = 2.3f\ (KHz)$ (F-5)

6.1.3 Kinetic Energy Computation for Series I & II Parameters

Modifying Eq. (F-3) and (F-4) above for Series II constants where Integrator gain = 250 and M = 10 slug

$\frac{322}{250} = 1.29$ $2 \times 1.29 = 2.58$

Series II $\Delta V = 1.29\ v_o = 2.58f$

from Eq. (F-5) above, for Run I

$KE = MV_o(2.3f)(KHz)$ (F-6)

For 100 knots, V_o = 170 ft/sec, (168.9 exactly)

KE = M (170) (2.3) f = 390 (f) foot pounds

KE = 9.5 x 12 x 390 f inch pounds

KE = 44,000 (f) inch pounds (F-7)

For 50 knots,

KE = 22,000(f) inch pounds (F-8)

In Series II Tests where M = 10 and Integrator gain is 250 volts per volt-second,

For 100 knots,

KE = 52,500(f) inch pounds (F-9)

50 knots,

KE = 26,250(f) inch pounds (F-10)

75 knots,

KE = 39,500(f) inch pounds (F-11)

6.2 Electronics

6.2.1 Circuit Response

1. Accelerometer charge amplifier (pre-amp)
   Measured response of this amplifier is shown in Figure F-8.

2. Integrator
   Measured response is shown in Figure F-8.

3. Integrator Input Filter (Series I only)
   Response is shown in Figure F-7.

4. Correction factors

   Series I - The correction factor for the pre-amp, the integrator input filter, and the integrator response is shown in Figure F-7.

   Series II - The correction factor for pre-amp and integrator response is shown in Figure F-8.

6.2.2 Derivation of Correction Factors

From the response curves shown in Figures F-7 and F-8 we may write for circuit response:

Pre-Amp Response = $(1 - \frac{t}{114}) = A_1(t)$, t in milliseconds response normalized to one.

Integrator Response = $e^{-t/80} = A_2(t)$ where 80 milliseconds is the measured time constant of the integrator.

High Pass Filter Response = $e^{-t/100} = A_3(t)$ where 100 milliseconds is the nominal time constant of the filter. The system response is then $A_1(t)A_2(t)A_3(t)$.

Because the response is not flat, it is necessary to specify the disturbing function to determine the integrator's response. From the nature of the impact, assume that a ramp function describes with sufficient accuracy the steadily rising force as the pole breaks, and dropping rapidly to zero. Then we write $f(t) = Kt$ with K so chosen that

$$\int_0^{t_1} f(t)dt = t_1$$

The integrator output will then be

$$v = \int_0^{t_1} f(t)A_1(t)A_2(t)A_3(t)dt$$

Substituting the appropriate values of $f(t)$ and A_1, A_2, A_3 and performing the indicated operations, the formulas shown in Figures F-7 and F-8 are obtained:

$$F(t) = \frac{2\tau^2}{114t}\left[(114 - 2\tau)\left(\frac{-t}{\tau} - 1\right) + \frac{t^2}{\tau}\right]e^{-t/\tau}$$

Substituting a few values of t, sufficient points are plotted for the purposes at hand, 15 and 26 milliseconds for ASE poles and 80 milliseconds for Belgian poles. These points were determined by evaluating the photographic data.

Note that correction factors for Belgian poles, where most of the force is exerted late in the episode, are high, 3 to 5, whereas correction factors for ASE poles are low because most of the impact is completed before substantial loss of circuit response occurs.

6.2.3 Circuit Operation

6.2.3.1 Development of Velocity Signal

Signal generated by the crystal accelerometer is amplified in its companion amplifier, the pre-amp (see Figure F-1) after which it is at a suitable level and impedance to operate the Integrator. The signal generated in the accelerometer is, as indicated by its name, an acceleration signal, and the integrator is required to convert it to a velocity signal in accordance with the relation $V = \int a dt$, or velocity is the time integral of acceleration. The integrator output voltage, which represents the desired velocity change, is usable only if a method is available to store it until it can be read out. This is done by a sample-and-hold circuit which digitizes the voltage, stores it digitally, and reads it out on demand through a digital to analog converter. In the data summary this output is called Channel 2.

Gating

To protect this channel from noise and other signals occurring outside the time slot of interest, the input is clamped by an F.E.T. gate operated from a timing circuit which holds the gate open for 30 milliseconds after arrival of the impact signal.

Reset

After readout, the circuit may be reset manually if desired, but will in any event be reset just before impact by a switch installed alongside the track.

Panoramic Channel

In order to make the circuit more flexible and to handle events which did not fall in the 30 millisecond time slot of Channel 2, a second recording method was used. In this channel the integrator is not gated, but has a discharge time constant which is long enough to hold data of interest,

but short enough that it will self-discharge in the time between launch and impact. This was set at 0.08 sec in the circuitry of Channel 1.

Readout

However, in order to record the varying output of this integrator, a continuous recording method is required, and the simplest to implement was a tape recorder operated from the output of a voltage to frequency converter: the integrator output voltage is converted to a proportional frequency, and the frequency which is in the range 100 Hz to 3000 Hz is recorded on tape.

6.2.4 Data Reduction - Method 1

For data reduction, two methods were used, as indicated in the system block diagram, Figure F-1. In one, the tape output is recorded on a chart recorder having a frequency response up to 5 KHz, after which the value of the frequency versus time is determined by counting cycles, and the data is plotted as in Figures F-2, F-3, F-4, and F-5.

If the time duration of the impact episode is not apparent by observation of the above plots, it must be ascertained by reduction of the optical data and this time then used in the chart.

Example: As an example, consider Figure F-3, in which the record extends more than 400 milliseconds. Photographic study shows the last leg of the tower breaking at 80 milliseconds. Accordingly, it must be assumed that signals occurring after 80 milliseconds are due to other causes such as structural vibration, and the impact data terminates at 80 milliseconds where f = 1.5 KHz. Applying the correction factor from Figure F-8 for 80 milliseconds, (3.4), the corrected frequency is 1.5 x 3.4 = 5.1 KHz. Applying the appropriate formula, Eq. (F-11)

KE = 39,500 x 5.1 = 200,000 in. #

Data Reduction - Method 2

The second method of data reduction of the tape record is to pass the signal which is essentially an FM signal, through a limiter and into an FM demodulator as indicated in Figure F-1. The demodulator is calibrated by using steady state signals from an oscillator, and the calibration plotted (Figure F-9). Then when the demodulator output is displayed on a memory oscilloscope, the voltage versus time plot becomes the same as that made from the chart recorder. Voltage is then converted to frequency by the calibration chart, Figure F-9, and the KE computed as before.

6.2.5 Auxiliary Circuitry

6.2.5.1 Power Supply

To satisfy the requirements of portability and constant voltage, a nickel-cadmium battery was used. Additional voltage regulation was not needed because of the extremely flat discharge characteristics of this type of battery. Also, the low impedance prevented any instabilities due to power supply coupling.

The battery used consisted of 30 cells, each 1.2V, connected in series to give voltage of -12V, +12V, and +24V by appropriate taps. Load balancing resistors are added across the lightly loaded sections so that the entire battery will discharge at the same rate. The capacity of each cell is 4 ampere-hours, which at the normal load of about 0.2 amps gives 8 hours of operation, continuous or intermittent, and in practice was found to require recharging only once a week.

6.2.5.2 Control Circuit

In order to open and close the gate to Channel 2, a circuit is required to detect the arrival of impact signals and open the gate for the prescribed time. This is done on Board M_3. Threshold detection is by operational amplifier UIA which is biased to -0.2g equivalent voltage (20 m.v.).

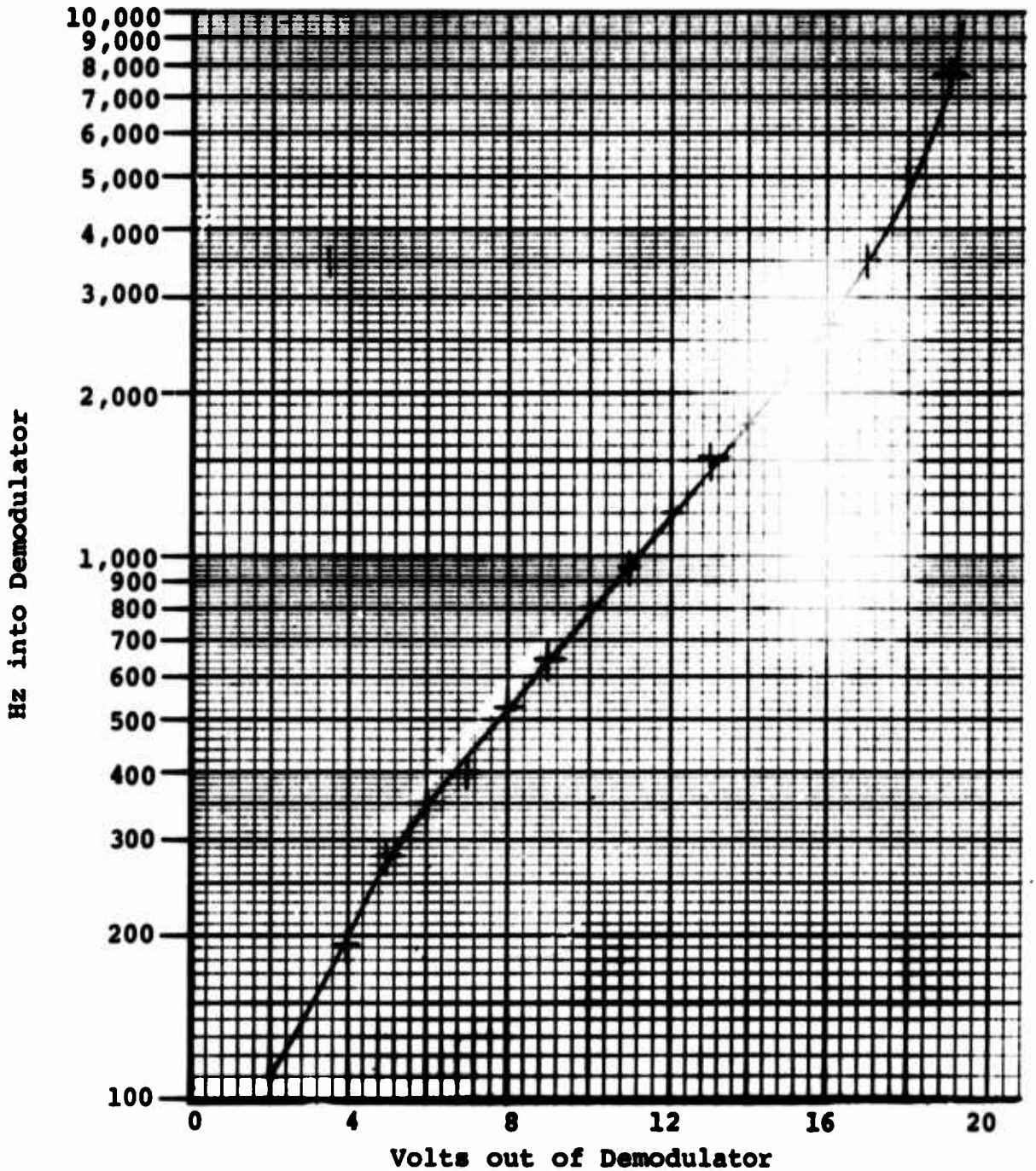

Figure F-9 Demodulator Calibration

When the signal exceeds this threshold, the output goes from -10V to +10V initiating the timing cycle. Timing is done by a 74121 one-shot followed by a 7479 Latch which prevents further timing cycles until it has been RESET, either manually during test, or by the track switch during a run. Nominal gate widths of 10, 15, 20 and 30 milliseconds and test pulse widths of 40 and 80 milliseconds are switch selectable, as indicated in 6.2.5.4 and 6.2.5.5.

6.2.5.3 Test Signals

During design, test signals of 0.33 Volt and 1.65 Volt amplitude, and 1.0 and 5.0 millisecond widths, switch selectable, were provided. After tests showed that the impact episodes were of considerably greater duration, the test pulse widths were changed to 40 milliseconds and 80 milliseconds.

In the equipment, these signals are fed directly to the integrator, a procedure which is adequate for checking integrator, sample-and-hold, and voltage-to-frequency converter performance. During data evaluation the signals were fed into the pre-amp through an accelerometer to provide the proper source impedance.

6.2.5.4 Gate Width Switch Settings - M3 Board

S6↓	S7↓	11 milliseconds
S6↑	S7↓	16 milliseconds
S6↓	S7↑	22 milliseconds
S6↑	S7↑	33 milliseconds

↑ is up, or away from terminal board

↓ is down, or toward terminal board

6.2.5.5 Test Pulse Width Switch Settings - M3 Board

S5↓	40 milliseconds
S5↑	80 milliseconds

6.3 Calibration by Impact

The impactor was instrumented and suspended by ropes so that it was free to swing. In front a weight consisting of an aluminum bar was swung as a pendulum to strike the impactor.

The impact equation is

$$V_3 = V_1 \frac{(M_1 - eM_2)}{(M_1 + M_2)} \qquad e = 0.76 \text{ (Determined by experiment)}$$

$$V_4 = V_1 \frac{(M_1)(1 + e)}{(M_1 + M_2)} \qquad e = \frac{h_2}{h_1}$$ Where h_1 = initial height of M_1, h_2 = rebound height

where M_1 = Mass (or weight) of pendulum = 12.2 pounds

M_2 = Mass (or weight) of impactor = 305 pounds

V_1 = Velocity of pendulum at moment of contact

V_2 = Velocity of impactor before contact, = 0

V_3 = Velocity of pendulum after contact

V_4 = Velocity of impactor after contact

To simulate an impact of 4000 in. lb. at 50 mph, when M_2 = 305 lb.,

V_4 = 0.48 ft./sec.

To compute V_1, set V_4 = 0.48 ft./sec.

Using impact formulas above, V_1 = 7.1 ft./sec.

From the relation $V = \sqrt{2gh}$, h_1 = 9.7 inches

The pendulum is then pulled back until it has risen 9.7 inches and released so that it strikes the impactor squarely, no energy going into rotation or lateral velocity. Several tests are run and the average compared with the design output of the electronics for V = 0.48 ft./sec. Data for several runs at 2000, 4000, and 6000 inch pounds equivalent are tabulated in Table F-2.

TABLE F-2 CALIBRATION DATA

KE	Accel. 1	Accel. 2	Average	Design Value	Error
2000 in. lb.	2.6	2.6	2.6	2.5	
	2.75	2.7	2.73		
	2.75	2.7	2.73		
	2.7	2.7	2.7		
	2.3	2.6	2.45		
	2.7	2.5	2.6		
	2.8	2.6	2.7		
			2.64	2.5	5% High
4000 in. lb.	6.4	4.1	5.2	5.0	
	5.8	4.4	5.1		
	4.7	5.5	5.1		
	4.1	5.0	4.5		
	5.0	4.2	4.6		
	4.8	4.6	4.7		
			4.9	5.0	2% Low
6000 in. lb.			7.1	7.5	5.5 Low

These last readings were estimated to be low because of the difficulty in making a square impact when the pendulum was drawn back 50 inches.

APPENDIX G

KINETIC ENERGY OF A TUMBLING SECTION OF BELGIAN STRUCTURE

Dr. Roy C. Spencer

This Appendix contains the calculations for evaluating the level of kinetic energy contained in the translation and rotation of a section of the Belgian structure which hurled forward of the impactor upon impact.

APPENDIX G

Kinetic Energy of a Tumbling Section of Belgian Structure

1.0 Introduction

This section makes use of the NASA movie films to analyze the kinetic energy of translation and of rotation of a section of the Belgian pole that wrapped around the impactor on impact and then was catapulted forward of the impactor.

1.1 Summary

An approximate 5 ft. section of Belgian pole was propelled ahead of the impactor at a ground speed of approximately 154 ft/sec, 41% faster than the carriage speed of 109 ft/sec. The section weighed 5.2 lbs.

The translational kinetic energy was	2,016 ft lbs
The rotational kinetic energy was	180 ft lbs
Total Kinetic Energy	2,196 ft lbs

2.0 Arrangement of Cameras

Two NASA high speed cameras were used with each of the impact tests conducted at Langley Field. One at 400 frames per second was placed on the ground opposite the impact site. The second at 400 frames per second was attached to the carriage on the support of the forward wheel, and took continuous pictures of the vicinity of the impactor. A third high speed camera, placed on the ground, operated at 4,000 frames per second, but after initial tests, was not used because the 400 frames-per-second camera was considered to be adequate. The following

analysis relates to the pictures of the first camera (400 frames per second) made of an impact with a Belgian pole.

3.0 Velocities at Impact

3.1 Carriage Velocity

The officially reported speed at impact was 73 knots. An independent analysis, given below, leads to a slightly lower value.

The individual movie frames were projected onto a screen with squares of arbitrary size. It was noted that the distance of 64.5 in. between centers of the extreme stripes painted on the impactor in Figure G-1 covered 1.9 squares. This is 2.829 ft per square.

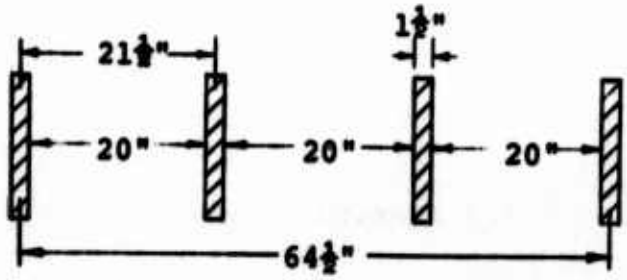

Figure G-1 Pattern of Stripes on Side of Impactor

To obtain the apparent speed of the carriage, the position of the upper left corner of the truss was plotted in Figure G-2 versus frame number. The slope was 0.0963 squares per frame. With a camera speed of 400 frames per second, this was

$$0.0963 \times 400 = 38.52 \text{ squares per sec}$$
$$= 38.52 \times 2.829 = 108.97 \text{ ft/sec}$$

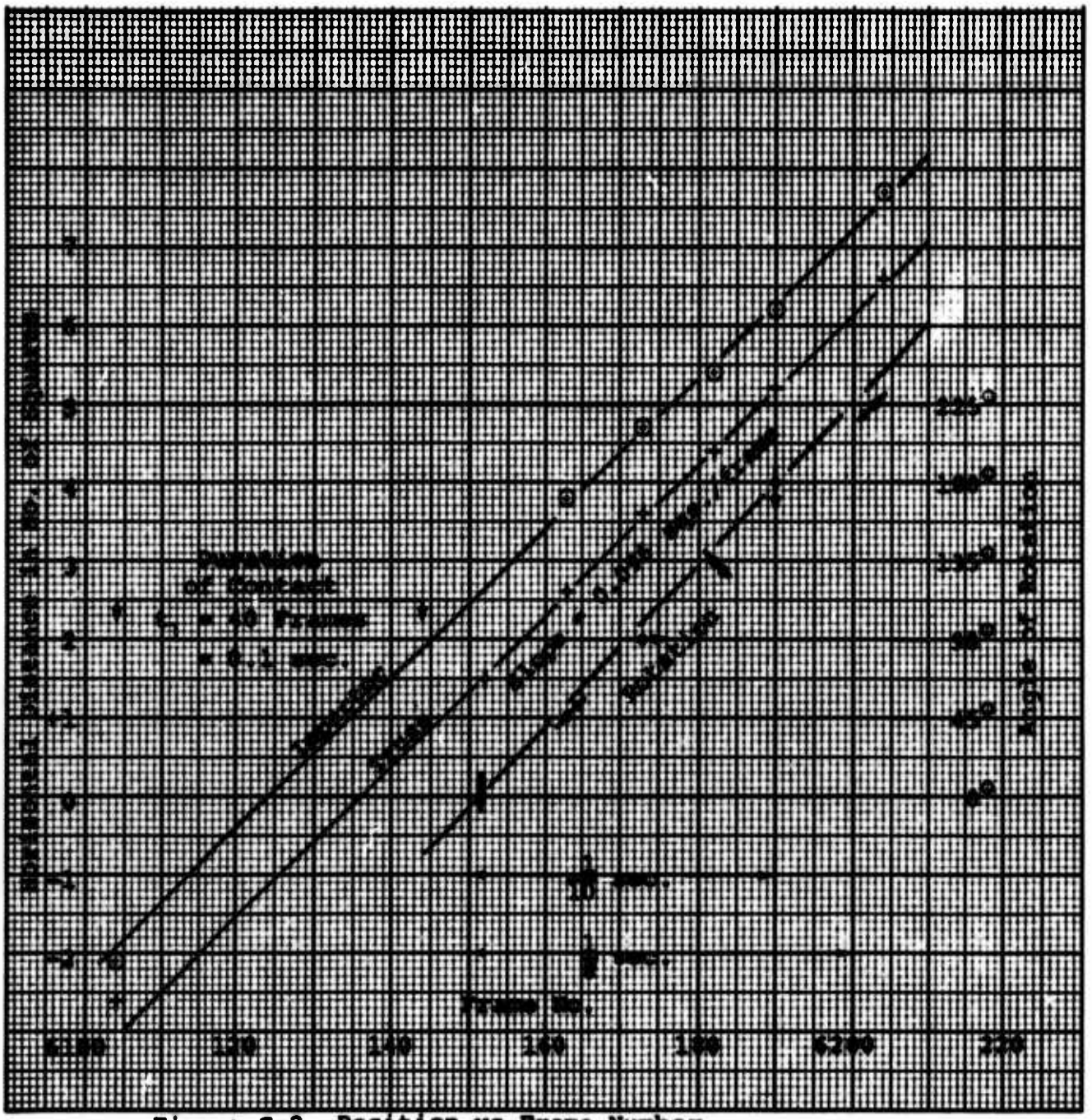

Figure G-2 Position vs Frame Number

Since

$$1 \text{ knot} = 6076 \text{ ft/hr} = \frac{6076}{3600}\frac{\text{ft}}{\text{sec}} = 1.6878 \text{ ft/sec},$$

the apparent speed is

$$\frac{108.97}{1.6878} = 64.56 \text{ knots}$$

This appears to be 11.6% lower than the 73 knots officially reported, but there is one obvious correction. The stripes on the impactor were three feet closer to the camera than the truss. This is the width of the impactor. Assuming that the camera was placed 60 feet from the impact site, the stripes would appear to subtend a 5% larger angle than if they were at the position of the truss. To allow for this, we should increase the 64.56 knots by 5% to yield 67.8 knots. This leaves a residual difference of 7.7%, which could arise in three ways.

a. The official record of the speed may be off, but this is unlikely, considering that Langley Field has been testing airplane tires for 20 years with this carriage, and they record the speed at four different points along the track.

b. The stated frame speed of 400 per second may be off. On some runs, a red light was made to flash at known intervals of time. This is recorded on the original film and might be a source of calibration. In the case of the 4000 frame per second camera, it was stated that a finite amount of time and quite a length of film was used up before the camera attained the rated speed. It is unlikely that this is the case with the 400 frame per second camera.

c. Distortion in the camera (and/or the projector) may cause a slight error. Although distortion is not apparent in the individual frames, one photographer at Langley Field stated that the high speed cameras were designed for maximum photographic speed and could not be depended upon for accurate scaling in subsequent analysis.

3.2 Impactor Velocity

The position of a corner of the impactor is also plotted on Figure G-2 vs frame number. The straight line through the small circles is drawn parallel to that for the truss, indicating that, within graphical accuracy, both impactor and truss are traveling at the same speed. However, the 5% correction again applies so that the impactor is actually moving 5% slower than the truss or carriage, or 5.45 ft./second slower.

The weight of the impactor is about 300 lbs. A 5% loss of speed could be caused by slamming into a stationary mass of 15 lbs. which then travels along with the impactor.

The interval t_1 between first impact and final contact of the tumbling section was 40 frames, or 0.10 sec. The motion of the impactor subsequent to this should be a linear term plus a damped sinusoid, with a period of about 0.7 sec. The post impact (circled) data points cover a period of about 0.1 sec. which is 51° of phase. However, no departure from linearity is observed greater than could be explained by statistical error.

4.0 Motion of Tumbling Section of Belgian Pole

Following the initial impact on the Belgian pole, the upper portion started to wrap around the impactor, bounced, and then was flipped forward of the impactor when it broke off. The somersaulting section weighed 5.2 lbs. Its orientation is plotted in Figure G-2 as a function of frame number. Due to the direction of the camera axis, the horizontal and 45° orientations may not be as precise as the vertical positions. It is noted that the section rotated one-half revolution in a time interval of 40 frames, or 0.1 sec. This is a rate of rotation of 5 revolutions per second, or 10π radians per second.

$$\omega = 10\pi$$

4.1 Kinetic Energy of Translation

The forward speed of the tumbling section obviously exceeds that of the impactor. While the section rotated 180° as mentioned in the previous paragraph, it progressed 5.5 squares compared to the 3.9 squares for the truss. This is a factor of 1.410, or 153.675 ft/sec. Assuming that the pole section is in the plane of the midsection of the impactor, we should increase the speed by 2.5% to

157.52 ft/sec.

The kinetic energy of translation in the horizontal direction is

$$KE = \frac{1}{2}\frac{m}{g}v^2 \qquad \text{(G-1)}$$

$$= \frac{1}{2}\frac{5.2 \text{ lb.}}{32.2 \text{ ft/sec}^2}(157.52)^2 \frac{\text{ft}^2}{\text{sec}^2} = 0.08125 \times 24812$$

$$= 2016 \text{ ft. lbs.}$$

4.1.1 Comparison With Kinetic Energy of Free Fall

The above value is large compared to the kinetic energy of free fall from the peak height of the trajectory. Since the distance of fall is

$$h = \frac{1}{2}gt^2 = 16t^2 \qquad \text{(G-2)}$$

the KE of free fall in ft. lbs. equals the loss in potential energy,

$$mh = 83.2t^2, \text{ t in seconds} \qquad \text{(G-3)}$$

If t = 0.1 sec.,

$$mh = 0.83 \text{ ft. lbs.}$$

4.2 Kinetic Energy of Rotation (Approximate)

The kinetic energy of rotation in ft. lbs. is

$$KE = \frac{1}{2}I\omega^2 \qquad \text{(G-4)}$$

where ω is the angular velocity in radians per second and I is the moment of inertia

$$I = \int r^2 dm = mk^2 \qquad \text{(G-5)}$$

where k is the radius of gyration.

As a first approximation, the 5.2 lb. mass of the rotating section is assumed to be uniformly distributed along its length. Then according to the reference books,

$$I = mk^2 = \frac{l^2}{12}m = \frac{5^2}{12} \times \frac{5.2}{32.2} = 0.337 \text{ slug ft.}^2 \qquad \text{(G-6)}$$

Using $\omega = 10\pi$

$$KE = \frac{1}{2}I\omega^2 = \frac{1}{2} \times 0.337 \times (10\pi)^2 = 0.1685 \times 986.96$$

$$= 166 \text{ ft. lbs.}$$

This is much less than the 2016 ft. lbs. of kinetic energy of translation.

An improved calculation is made in the following paragraph.

4.2.1 Kinetic Energy of Rotation (Improved)

The approximate calculation was based on the value of k^2 for a uniform bar of length 5 feet

$$k = \frac{L}{\sqrt{12}} = \frac{60 \text{ in.}}{\sqrt{12}} = 17.32 \text{ in.} \qquad \text{(G-7)}$$

Appendix H describes how an experimental value of

$$k = 18 \text{ in.}$$

was obtained. This is 3.92% greater than the value used, which leads to an 8% increase in kinetic energy, or

$$KE = 180 \text{ ft. lbs.}$$

5.0 Conclusion

1. An independent analysis results in a velocity of 67.8 knots for the carriage, compared to the 73 knots announced. This is more an indication of the consistency of the analysis of the high speed films, rather than a criticism of the Langley Field speed measurements.

2. The approximate 5 ft. section of Belgian pole was propelled ahead of the impactor at a ground speed of 154 ft/sec. This is 41% faster than the carriage speed of 109 ft/sec. The translational kinetic energy of this section with a mass of 5.2 lbs. was

2016 ft. lbs.

3. The kinetic energy of rotation of this section was 167 ft. lbs. based on a uniform distribution of mass over a 5 ft. length. Using an experimental value of radius of gyration this value was increased to 180 ft. lbs.

4. The sum of the rotational and horizontal translational kinetic energies was

2196 ft. lbs.

APPENDIX H

EXPERIMENTAL DETERMINATION OF RADIUS OF GYRATION

Dr. Roy C. Spencer

This Appendix describes the theory and method for experimentally determining the radius of gyration of an irregular body. This value is needed in the determination of the kinetic energy contained in the rotational motion of an irregular body, as in Appendix G.

APPENDIX H

Experimental Determination of Radius of Gyration

1.0 General

The moment of inertia I of a body about a particular axis is

$$I = mk^2 \qquad \text{(H-1)}$$

where m is the mass and k is the radius of gyration about the axis. In general, there are three moments of inertia, but we are interested here with the one (or two) moments about a transverse axis through the center of gravity (c.g.).

For example, the radius of gyration for a uniform bar of length L is

$$k = \frac{L}{\sqrt{12}} = \frac{L/2}{\sqrt{3}} \qquad \text{(H-2)}$$

Experimentally, k can be measured by suspending the body from two cords as in Figure H-1. This is a "bifilar suspension". The application and derivation of the theory are contained in this Appendix in the absence of any reference.

In Figure H-1, the irregular body is suspended by two cords of lengths ℓ_1 and ℓ_2 attached at points A and B at distances $\pm$ a from the center of gravity (c.g.). The c.g. is at a distance ℓ_c below the tops of the support cords.

2.0 Modes of Vibration of Bifilar Suspension

There are three possible modes of vibration.

Mode 1: The first mode occurs when the body is allowed to swing through a small arc in and out of the plane of Figure

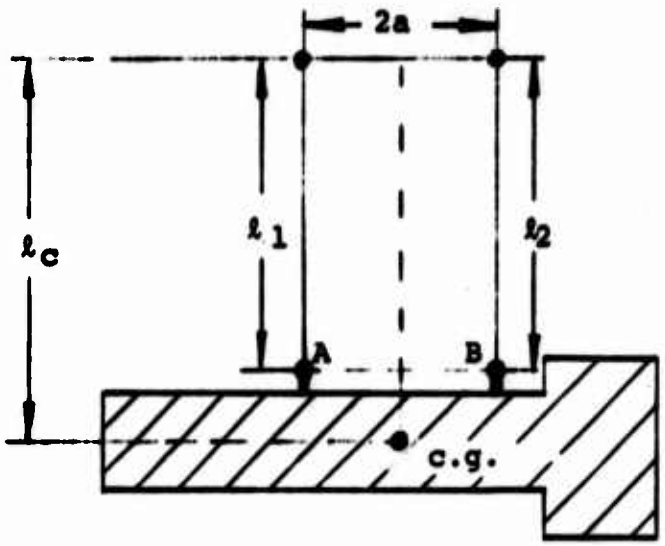

Figure H - 1 Bifilar Pendulum Supports

H-1. The period is then approximated by the period of a simple pendulum of length ℓ_c given by the formula

$$T = 2\pi\sqrt{\frac{\ell}{g}} \qquad \text{(H-3)}$$

where g in the acceleration of gravity

$$g = 980 \text{ cm/sec}^2 = 32 \text{ ft/sec}^2 \qquad \text{(H-4)}$$

There may be two small corrections. The first, due to the finite angle of oscillation, is neglected. The second, due to the radius of gyration about the longitudinal axis, is also neglected. The period obtained in this way is an initial experimental check against the value obtained from Equation H-3.

Mode 2: If we let the mass swing in the plane of Figure H-1, the motion is one of translation and the rotational moments of inertia do not come into the problem. The equivalent simple pendulum length is that of ℓ_1 or ℓ_2, assumed equal. The experimentally determined period should check with Equation H-3.

Mode 3: The mass is forced to rotate through a small angle ϕ about a vertical axis through the center of gravity as in Figure H-2. This brings in the rotational moment of inertia in which we are interested. The radius of gyration is k. It will be proved later that the period of oscillation is given by

$$T_k = 2\pi \frac{k}{a}\sqrt{\frac{\ell}{g}}, \qquad \ell = \ell_1 = \ell_2 \qquad \text{(H-5)}$$

This is k/a times the period in Mode 2, Equation (H-3). Again, small angles are assumed. Knowing the distance a, the value of k is given by a times the ratio of periods.

$$k = a \frac{T_k}{T} \qquad \text{(H-6)}$$

Using this method, the radius of gyration of the section of Belgian pole (See Appendix G) was experimentally determined to be

$$k = 18 \text{ inches}$$

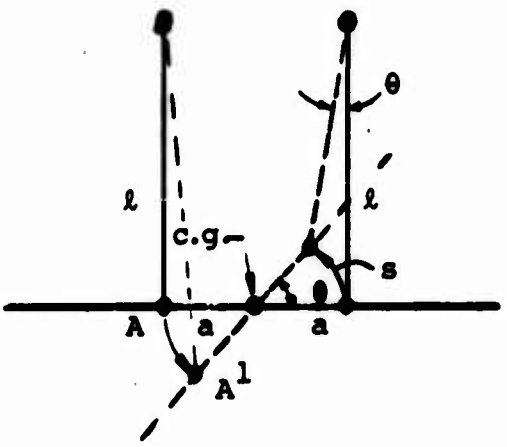

Figure H-2 Motion of a Bifilar Pendulum

3.0 Theory of the Bifilar Pendulum

From Figure H-2, one notes that as the mass rotates about the c.g. through a small angle ϕ, the cord deflects about a vertical angle θ. The arc length s is given by

$$s = \ell\theta = a\phi \qquad \text{(H-7)}$$

For a small angle of rotation the mass is lifted up a height

$$h = (1 - \cos\theta) \triangleq \frac{\ell}{2}\theta^2$$

so that the potential energy in absolute units is

$$mgh = mg\ell\theta^2/2$$

The restoring force at each support point is

$$\frac{1}{2} mg \sin\theta \triangleq \frac{1}{2} mg \frac{s}{\ell}$$

The two restoring forces combine to form a restoring torque. This is the sum of the forces times the radius a.

$$mga \frac{s}{\ell} = ma^2 \frac{g}{\ell} \phi \qquad \text{(H-8)}$$

The product of the moment of inertia I times the angular acceleration must equal the sum of the torques.

$$I \frac{d^2\phi}{dt^2} + ma^2 \frac{g}{\ell} = 0 \qquad \text{(H-9)}$$

On substituting $I = mk^2$

$$\frac{d^2\phi}{dt^2} + \frac{a^2}{k^2} \frac{g}{\ell} \phi = 0 \qquad \text{(H-10)}$$

Now, compare this with the usual differential equation for simple harmonic motion

$$\frac{d^2\phi}{dt^2} + \omega^2\phi = 0 \qquad \text{(H-11)}$$

where

$$\omega = \frac{2\pi}{T} \qquad \text{(H-12)}$$

It follows that T_k, the period of the bifilar pendulum is

$$T_k = 2\pi \frac{k}{a} \sqrt{\frac{\ell}{g}}$$

This is k/a times the period for the simple pendulum, as stated earlier, in Equation (H-5).

GPO 870-288